

Hierarchical Fuzzy Control of the UPFC and SVC located in AEP's Inez Area

Satish Maram

Thesis submitted to the Department of Electrical and Computer Engineering of the

Virginia Polytechnic Institute and State University

in partial fulfillment of the requirements for the degree of

Master of Sciences

in

Electrical Engineering

Lamine Mili (Chair)

Saifur Rahman

Yilu Liu

May 6th, 2003

Falls Church, Virginia.

Keywords: SVC, UPFC, Voltage Stability, Fuzzy control, Hierarchical control

Copyright 2003, Satish Maram

Hierarchical Fuzzy Control of the UPFC and SVC located in AEP's Inez Area

Satish Maram

Committee: Prof. Lamine Mili (Chair), Prof. Saifur Rahman, Prof. Yilu Liu

(ABSTRACT)

To reinforce its Inez network, which was operated close to its stability limits, American Electric Power (AEP) undertook two major developments, one being the installation of a Static Var Compensator (SVC) in November 1980 and the other one being the installation of the world's first Unified Power Flow Controller (UPFC) in 1998. The controllers in the system include the Automatic Voltage Regulators (AVRs) of the generators, the controllers of the SVC, and UPFC. To coordinate the control actions of these controllers and prevent voltage instability resulting from their fighting against each other, a two level hierarchical control scheme using fuzzy logic has been developed and its performance was assessed via simulations. The second level of the hierarchy determines the set points of the local controllers of the AVRs, SVC, and UPFC and defines the switching sequences of the capacitor banks, the goal being to maximize the reactive reserve margins of the Inez subsystem. Numerous simulations were carried out on this system to determine the actions of the fuzzy controller required to prevent the occurrence of voltage collapse under double contingency. Simulations have revealed the occurrence of nonlinear interactions between the machines resulting in stable limit cycles, nonlinear oscillations undergoing period doubling leading to chaos and possible voltage collapse. The proposed fuzzy scheme provides a fast, simple, and effective way to stretch the stability limit of the system for double contingency conditions, up to 175 MW in some cases. This is a significant increase in the system capacity.

Table of Contents

Chapter 1 Introduction 1

Chapter 2 Voltage Stability 6

2.1	Definition of basic concepts	6
2.2	Voltage stability problems	7
2.3	Causes of voltage instabilities	8
2.3.1	Short-term / transient dynamics	12
2.3.2	Longer-term voltage dynamics	12
2.4	Analysis of voltage stability	12
2.4.1	P-V Curves	13
2.5	Reactive power compensation and control	14
2.5.1	Reactive power transmission	15
2.5.2	Shunt capacitor banks	17
2.5.3	Static Var Compensators (SVCs)	18
2.6	Chapter summary	18

Chapter 3 UPFC and SVC Modeling and Control 19

3.1	Flexible AC Transmission Systems (FACTS)	19
3.2	Types of FACTS controllers	20
3.2.1	Principles of the series controllers	20
3.2.2	Principles of the shunt controllers	20
3.2.3	Principles of the combined series-series controllers	21
3.2.4	Principles of the combined series-shunt controllers	21

3.3	Principles of the Static Var Compensators (SVCs)	21
3.3.1	V-I characteristics of an SVC	22
3.3.2	Prevention of voltage instability with the SVC	23
3.3.3	Modeling of SVC in Eurostag	24
3.4	Unified Power Flow Controller (UPFC)	26
3.4.1	Basic operating principles	26
3.4.2	Transmission control capabilities	28
3.4.3	Control and dynamic performance	29
3.4.4	Modeling of UPFC in Eurostag	31
3.5	Chapter Summary	35

Chapter 4 Description of the Fuzzy hierarchical controller 36

4.1	Fuzzy logic	36
4.2	Why Fuzzy?	37
4.3	Fuzzy systems	37
4.4	Fuzzy sets	38
4.4.1	Membership function	39
4.5	Fuzzifier	40
4.6	Defuzzifier	42
4.6.1	Centroid defuzzifier	42
4.6.2	Center average defuzzifier	42
4.6.3	Maximum defuzzifier	43
4.7	Fuzzy rule base – IF-THEN rules	43
4.8	Description of the fuzzy inference engine	45
4.8.1	Composition based inference	46
4.8.2	Individual rule-based inference	46
4.9	Hierarchical fuzzy control	46
4.10	Basic concepts of pattern recognition (PR)	50
4.10.1	Sensors and acquisition	50

4.10.2	Signal conditioning or preprocessing	51
4.10.3	Segmentation (Low level feature extraction)	51
4.10.4	Feature extraction	52
4.10.5	Selecting features	52
4.10.6	Classification	53
4.11	Chapter summary	54

Chapter 5 Design and Implementation of the INEZ system in Eurostag 55

5.1	Transmission line model	55
5.2	Load modeling	56
5.2.1	Dynamic load modeling	57
5.3	Generator modeling	58
5.4	Step-down transformer modeling	59
5.5	Capacitor banks	62
5.6	Static Var Compensator (SVC) modeling in Eurostag	63
5.7	Unified Power Flow Controller (UPFC)	64
5.8	Chapter summary	66

Chapter 6 Simulation Results of the INEZ system 72

6.1	Steady-state analysis	72
6.2	Transient analysis	73
6.2.1	5% Load increase on the system	74
6.2.2	Single-contingency cases	78
6.2.3	Double-contingency cases	80
6.3	Fuzzy logic controller	84
6.4	Self-excited dynamic non-linear oscillations	85

Chapter 7 Conclusion	91
References	93
Vita	96

List of figures

Chapter 2 Voltage Stability

Fig. 2.1	Time duration of disturbances affecting voltage stability	8
Fig. 2.2	Voltage profile of the Inez system for no contingencies	9
Fig. 2.3	Voltage profile of the Inez system for single contingency on line 05SPRIG1-05JOHNSC	10
Fig. 2.4	Voltage profile of the Inez system for double contingency on line 05SPRIG1-05JOHNSC and 05BSAND-05INEZ	11
Fig. 2.5	Normalized P-V curves for a fixed source and reactance network	13
Fig. 2.6	Plots of active load (P) vs voltage (V) at various buses of the Inez system	15

Chapter 3 UPFC and SVC modeling and control

Fig. 3.1	Voltage-Current Characteristics of SVC	22
Fig. 3.2	Block diagram of SVC	24
Fig. 3.3	Generalized block diagram of SVC	25
Fig. 3.4	Representation of the UPFC in a two-machine power system	27
Fig. 3.5	UPFC implementation by two back-to-back voltage source converters	28
Fig. 3.6	Principle UPFC control scheme	30
Fig. 3.7	Principle of operation of the shunt part of the UPFC	30
Fig. 3.8	Principle of operation of the series part of the UPFC	31
Fig. 3.9	Dynamic model of UPFC in Eurostag	32
Fig. 3.10	Control of the series part	33
Fig. 3.11	Model of shunt part used in Eurostag	34
Fig. 3.12	Shunt part control	34

Chapter 4 Description of the fuzzy hierarchical controller

Fig. 4.1	Configuration of a pure fuzzy system	38
Fig. 4.2	Configuration of a Takagi-Sugeno-Kang fuzzy system	39
Fig. 4.3	Configuration of a fuzzy system with fuzzifier and defuzzifier	40
Fig. 4.4	Hierarchical voltage control scheme for the Inez system	49
Fig. 4.5	Generic block diagram of a pattern recognition system	51

Chapter 5

Fig. 5.1	Equivalent pi- circuit of a transmission line	55
Fig. 5.2	Modeling of a line in Eurostag	56
Fig. 5.3	Constant impedance load as entered at each node in Eurostag	57
Fig. 5.4	Parameter's values of the induction motor model used to represent the load of the INEZ subsystem	58
Fig. 5.5	First set of data for a synchronous generator as modeled in Eurostag	60
Fig. 5.6	Second set of data of a synchronous generator as modeled in Eurostag	61
Fig. 5.7	Transformer equivalent circuit	61
Fig. 5.8	Transformer modeling in Eurostag	62
Fig. 5.9	Capacitor banks at the Beaver Creek and Inez buses	63
Fig. 5.10	Generalized Block diagram of SVC with conductance G and susceptance B	63
Fig. 5.11	Capacitor bank as modeled in Eurostag	64
Fig. 5.12	SVC Implementation in Eurostag	65
Fig. 5.13	Dynamic model of UPFC in Eurostag	65
Fig. 5.14	Model of the complete interface between the UPFC and the transmission network	66
Fig. 5.15	Macrobloc main scheme of the SVC	67
Fig. 5.16	Macrobloc upfc_se (series part control) connected to 05INEZ node	68
Fig. 5.17	Macrobloc upfc_sh (shunt part control) connected to 05INEZ node	69
Fig. 5.18	Macrobloc interup1 (Injector 1) connected to 05INEZ node	70
Fig. 5.19	Macrobloc interup2 (Injector 2) connected to UPFCNODE	71

Chapter 6

Fig. 6.1	P-V plots of the system without UPFC and SVC	73
Fig. 6.2	P-V plots of the system with the UPFC and SVC	74
Fig. 6.3	Q-V plots of the system without UPFC and SVC	75
Fig. 6.4	Q-V of the system with the UPFC and SVC	75
Fig. 6.5	Voltage magnitude and angle plot of the 05INEZ node with the UPFC and SVC not connected to the network	76
Fig. 6.6	Voltage magnitude and angle plot of the 05Baker node with the UPFC and SVC not connected to the network	77
Fig. 6.7	Voltage magnitude and angle plot of the 05Inez node with the UPFC and SVC connected to the network	77
Fig. 6.8	Voltage magnitude and angle plot of the 05Baker node with the UPFC and SVC connected to the network	78
Fig. 6.9	Voltage magnitude and angle plot of the 05Inez node with the UPFC and SVC connected to the network when Line 05HATFLD-05BORLND is disconnected at $t=20$ seconds following an increment in P and Q load by 5% throughout the network	79
Fig. 6.10	Voltage magnitude and angle plot of the 05Baker node with the UPFC and SVC connected to the network when Line 05HATFLD-05BORLND is disconnected at $t=20$ seconds following an increment in P and Q load by 5% throughout the network	80
Fig. 6.11	Voltage magnitude and angle plot of the 05INEZ node with the UPFC and SVC connected to the network with Line 05HATFLD-05BORLND and Line 05BUSSYV-05THELMA opened	81
Fig. 6.12	Voltage magnitude and angle plot of the 05BAKER node with the UPFC and SVC connected to the network with Line 05HATFLD-05BORLND and Line 05BUSSYV-05THELMA opened	82
Fig. 6.13	Voltage magnitude and angle plot of the 05INEZ node with the UPFC and SVC connected to the network with Line 05HATFLD-05BORLND and Line	82

	05BUSSYV-05THELMA opened and with actions of the controllers coordinated	
Fig. 6.14	Voltage and voltage angle plot of the 05BAKER node with the UPFC and SVC connected to the network with Line 05HATFLD-05BORLND and Line 05BUSSYV-05THELMA opened and with actions of the controllers coordinated	83
Fig. 6.15	Variation of the voltage magnitude V with the reactive power load	86
Fig. 6.16	Voltage versus Time plot at the 05BAKER node	88
Fig. 6.17	Zooming in at point H ₁ in Fig. 6.16, showing persistent oscillations at time t=65 seconds	88
Fig. 6.18	Zooming in on point H ₂ in Fig. 6.16, showing damped oscillations at time t=85 seconds	89
Fig. 6.19	Voltage-Time plot at Node 05THELMA	90

List of Tables

Chapter 4

Table 4.1 Example of nested IF- THEN loops exhibiting the hierarchy of operations 48

Chapter 6

Table 6.1 Example of nested IF- THEN loops exhibiting the hierarchy of operations 84

Chapter 1

Introduction

Problem Statement

The traditional mid-west service territory of AEP hosts a collection of power plants mainly sited along the Ohio River and its tributaries. In the eastern and southern parts of these water channels, a backbone of long transmission lines at the 765 kV and 345 kV voltage levels energizes a 138-kV sub-transmission network that spans over the Tri-state and the Inez areas located in the central Appalachian region. The load in these areas consists of widely dispersed small rural communities and a fast growing industrial sector dominated by the coal mining industry [23]. As a result, the Inez 138-kV network has been pushed closer to its stability limits, leaving not enough reserve margins to withstand multiple contingencies or planned equipment outages. Prior to the installation of voltage support equipment, the Inez sub-transmission network suffered from severe voltage depressions, sometimes leading to blackouts whenever major double contingencies occurred.

To reinforce the Inez 138-kV network, AEP undertook two major developments in the area. The first development took place in November 1980 with the connection of a ± 125 -MVAR Static Var Compensator (SVC) along with four 50-MVAR mechanically-switched shunt capacitors to the 138-kV bus bars of the Beaver Creek Station [23]. This gives a total reactive power capability of + 325 MVAR for the installed Static Var System (SVS). The 138-kV bus-bar voltage is regulated by a control scheme providing a coordinated control of the four capacitor banks together with the two thyristor-controlled reactors (TCRs) and the two thyristor switched capacitors (TSCs) that form the SVC.

The second major development took place at the Inez Station [24-26] between mid 1997 and early 1998 with the installation of the world's first Unified Power Flow Controller (UPFC). The Inez project was carried out in two main phases [24]. During the first phase of the project, which was completed in July 1997, a ± 160 -MVAR Static Synchronous Compensator (STATCOM) was connected to the Inez 138-kV bus bars. The STATCOM's role is manifold; it provides reactive support to the Inez area, regulates the voltage at the Inez station, and remotely switches on and off the series reactor at the Big Sandy Station and several other capacitor banks in the neighboring stations.

During the second phase of the Inez project [24-26], which was completed in early 1998, a ± 160 -MVA Static Synchronous Series Compensator (SSSC) was connected to the dc terminals of the STATCOM to form a ± 320 -MVA UPFC. In the event where the STATCOM is disconnected or a larger reactive power support is needed in the area, the SSSC can be converted into a second STATCOM thanks to the addition of a spare shunt transformer [7]. The controllers of the UPFC are able to independently control the voltage at the Inez station and the real and the reactive power flow at the newly installed 950 MVA, 138-kV Inez-Big Sandy line [7]. As indicated in [24], they also regulate the voltages at the Johns Creek, Sprigg, and Logan Stations by sending switching signals to the six shunt capacitor banks sited there, four of them being newly installed.

While it is shown in a simple example of a two-machine system [27] that the inclusion of an UPFC in one of the two tie-lines significantly increases the transient stability limits of the system, a comprehensive study still needs to be carried out in the Inez area. It is stated in [24] that it is required to optimize the setting of the UPFC controls so that the reactive reserves in the Inez area are maximized under contingencies. This optimization should account for all the interactions that may occur in the system, which comprises harmonic and control interactions. Control interactions are expected to occur between the AVRs of the generators at Big Sandy and Baker and the controllers of the SVC and UPFC, which also send control signals to the reactors and the ten shunt capacitor banks located in the area. Interactions of these controllers with the dynamic loads of the subsystem may also occur. If not coordinated, these controllers may fight

one against the other to produce instabilities. Coordinating their actions is required to optimize the voltage stability margins in the Inez area and improve the damping of the transient and dynamic oscillations under contingencies.

Stat-of-the art in fuzzy control as applied to power systems

Over the last decade, fuzzy logic has gained a lot of appreciation from many engineering fields. The electric power industry is no exception. With the advent of powerful and cheap computers, digital control is being used in a growing number of power system applications. Many new effective algorithms have been developed and implemented in real time. Fuzzy logic is a new control approach with a great potential for real-time applications.

According to Schoder, Hasanovic, and Feliachi [19], “Fuzzy control design is attractive for nonlinear systems applications because it does not require mathematical model, and it can cover a wide range of operating conditions.” The last few years have seen numerous papers being published applying fuzzy control to achieve better results in a wide array of power system tasks. Voltage stability, power system simulation, damping control, transient analysis, and load flow studies are few such applications.

Efficient load flow methods [21], which make use of fuzzy logic to reduce the number of iterations and decrease computation time, have been developed and tested successfully. With increasing availability of fuzzy knowledge base, new types of fuzzy controllers for nonlinear systems have been proposed recently, like the one that uses sliding-mode control [31] to give good transient performance and system robustness. Fuzzy logic has also been used in transient stability analysis of power systems with SVC [32] and to design supervisory controllers for power system stabilizers [20]. Fuzzy-controlled UPFC has been demonstrated to enhance transient and dynamic stability and power system damping [18, 19].

Contribution of this Research

Researchers have been showing a growing interest in fuzzy logic to design new controllers because of its ability to effectively implement nonlinear control without much complexity. The INEZ case is one such example where the interactions between nonlinear devices need to be controlled and coordinated. There has been considerable amount of work done to develop new controllers for the UPFC [18, 19] but none of them addresses the problem of control coordination of multiple FACTS devices by means of fuzzy logic. This research has filled this gap since it has achieved the design, development, and testing of a two-level hierarchical fuzzy scheme to control and coordinate the actions of the UPFC, the SVC, and the Automatic Voltage Regulators (AVRs) of the generators in the INEZ region.

To this end, extensive simulation studies were performed to build the knowledge base used to develop the fuzzy rules. Prior to this control, the INEZ system suffered from voltage collapse under heavy loading and double contingency conditions despite the presence of the UPFC and SVC in the system. This could be attributed to the poor coordination of the controllers of these devices. The proposed fuzzy scheme provides a fast, simple and effective scheme to stretch the stability limit of the system for double contingency cases. In some cases, the loadability of the system was increased by about 175 MW while operating under double contingencies. This is a significant increase in the system capacity.

The two-level hierarchy that supervises the SVC and the UPFC facilitates fast availability of reactive power support in the event of major perturbations in the system, thus giving the system a certain amount of robustness against dynamic voltage instabilities. The possible mode interactions between the dynamic loads of the system and these controllers have also been accounted for, and suitable parameter adjustments of the SVC and FACTS controllers have been made via the fuzzy rules to provide effective damping of these oscillations. Finally, investigations have been done for the possible incorporation of pattern recognition into the fuzzy logic scheme to enhance its

performance and effectiveness. This incorporation would add a whole new dimension to the scheme making it applicable to any power network.

Organization of this report

The report is divided into 7 chapters. The first chapter is an introduction and provides the problem statement, state of the art, and contribution of this research. Chapter 2 gives an introduction to the concepts and definitions related to voltage stability problems in power systems. It also gives a concise description of the stability situation in the INEZ system. The third chapter deals with basic operating principles of FACTS devices and provides detailed discussions about the structures, operation, and control of the SVC and the UPFC. Chapter 4 presents a brief introduction to Fuzzy Logic Control (FLC) to show that this powerful and flexible method can be used at different levels of the hierarchical controller to accomplish the desired control. In chapter 5, the details of the modeling of various components of the INEZ power system as implemented in Eurostag have been shown along with screen shots from the computer program Eurostag. The sixth chapter gives the results obtained during the course of this research. Numerous graphs showing the behavior of the system in various conditions have been included to illustrate the analysis. Lastly, Chapter 7 includes the conclusions and proposed future work to further this research.

Chapter 2

Voltage Stability

In recent years, voltage instability has been responsible for many major network collapses throughout the world; hence the growing interest of power engineers and researchers to address this problem. This chapter provides an introduction to the concepts and definitions related to voltage stability problems in power systems. It also gives a concise description of the stability problems of the INEZ system. Observations made from extensive simulations using the software program Eurostag have been included to give a better understanding about the dynamic behavior of this system under various operating conditions and contingencies. Static voltage stability analysis based on the P-V and V-Q curves has also been presented. Let us start this chapter with the definition of the term “Voltage Stability.”

2.1 Definition of basic concepts

According to Carson W. Taylor [1], *“A power system at a given operating state is small-disturbance voltage stable if, following small disturbances, voltages near loads are identical or close to the pre-disturbance values.”* In other words we can say voltage stability is the ability of the system to maintain steady voltages in a pre-decided range (typically 1 p.u. \pm 10 %) after being subject to a disturbance.

The maximum power transfer limit of the network does not necessarily determine the voltage stability limit. There are numerous factors that determine this limit as it can be seen briefly through the course of this chapter.

In general, voltage stability involves disturbances of substantial magnitude. Such disturbances include large increases in loads and loss of heavily loaded lines, which leads

to an increase in the amount of power transfer on other lines. The outcome of voltage instability is usually a progressive and uncontrollable voltage decay, which may lead to a complete voltage collapse (black out). The inability of the network to meet the reactive power demand is one of the major reasons for voltage instability. Voltage instability is most likely to occur in a highly stressed network (such as the INEZ network), leading to a voltage collapse in some of its parts and load shedding in other parts.

2.2 Voltage Instability Problems

Voltage instability is of much concern in a growing number of power systems. This is mainly due to the ever-increasing demand for power in conjunction with the inherent difficulties in building new transmission lines to transport power from remote generation units to load centers, consequently, the existing transmission networks are being operated closer to their stability or capacity limits.

Regarding the INEZ area, it is a coal-mining region characterized by many highly concentrated loads. Over the last few years, the load in this area has increased multifold, where as no new transmission lines were built. The increased load has driven the system to operate close to its stability limits, making it highly vulnerable to voltage collapse in a double contingency case. This will be demonstrated in Figures 2.1, 2.2 and 2.3. These figures display the voltage profile of the INEZ system for no contingency, single contingency, and double contingencies, respectively. Fig. 2.1 shows the INEZ system voltage profile in the no contingency case. As observed in that figure, all the voltages are close to 1 p.u and all the angles are small. Fig. 2.2 depicts the load profile for a single contingency applied on Line 05JOHNSC-05SPRIG1. For that case, the network is mildly stressed since one observes the following:

1. The voltages of the buses to which UPFC, SVC, and capacitor banks are connected, remain very close to 1 p.u. while the voltages of the other buses have dropped significantly and the angles have undergone a large increase.

- The voltages at the nodes located in the vicinity of the fault have dropped more than the other bus voltages.

Note that in all the single contingencies being tested, similar results were obtained.

Fig. 2.3 depicts the voltage profile of the INEZ system for double contingency. As seen, the nodal voltages pinpointed by ovals have dropped from 138 kV to a low value of about 100 kV. On the whole, the network is highly stressed and on the verge of voltage collapse.

2.3 Causes of Voltage Instabilities

In a power system, several disturbances may lead to voltage instability. These disturbances span from a couple of seconds to tens of minutes as depicted in Fig. 2.4. Few of them play a major role or participate significantly in a particular incident or scenario. The system characteristic and the type of disturbance determine their roles.

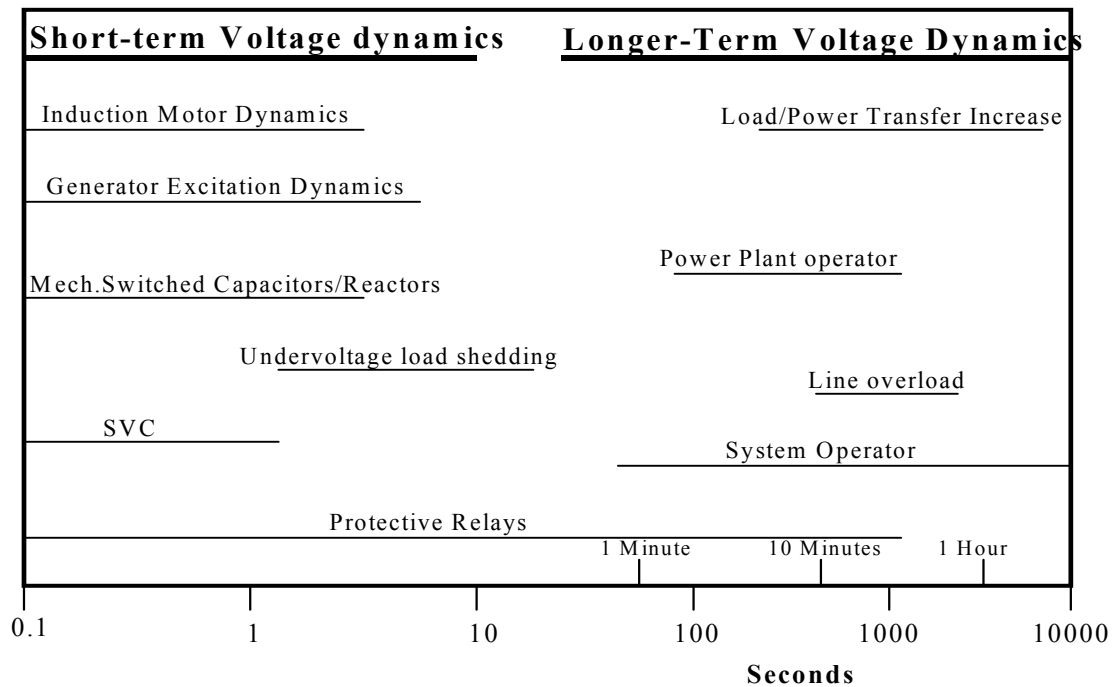


Fig. 2.1. Time duration of disturbances affecting Voltage stability. (Adapted from [1])

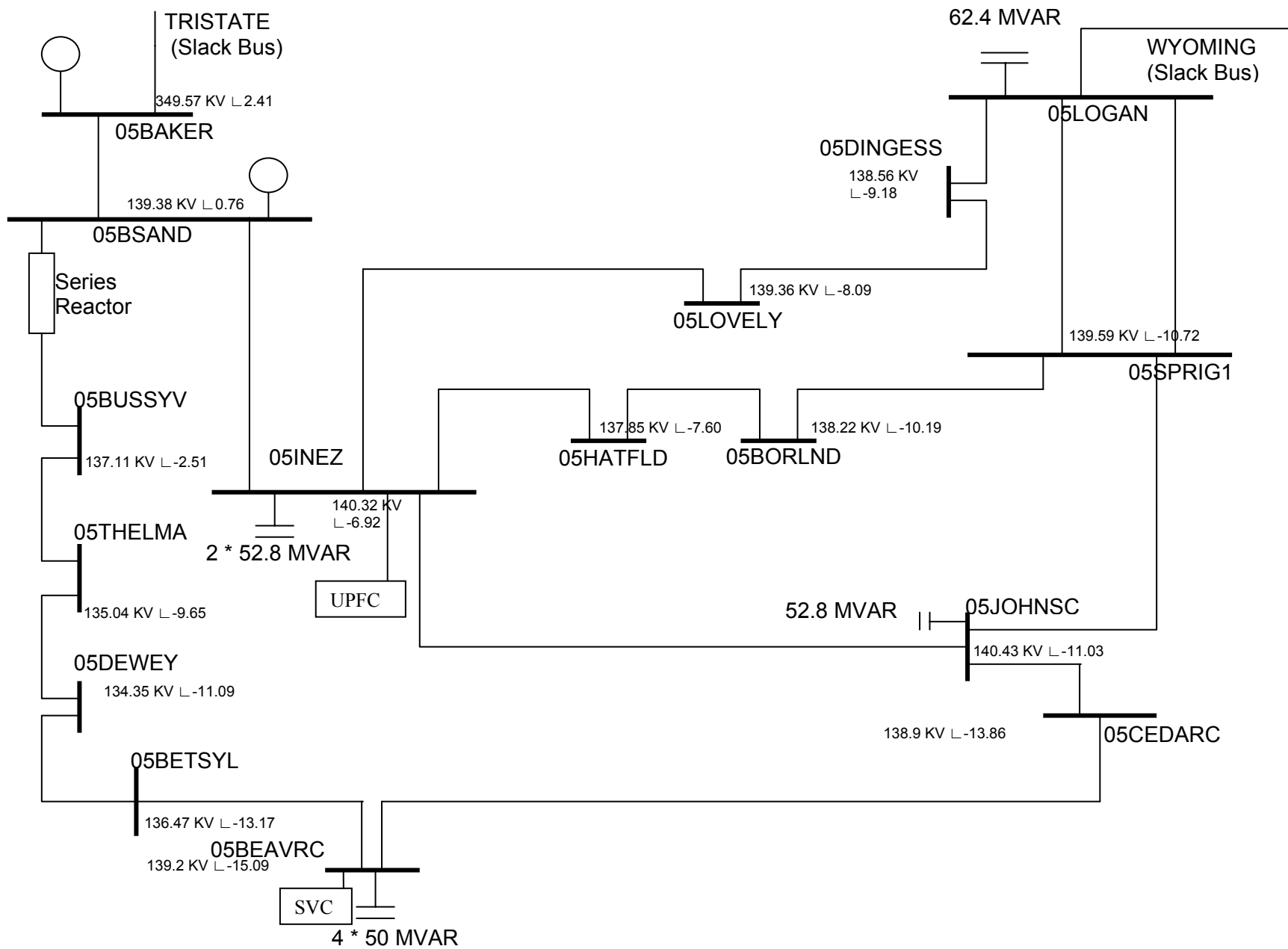


Fig. 2.2. Voltage Profile of the Inez System for no contingencies.

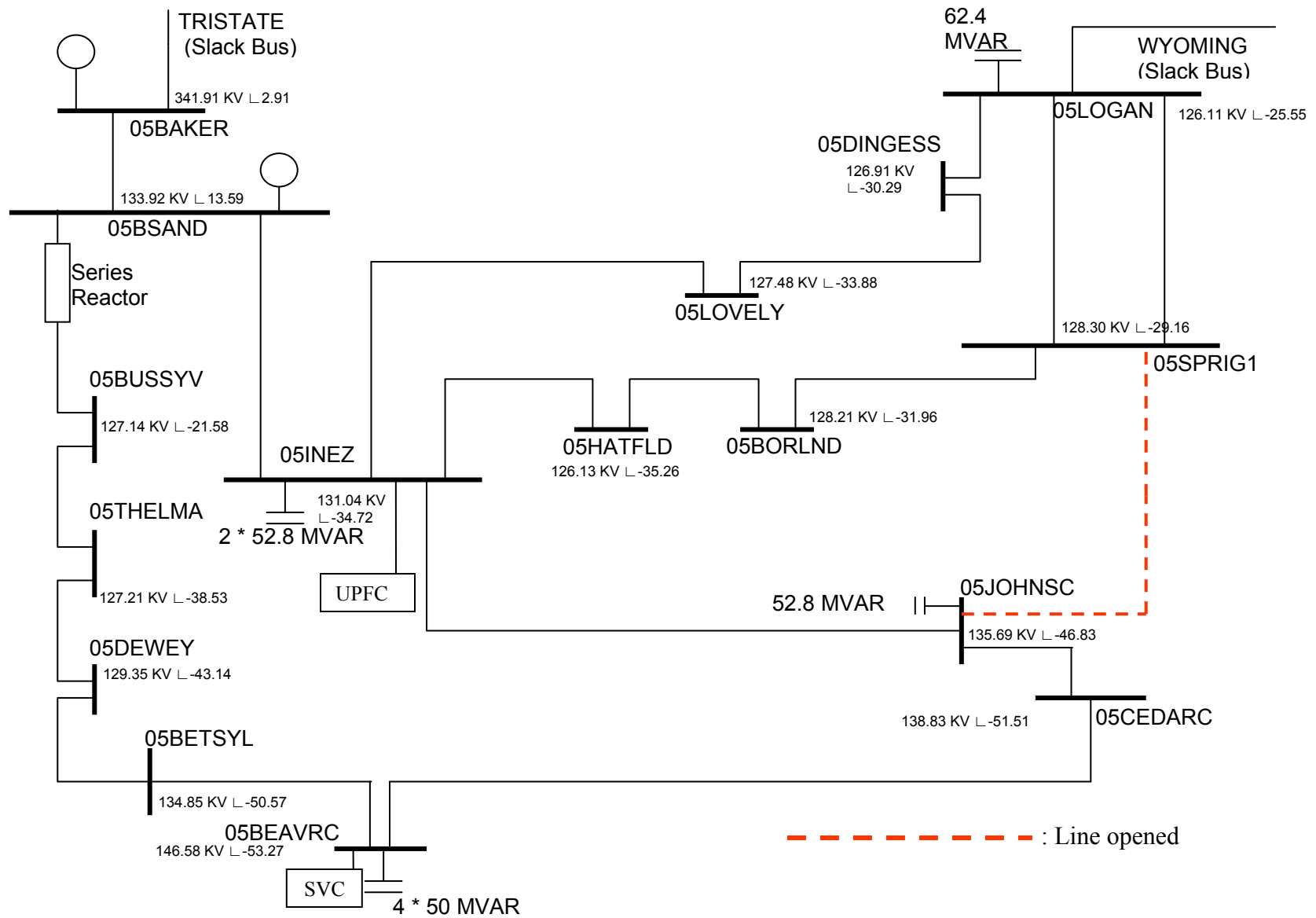


Fig. 2.3. Voltage Profile of the Inez System for single contingency on line 05SPRIG1-05JOHNSC

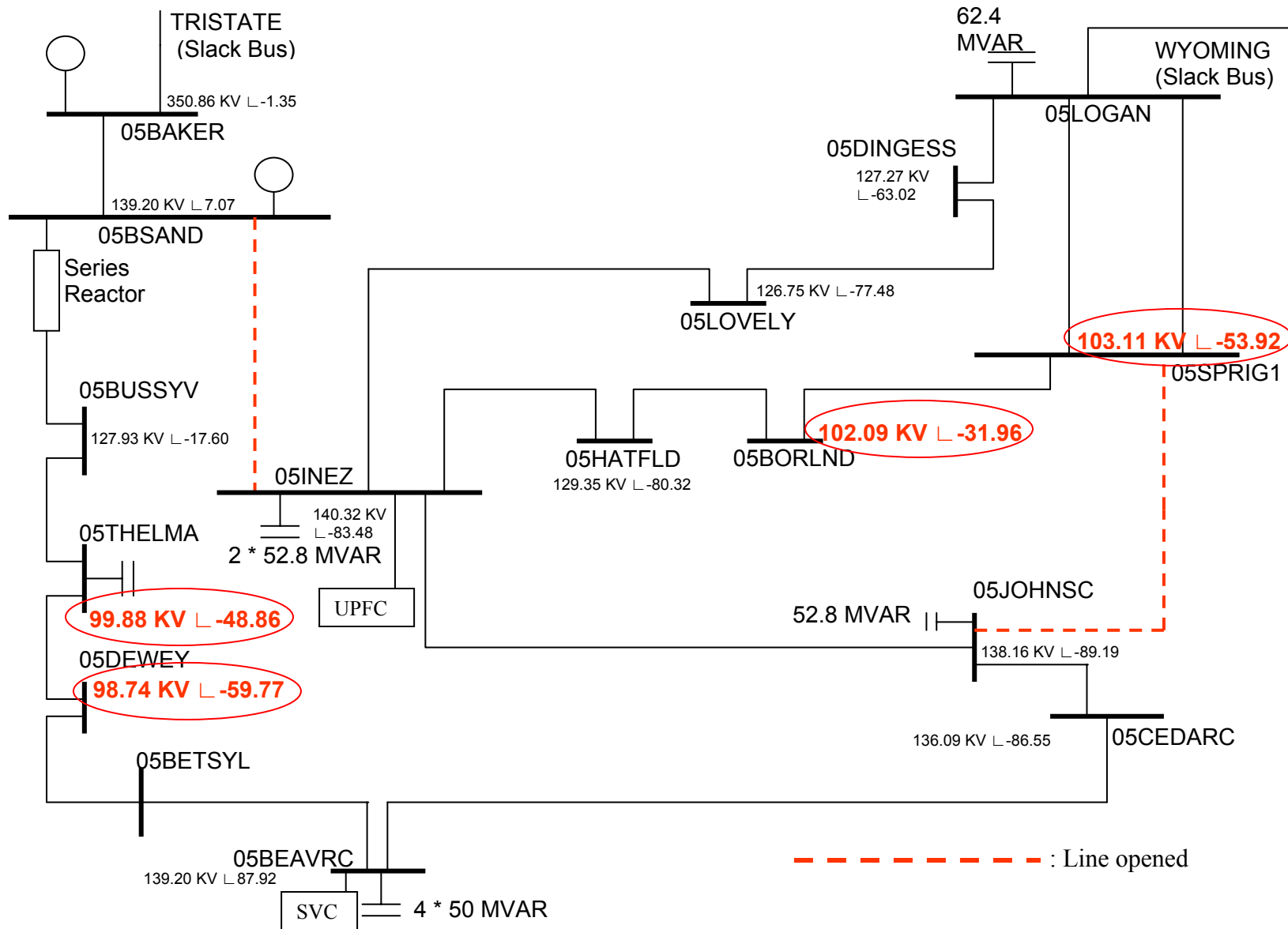


Fig. 2.4. Voltage Profile of the Inez System for double contingency on Line 05SPRIG1-05JOHNSC and Line 05BSAND-05INEZ

Fig 2.4 shows two general classifications of voltage instability phenomena based on time frames of operation, namely: short term or transient voltage instability and long-term voltage stability. Network topology and characteristics, especially electrical disturbances between load and generation centers, have a significant impact on the system's voltage dynamics.

2.3.1 Short-Term / Transient Dynamics

A usual time frame for short-term voltage dynamics is up to ten seconds, approximately. The driving forces of this type of instabilities are the dynamic loads, which tend to restore the consumption of power and the system's power electronic devices, which tend to damp them in a time frame of seconds. Examples of such loads and devices include induction motors, HVDC and FACTS controllers and generator AVRs, to cite a few. Events falling under this short-term dynamics include induction motor stalling, oscillation of generators, and spikes due to switching on and off of devices.

2.3.2 Longer-Term Voltage Dynamics

After the system sustains the disturbances causing short-term instability, other phenomena come into play. The latter operate in a time frame of a few minutes to a few tens of minutes. Some examples of such events can be seen in Fig.2-4. Few other examples in this category are frequency problems resulting from generation-load imbalance irrespective of the network.

2.4 Analysis of Voltage Stability

This section provides an analysis of the stability of the INEZ network.

2.4.1 P-V Curves

The relationships between the active power transmitted, the receiving end voltages, and the reactive power injected are important when studying the characteristics of transmission systems. Fig 2.5 gives the family of normalized P-V curves for an elementary radial network. The voltage and power is plotted for various values of power factor with the sending side voltage kept constant.

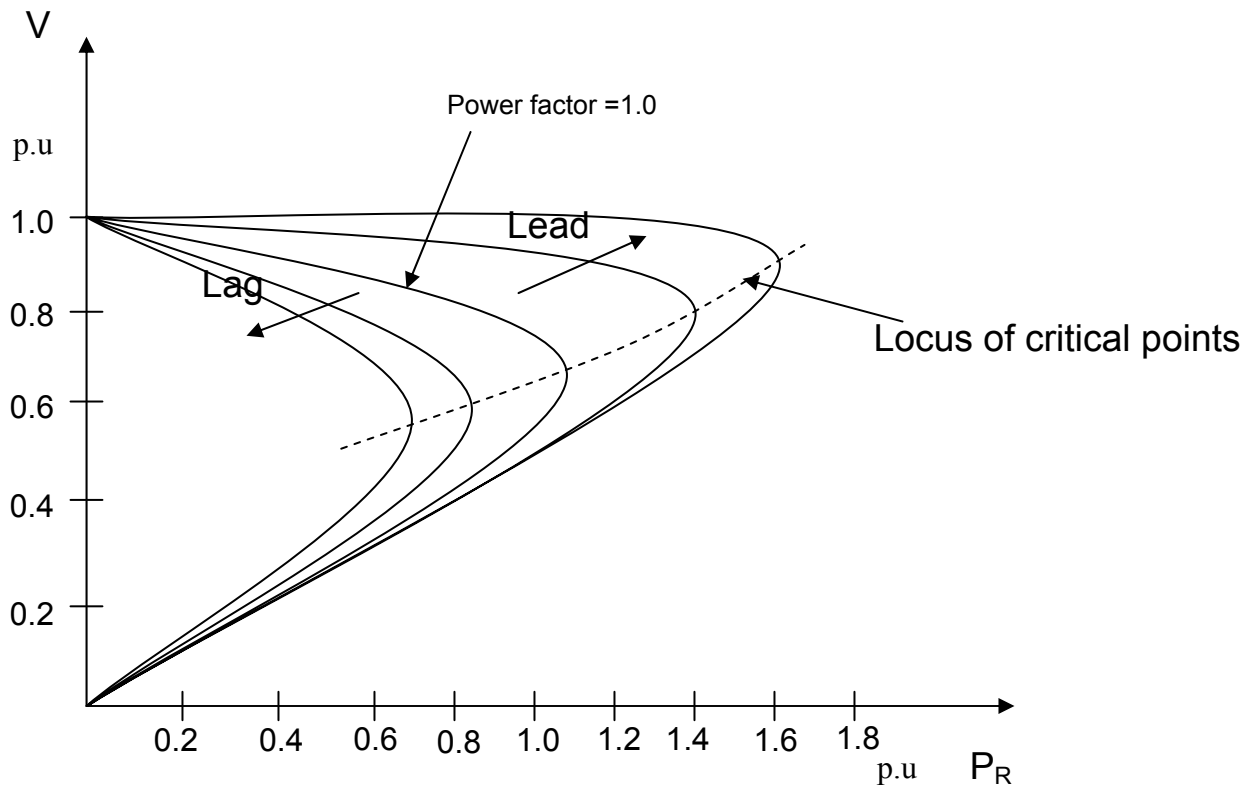


Fig. 2.5. Normalized P-V curves for a fixed source and reactance network.

The dashed line in Fig. 2.5 shows the locus of points of voltage collapse, referred to as the critical points or saddle node bifurcation points. These points determine the steady-state loadability limits of the system for voltage stability of the network. Only the equilibrium points above the critical points represent stable operating conditions. The loci below the dashed line are that of unstable equilibrium points.

When used to study a large meshed network, P represents the total load in an area, and V represents the voltage at a critical bus or the bus under consideration. Voltages at several buses can be plotted versus P to understand the effect of load on each of them. The curves in Figure 2-6 represent the voltages at few buses of the INEZ system, which were chosen based on their response to changes in load. They are associated with the operation of the network for different loading conditions.

The curves were plotted by carrying out numerous load flow calculations on the INEZ system using the software program Eurostag. The load in the area was increased gradually while keeping the power factor constant. As seen in Fig.2.6, beyond the load of around 1000 MW, the voltage dropped rapidly below the accepted range of $\pm 10\%$, and beyond a load of 1100MW, the load flow program no longer converged. This is the steady-state voltage stability limit of the network. However, the maximum power transferred through the network can be increased with shunt compensation. One of the challenges for this research was to increase the loadability of the system using the coordinated action of the UPFC, the SVC, and the capacitor banks as will be shown in Chapter 5.

2.5 Reactive Power Compensation and Control

One of the most effective ways to improve the power transfer capability and voltage stability of a system is reactive power compensation. There exist two classes of compensation methods. The first class is based on the connection type, namely series and shunt compensation, while the second class is based on the operation, namely, active and passive compensation. In active compensation, the voltage and other variables are controlled by a feedback control loops. Some common forms of reactive power compensation are series capacitors, shunt capacitor banks, series reactors, and static var compensators, to cite a few.

2.5.1 Reactive Power Transmission

As already discussed, one major aspect of voltage stability is the capability of a system to transfer reactive power from sources to sinks under steady operating conditions. Reactive power transmission is mainly dependent on the difference in nodal voltage magnitudes across the network. It flows from a higher to a lower voltage value. This is similar to heat transfer from an object at a higher temperature to a body at a lower temperature. Note that transmission of reactive power across large nodal voltage angles, even with substantial voltage magnitude gradients, may be difficult to achieve.

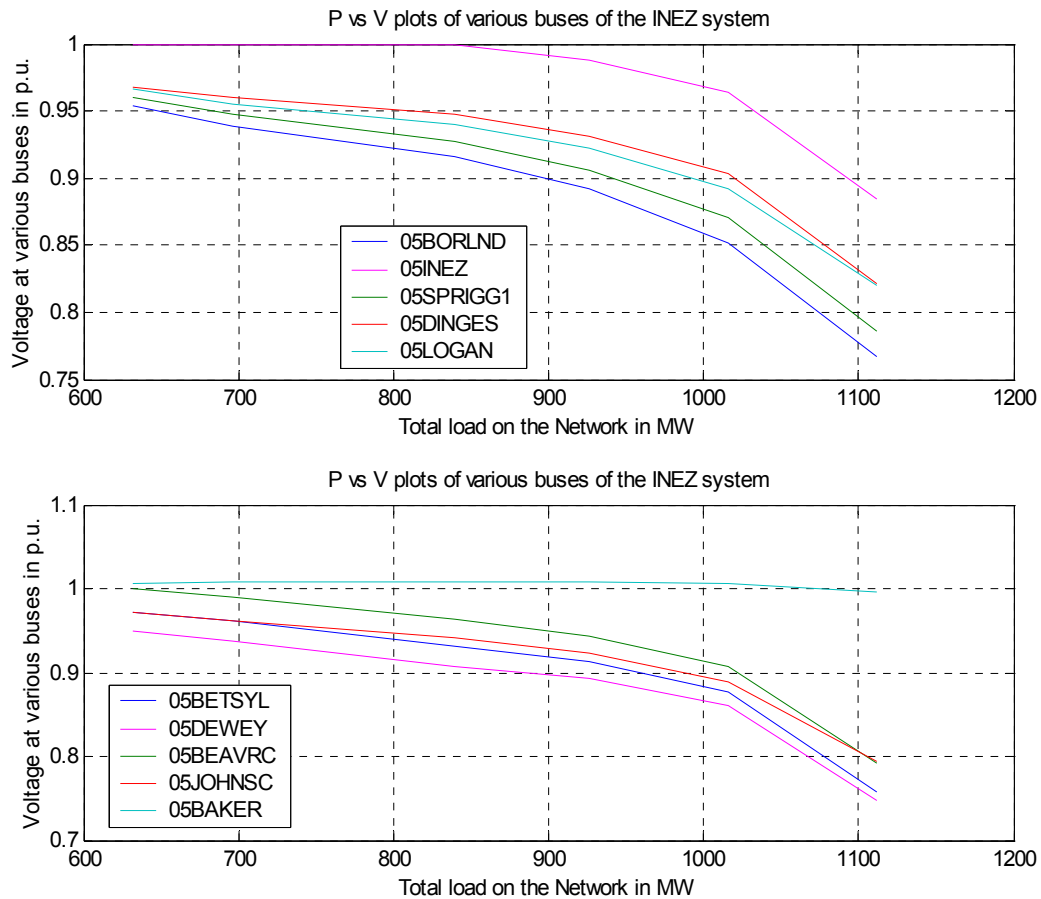


Fig. 2.6. Plots of active load (P) vs. voltage (V) at various buses of the INEZ system.

Some of the reasons for minimizing transfer of reactive power through the network include the following:

- a. To minimize the real and reactive losses for economic considerations. This can be illustrated by the following simple set of equations [2]:

$$I^2 = \bar{I} \bar{I}^* = \left[\frac{P - jQ}{\bar{V}^*} \right] \left[\frac{P + jQ}{\bar{V}} \right] = \frac{P^2 + Q^2}{V^2} \quad (2.1)$$

$$P_{loss} = I^2 R = \frac{P^2 + Q^2}{V^2} R \quad (2.2)$$

$$Q_{loss} = I^2 X = \frac{P^2 + Q^2}{V^2} X \quad (2.3)$$

Note that the real and reactive losses across the series impedance of the transmission line are given by $I^2 R$ and $I^2 X$, respectively. Observing the above equations we can see that the losses are minimized when the reactive power transfer is low and the bus voltages are high;

- b. To minimize the temporary over-voltage and hence, achieve a faster recovery, the reactive power transfer mainly determines the magnitude of the over-voltage.;
- c. Handling large amounts of reactive power consumed by the load requires equipment of larger size and rating, which leads to a higher cost of installation and operation.

We have seen that transmission of reactive power over long distances is not economically viable as it results in a prohibitive amount of losses. Hence, reactive power generation must be as close to the point of consumption as possible. The INEZ system has capacitor banks that are distributed over the entire system, with concentrated sources of reactive power at two buses, namely 05INEZ and 05BEAVRC. In addition to the

capacitor banks, the system has a UPFC and SVC, making the total reactive power rating of these buses as high as 425.6 MVAR at 05INEZ and 325 MVAR at 05BEAVRC.

2.5.2 Shunt Capacitor Banks

Shunt capacitor banks are one of the most inexpensive methods of reactive power compensation aimed at providing voltage support to the transmission system. They are usually connected to the buses rather than to the lines, with the primary purposes being voltage control and load stabilization. By correcting the receiving end power factor, these banks can be used up to a certain limit to effectively increase the voltage stability limits of the system and help in preventing voltage collapse in many situations.

Shunt capacitor banks are often switched manually with voltage relay backups operating when the voltage goes out-of-range. Shunt capacitor banks are very useful in facilitating the operation of the generators near unity power factor, hence maximizing the fast acting reactive reserve and thereby improving voltage stability. The INEZ system has in all 10 capacitor banks to give a total shunt compensation of 526.4 MVAR distributed all over the network and providing reactive power support.

Mechanically-switched shunt capacitor banks have the advantage of much lower costs compared to the other methods of compensation like static var systems. However, they have a number of disadvantages and limitations from the voltage stability and control viewpoint. For example, unlike SVCs, they do not provide precise and rapid voltage control of the system. Also in systems heavily compensated by shunt capacitors, voltage regulation tends to be poor and stable operation is not possible beyond a certain level of compensation. The most important shortcoming of shunt capacitor banks is their inability to provide fast compensation under voltage contingencies. The reactive power output of these banks is proportional to the square of the voltage; consequently, in conditions where the voltage is dropping, the var support also drops, thus not serving its primary purpose. For transient voltage instability, the capacitor banks are not fast enough to prevent induction motor stalling.

2.5.3 Static Var Compensators

Static Var Compensators regulate the voltage up to their maximum capacitive limit and overcome the shortcomings of capacitor banks. These systems experience no voltage control or instability problems as long as they operate within their rated regulating range. Advantages of these systems are precise, fast voltage regulation, and transient free capacitor bank switching.

Static Var Compensators (SVCs) are more effective in preventing transient voltage oscillations in areas with concentrated motor loads, as in the case of the INEZ system, when compared to shunt capacitors. The SVCs performance is critical in cases of low voltage where the shunt capacitor's output is lower than their rating. The modeling, construction, and operation of the SVC will be discussed in detail later in Chapter 3. At present, it would be enough to know that the SVCs perform better than the capacitor banks in most of the situations.

2.6 Chapter Summary

This chapter gives an insight into the different aspects of voltage stability and the basic concepts associated with it. The behavior of the INEZ system to different levels of loading has been presented in the form of P-V curves plotted for various buses. We have seen that voltage stability and collapse is a dynamic phenomenon of large magnitude. Various methods aimed at increasing the voltage stability limit of the power system with reactive power compensation were also presented.

Chapter 3

UPFC and SVC Modeling and Control

Power electronic devices have had a revolutionary impact on the electric power systems around the world. The availability and application of thyristors has resulted in a new breed of thyristor-based fast operating devices devised for control and switching operations. Flexible AC Transmission System (FACTS) devices are new comings, which have found a wide spread application in the power industry for active and reactive power control. This chapter deals with basic operating principles of FACTS devices and provides detailed discussions about the structures, operation, and control of the SVC and the UPFC.

3.1 Flexible AC Transmission System (FACTS)

Devised by Hingorani [7], FACTS devices are based on power electronic controllers that enhance the capacity of the transmission lines. These controllers are fast and increase the stability operating limits of the transmission systems when their controllers are properly tuned. These devices provide control of the power system through appropriate compensation of network parameters, such as line series impedance, line shunt impedance, current, voltage, and real and reactive power. They help the operation of the power network closer to its thermal limits. The FACTS technology encompasses a combination of various controllers, each of which can be applied individually or in a co-ordination with other devices to control the interrelated parameters of the system as mentioned above.

3.2 Types of FACTS controllers

FACTS controllers can be broadly divided into four categories, which include series controllers, shunt controllers, combined series-series controllers, and combined series-shunt controllers. Their operation and usage are described next.

3.2.1 Principles of the Series Controllers

A series controller may be regarded as a variable reactive or capacitive impedance whose value is adjusted to damp various oscillations that can take place in the system. This is achieved by injecting an appropriate voltage phasor in series with the line; this voltage phasor can be viewed as the voltage across an impedance in series with the line. If the line voltage is in phase quadrature with the line current, the series controller absorbs or produces reactive power, while if it is not, the controllers absorbs or produces real and reactive power. Examples of such controllers are Static Synchronous Series Compensator (SSSC), Thyristor-Switched Series Capacitor (TSSC), Thyristor-Controlled Series Reactor (TCSR), to cite a few. They can be effectively used to control current and power flow in the system and to damp system's oscillations.

3.2.2 Principles of the Shunt Controllers

Shunt controllers are similar to the series controllers with the difference being that they inject current into the system at the point where they are connected. A variable shunt impedance connected to a line causes a variable current flow by injecting a current into the system. If the injected current is in phase quadrature with the line voltage, the controller adjusts reactive power while if the current is not in phase quadrature, the controller adjusts real power. Examples of such systems are Static Synchronous Generator (SSG), Static Var Compensator (SVC). They can be used as a good way to control the voltage in and around the point of connection by injecting active or reactive current into the system.

3.2.3 Principles of the Combined Series-Series Controllers

A combined series-series controller may have two configurations. One configuration consists of series controllers operating in a coordinated manner in a multilane transmission system. The other configuration provides independent reactive power control for each line of a multilane transmission system and, at the same time, facilitates real power transfer through the power link. An example of this type of controller is the Interline Power Flow Controller (IPFC), which helps in balancing both the real and reactive power flows on the lines.

3.2.4 Principles of Combined Series-Shunt Controllers

A combined series-shunt controller may have two configurations, one being two separate series and shunt controllers that operate in a coordinated manner and the other one being an interconnected series and shunt components. In each configuration, the shunt component injects a current into the system while the series component injects a series voltage. When these two elements are unified, a real power can be exchanged between them via the power link. Examples of such controllers are UPFC and Thyristor-Controlled Phase-Shifting Transformer (TCPST). These make use of the advantages of both series and shunt controllers and, hence, facilitate effective and independent power/current flow and line voltage control.

3.3 Principles of the Static Var Compensators (SVCs)

The IEEE definition of the SVC [7] is as follows: “*A shunt connected static var generator or absorber whose output is adjusted to exchange capacitive or inductive current so as to maintain or control specific parameters of the electrical power system (typically bus voltage).*”

In other words, an SVC is a static var generator whose output is varied in order to maintain or control the specific parameters of an electric power system. SVCs are primarily used in power systems for voltage control or for improving system stability. This section presents a detailed overview of the principles and design of an SVC.

3.3.1 V-I characteristics of an SVC

As shown in Fig 3.1., the dynamic characteristics of an SVC are the plots of bus voltages versus current or reactive power. In Fig 3.1., the voltage V_{ref} is the voltage at the terminals of the SVC when it is neither absorbing nor generating any reactive power. The reference voltage value can be varied between the maximum and minimum limits, $V_{ref\ max}$ and $V_{ref\ min}$, using the SVC control system. The linear range of the SVC control passing through V_{ref} is the control range over which the voltage varies linearly with the current or reactive power. In this range, the power is varied from capacitive to inductive.

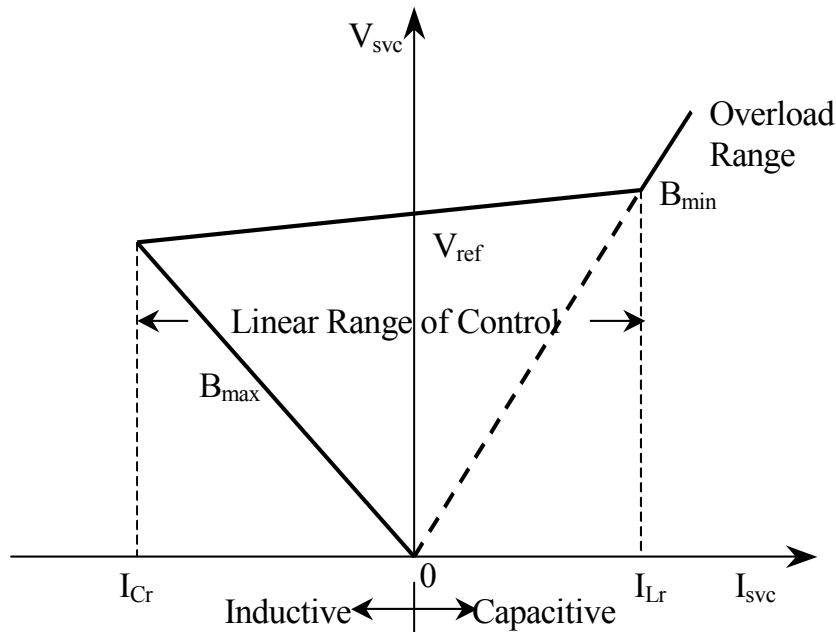


Fig. 3.1. Voltage – Current Characteristics of the SVC

The slope or droop of the V-I characteristic is the ratio of change in voltage magnitude to the change in current magnitude over the linear control range. This slope is given by

$$K_{sl} = \frac{\Delta V}{\Delta I} \Omega, \quad (3.1)$$

where ΔV denotes the change in voltage magnitude (V) and ΔI denotes the change in current magnitude (I).

The slope K_{sl} can be changed by the control system. Ideally, for voltage regulation it is required to maintain a flat voltage profile with a slope equal to zero. In practice, it is desirable to incorporate a finite slope of about 3-5% for the following reasons:

1. It reduces the reactive power rating of the SVC substantially for achieving similar control objectives;
2. It prevents the SVC from reaching its reactive-power limits too frequently;
3. It facilitates the sharing of reactive power among multiple compensators connected or operating in parallel.

Once the SVC's operating point crosses the linear controllable range, it enters the overload zone where it behaves like a fixed inductor or capacitor.

3.3.2 Prevention of Voltage Instability with the SVC

Voltage instability as discussed in the previous chapter is caused by the inability of the power system to meet the reactive power demand of the load. When the latter consists of induction motors, a drop in the bus voltage results in increased demand for reactive power and if the system cannot meet this demand, there will be a further decay in the voltage. This process may continue until a voltage collapse occurs. The voltage at a load bus is dependent on the magnitude of the load, the power factor, and the impedance of the line. For a given power factor, there exists a maximum power that can be transferred to the load and beyond which a voltage collapse inevitably occurs. In such a

case, appropriate control of the combined power factor of the load and that of the SVC could help preclude a too fast drop in the bus voltages as the load power increases and thereby, push further the point of voltage collapse. It also helps increase the damping capability of the system should a perturbation occurs.

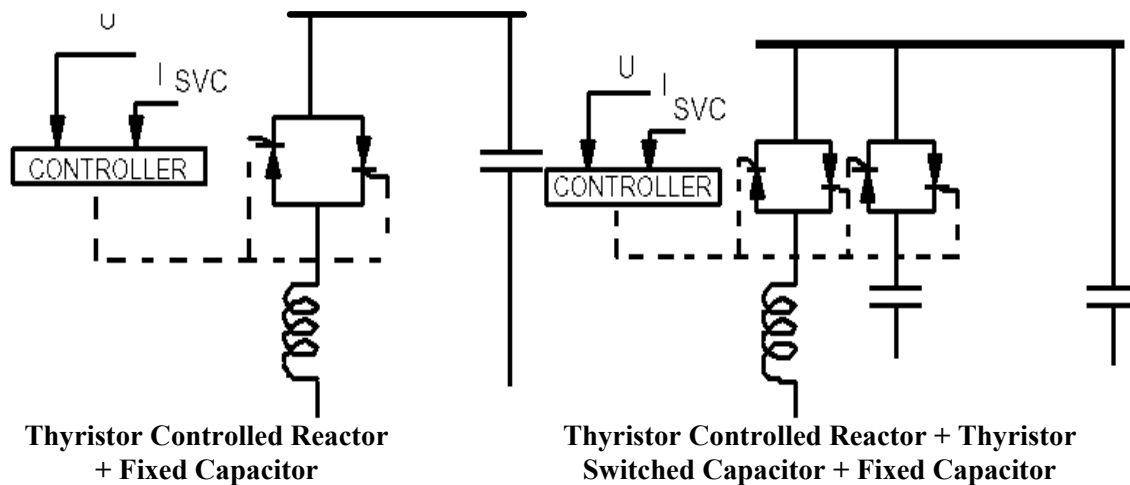


Fig. 3.2. Block Diagrams of SVC [8].

3.3.3 Modeling of SVC in Eurostag

In Eurostag, an SVC is modeled as a current injector at the bus to which it is connected. The Eurostag standard library utilizes the model described by Fig. 3.2. The generalized block diagram of the model used is depicted in Fig. 3.3

Eurostag assumes that one or several TSCs of equivalent rating are used to provide smoothing effect to the step-wise variation of the capacitor banks. This facilitates a vernier control of the reactive power generation. Based on the description made by CIGRE, the model allows us to implement functions such as current and voltage measurement, regulator, blocking in case of low voltage conditions, and delay in the thyristors firing instants and smoothing of the control signal.



Fig. 3.3. Generalized Block diagram of SVC [8].

a. Current and Voltage Measurement

The voltage of the bus to which the SVC is connected is measured and smoothed with a time constant. The current generated by the SVC is computed from the voltage and the admittance of the SVC. This current is multiplied by the slope of the V-I characteristics and smoothed with a time constant.

b. Regulator

The regulator includes a lead-lag function given by

$$F(s) = \frac{K(1 + sT1)}{(1 + sT2)}, \quad (3.2)$$

a variable gain, which helps to test the dynamic behavior of the system during the simulation, and a PID regulator.

c. Overvoltage Delay

A short circuit in the system causes the reactive power required by the controller to reach its maximum, which may lead to over-voltages on fault clearance. This model includes a protection loop that decreases the reactive power demand when the voltage value increases beyond a certain threshold value.

d. Smoothing and Firing Delay

The output of the regulator is smoothed and delayed with a real-time average value of 5ms. Before initiating control of the susceptance of the SVC, the amplitude of the signal is limited. There is a linear function between the control signal and the susceptance of the SVC.

3.4 Unified Power Flow Controller (UPFC)

The UPFC is the most versatile FACTS controller with capabilities of voltage regulation, series compensation, and phase shifting. The UPFC is a member of the family of compensators and power flow controllers. The latter utilize the synchronous voltage source (SVS) concept to provide a unique comprehensive capability of transmission system control [9]. The UPFC is able to control simultaneously or selectively all the parameters affecting power flow patterns in a transmission network, including voltage magnitudes and phases, and real and reactive powers. These basic capabilities make the UPFC the most powerful device in the present day transmission and control systems.

3.4.1 Basic Operating Principles

As illustrated in Fig 3.4, the UPFC is a generalized SVS represented at the fundamental frequency by controllable voltage phasor of magnitude V_{pq} and angle injected in series with the transmission line. Note that the angle ρ can be controlled over the full range from 0 to 2π . For the system shown in Fig 3.4, the SVS exchanges both real and reactive power with the transmission system. In the UPFC, the real power supplied to or absorbed from the system is provided by one of the end buses to which it is connected. This meets the objective of the UPFC to control power flow rather than increasing the generation capacity of the system.

As shown in Fig 3.5, the UPFC consists of two voltage-sourced converters, one in series and one in shunt, both using Gate Turn-Off (GTO) thyristor valves and operated from a common dc storage capacitor. This configuration facilitates free flow of real power between the ac terminals of the two converters in either direction while enabling each converter to independently generate or absorb reactive power at its own ac terminal. The series converter, referred to as Converter 2, injects a voltage with controllable magnitude V_{pq} and phase ρ in series with the line via an insertion transformer, thereby providing the main function of the UPFC. This injected voltage phasor acts as a synchronous ac voltage source that provides real and reactive power exchange between

the line and the ac systems. The reactive power exchanged at the terminal of series insertion transformer is generated internally while the real power exchanged is converted into dc power and appears on the dc link as a positive or negative real power demand.

By contrast, the shunt converter, referred to as Converter 1, supplies or absorbs the real power demanded by Converter 2 on the common dc link and supports the real power exchange resulting from the series voltage injection. It converts the dc power demand of Converter 2 into ac and couples it to the transmission line via a shunt-connected transformer. Converter 1 can also generate or absorb reactive power in addition to catering to the real power needs of Converter 2; consequently, it provides independent shunt reactive compensation for the line. It is to be noted that the reactive power exchanged is generated locally and hence, does not have to be transmitted by the line. On the other hand, there exists a closed path for the real power exchanged by the series voltage that is injected through the converters back to the line.

Thus, there can be a reactive power exchange between Converter 1 and the line by controlled or unity power factor operation. This exchange is independent of the reactive power exchanged by Converter 2.

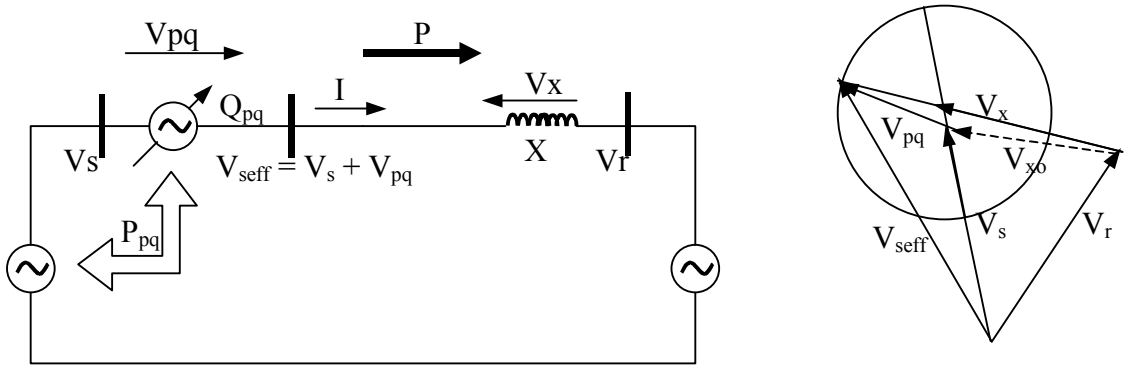


Fig. 3.4. Representation of the UPFC in a two-machine power system.

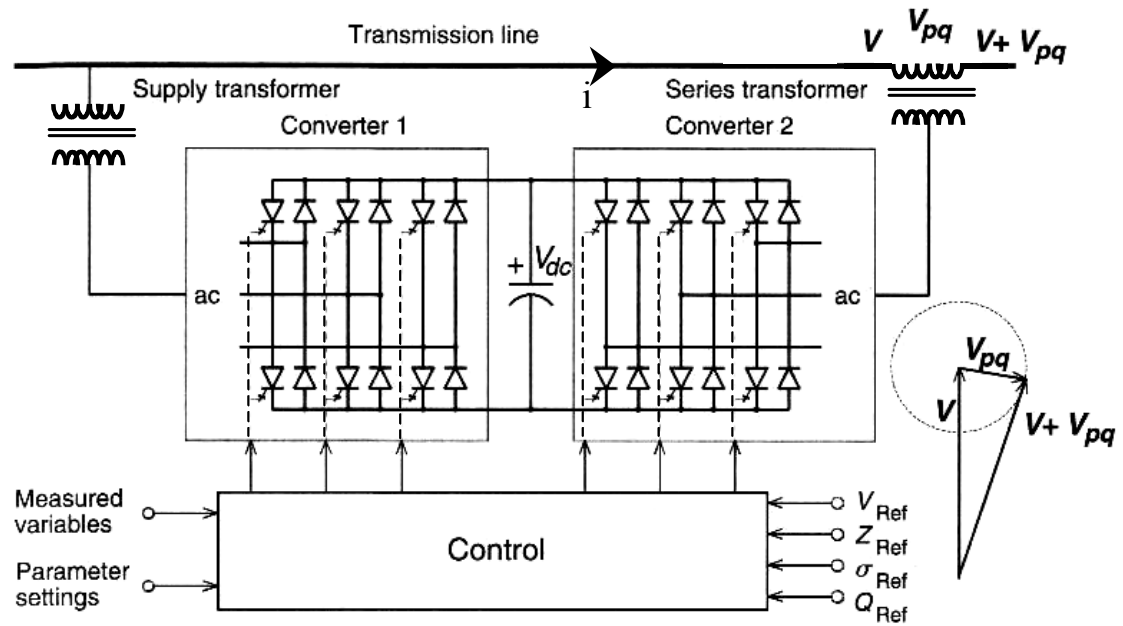


Fig. 3.5. UPFC implemented by two back-to-back voltage source converters.

3.4.2 Transmission Control Capabilities

The UPFC can fulfill the functions of reactive shunt compensation, series compensation, and phase angle regulation. Hence it can meet multiple control objectives by injecting a voltage phasor with appropriate amplitude and phase angle to the terminal voltage. The basic UPFC power flow control functions are

- Voltage regulation with continuously variable in-phase/out of phase voltage injection;
- Line-impedance compensation or series reactive compensation by the series injected voltage. This injected voltage phasor can be kept constant over a broad range of the line current while the voltage across the compensating impedance varies with the line current;
- Phase-shifting control that is achieved by injecting a voltage phasor with any particular angular relation with the terminal voltage. In other words the desired phase shift can be obtained without any change in the voltage magnitude;

- Simultaneous multifunction power flow control by an adequate adjustment of the terminal voltage, series impedance compensation, and phase shifting. This functional capability is unique to the UPFC; no other single conventional equipment has similar multifunction capability.

3.4.3 Control and Dynamic Performance

The ability of the UPFC to rapidly inject an ac-compensating voltage phasor with variable magnitude and angle in series with the line when needed, bestow it with superior operating characteristics. When equipped with suitable electronic controllers, the UPFC can not only establish an operating point within a wide range of possible P and Q flows on the line, but can also rapidly displace that operating point to another position.

a. Control of the Shunt Converter

The shunt converter draws a controlled current phasor from the line, the real part of which is determined by the real power requirement of the series converter while the reactive part can be set to any desired level within the converter's capability.

The shunt part of the UPFC has two modes of operation. The first operating mode achieves reactive power control. Here, the reference input is an inductive or capacitive Var request. This request is translated into a corresponding shunt current request by the shunt converter, which adjusts the gating of the converters to establish the desired current. The second operating mode achieves automatic voltage control. Here, the shunt converter reactive current is automatically regulated to maintain the transmission line voltage at the point of connection.

b. Control of the Series Converter

The series converter provides control over the angle of the voltage phasor injected in series with the line. Dependent on the operation mode of the UPFC, the voltage injected controls the power flow on the line. This converter has four operating modes, which are the direct voltage injection mode, the line impedance compensation mode, the phase

angle shifter mode and the automatic power flow control mode. They will be described next.

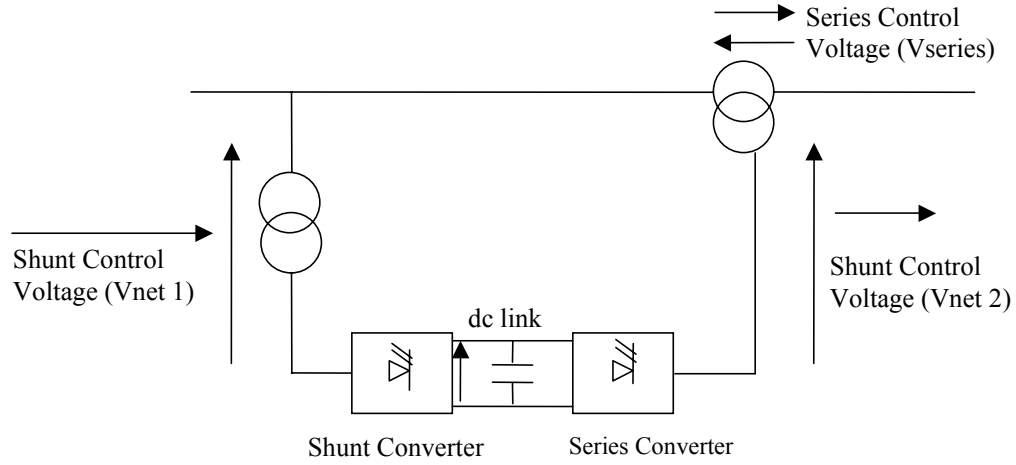


Fig. 3.6 Principle UPFC control scheme.

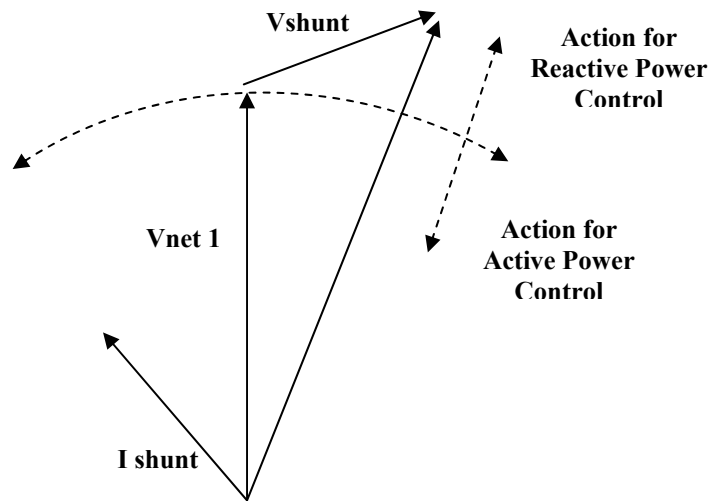


Fig. 3.7. Principle of operation of the shunt part of the UPFC.

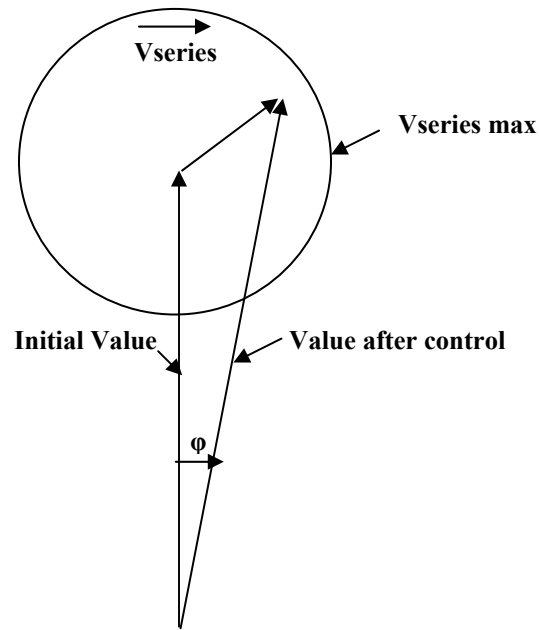


Fig. 3.8. Principle of operation of the series part of the UPFC [8].

In the direct voltage injection mode, the voltage is generated with the magnitude and phase as required by the reference input. One such example is the operation to purely supply reactive power to the system. In the line impedance compensation mode, the magnitude of the injected voltage is controlled according to the magnitude of the line current in such a way that the series injection emulates a reactive impedance when viewed from the line. When the UPFC is operating in the phase angle shifter mode, the injected voltage is controlled with respect to the reference input so that the output bus voltage phasor is shifted by a certain angle. Lastly, when the UPFC is in the automatic power flow control mode, the magnitude and angle of the injected voltage phasor is controlled so as to adjust the line current to achieve the required real or reactive power flow.

3.4.4 Modeling of UPFC in Eurostag

The model is implemented such that the series action is represented by a voltage source inserted in series across the line and the shunt action is represented by a current source injected in parallel. The constraints due to the size of the converters, the dc-voltage source, and the transformer, limit (i) the phase-shift angle and amplitude of the

voltage inserted by the shunt part and (ii) the current inserted by the series the part. Fig 3.9 gives the UPFC's dynamic model as implemented in Eurostag. The p-axis is in phase with voltage V_{net1} and the q-axis leads the p-axis by 90° .

a. Modeling principle of the series part

In Eurostag, the UPFC is modeled as a combination of 2 current injectors to obtain the required operation. For the series-voltage control, the line at which the UPFC is located is opened and two current injectors are placed in both ends to adjust their voltages.

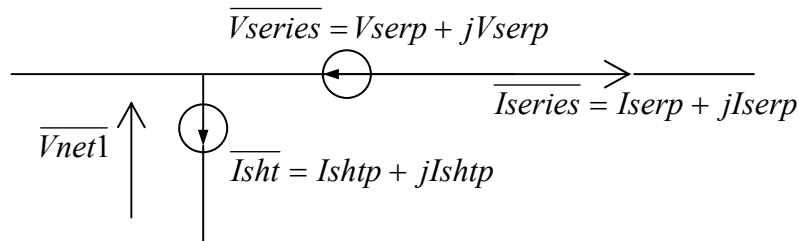


Fig. 3.9. Dynamic model of UPFC in Eurostag [8].

b. Control of the series part

The control of the active flows is obtained via the phase shift while the control of the reactive flow is achieved via the variation of the voltage amplitudes at the terminals. Fig. 3.10 illustrates the block diagram of the control of the series part. This control is implemented using the Macroblocks available in Eurostag. The series part has been provided with two types of protection, which are

- i. a current by-pass protection that brings the series voltage to zero in case the line is opened;
- ii. a hysteresis-type undervoltage protection that brings the series voltage to zero if the value of the injected voltage goes below a threshold value;

c. Modeling principle of the shunt part

The function of the shunt part is to maintain the voltage through a reactive power injection into the network and to supply the active power required by the series part. The shunt part is modeled as a current injector whose components are adequately controlled. Fig. 3.11 gives the shunt part model as used in Eurostag.

d. Control of the shunt part

The control of the shunt part consists of two loops. One of these loops is the fast control of the dc-voltage at the capacitor terminals between the two converters. It has the fastest response and outputs the active current absorbed by the shunt part. The second loop provides a voltage control, outputting the reactive current to be supplied by the shunt part. The latter comprises of an integral-type control of the voltage generated by the shunt converter. The calculation of the active current supplied by this shunt part is done such that the total active power generated by the shunt part almost instantly matches that used by the series part. In addition, the shunt part has an undervoltage protection which brings the reactive power to zero when the threshold is exceeded. The shunt part's active current is given a certain priority to ensure that the capacitor voltage is being controlled more than the reactive power exchange.

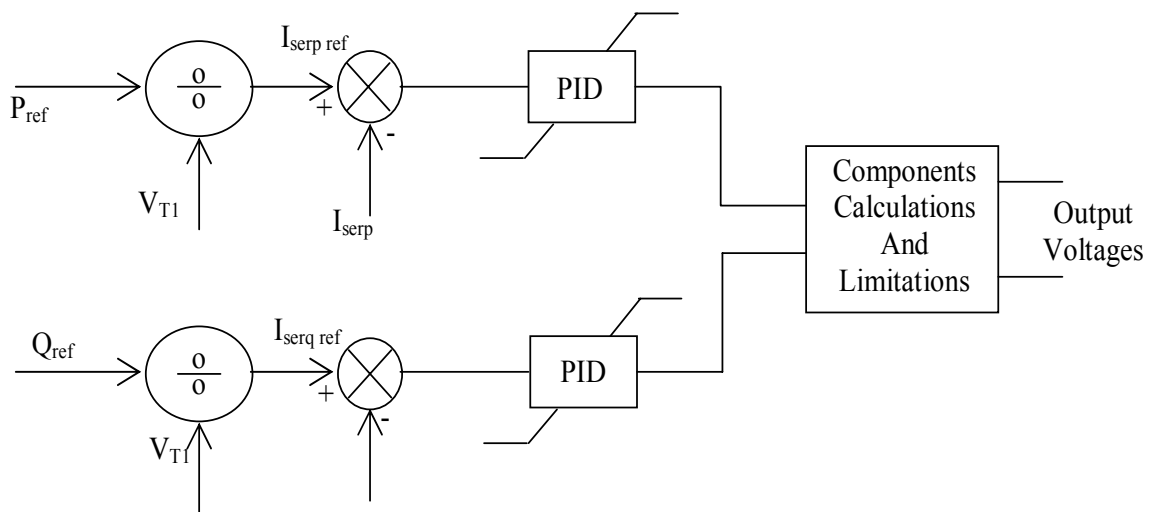


Fig. 3.10. Control of the series part [Taken from 8].

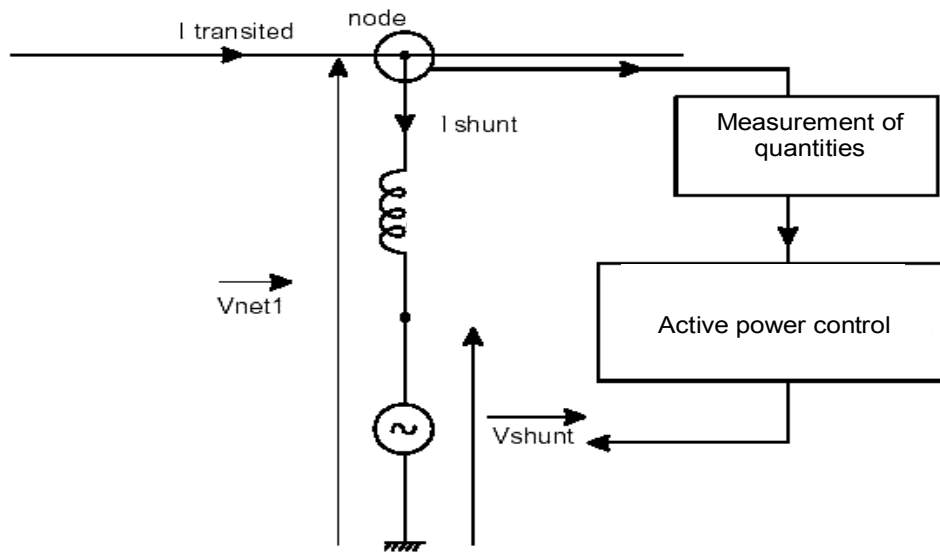


Fig. 3.11. Model of Shunt part used in Eurostag (Taken from [8]).

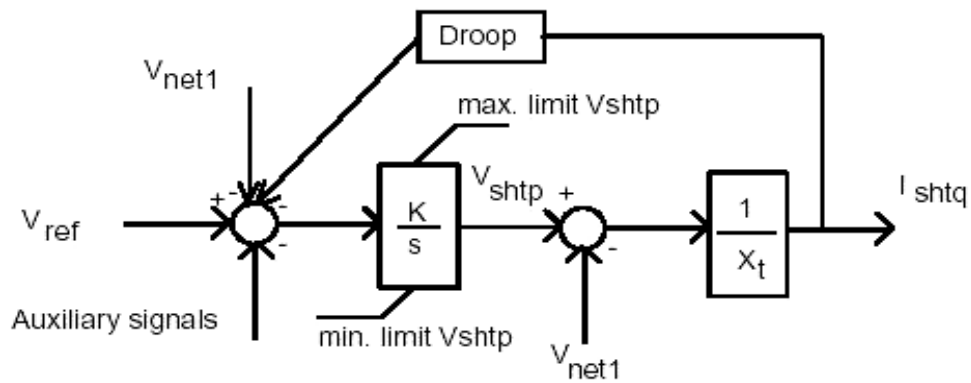


Fig. 3.12. Shunt part Control [Taken from 8].

To summarize, the two injectors are governed by four Macroblocks, three of which are linked to the series injector and one to the shunt part. The first Macroblock comprises the control system, measurements, and setpoints, and outputs the phase and magnitude of the series injection voltage. The second macroblock comprises the dc-voltage control of the capacitor.

3.5 Chapter Summary

The advent of FACTS devices has been a boon to the power industry. These devices provide fast and effective control of the various parameters of the power system to stretch their stability limits up to the thermal limits. The SVC has been in use from the last 37 years and ever since, it has been a very reliable source of reactive power to provide voltage support to the network. The UPFC is one of the most versatile FACTS devices, providing independent control of the voltage, real and reactive power of the transmission under its supervision. As quoted by Gyugi and Schauder [10], we may say, *“The UPFC installation at Inez represents a milestone in establishing the superiority of modern transmission system control with the use of high power switching converters.”*

Chapter 4

Description of the Fuzzy hierarchical controller

“What makes society turn is science, and the language of science is math, and the structure of math is logic, and the bedrock of logic is Aristotle, and that’s what goes out with fuzzy.” — Bart Kosko [6]

Uncertainty in the form of ambiguity makes the real world a complex place. Humans have been able to address this problem of ambiguity with their ability to think and adapt to an ever changing environment. Because of their inability to think and adapt, computers and other electronic devices, though designed by human, are not capable of addressing complex and ambiguous situations.

In this section, a brief introduction to Fuzzy Logic Control (FLC) is presented to show that this powerful and flexible method can be used at different levels of the hierarchical controller to accomplish the desired control. At this stage, however, perhaps only the system level “coordination” is of most interest.

4.1 Fuzzy Logic

The dictionary meaning of the word “fuzzy” is “not clear, indistinct, non coherent, vague”. By contrast, in the technical sense, fuzzy systems are precisely defined systems, and fuzzy control is a precisely defined method of non-linear control. The main goal of fuzzy logic is to mimic (and improve on) “human-like” reasoning. *“Fuzzy systems are knowledge-based or rule-based systems”* [4]. Specifically, the key components of fuzzy system’s knowledge base are a set of IF-THEN rules obtained from human

knowledge and expertise. The fuzzy systems are multi-input-single-output mappings from a real-valued vector to a real-valued scalar.

4.2 Why Fuzzy?

Natural language is one of the most powerful forms of conveying information. The conventional mathematical methods have not fully tapped this potential of language. According to Timothy J. Ross [5], “scientists have said, the human thinking process is based primarily on conceptual patterns and mental images rather than on numerical quantities”. So if the problem of making computers with the ability to solve complex issues has to be solved, the human thought process has to be modeled. The best way to do this is to use models that attempt to emulate the natural language; the advent of fuzzy logic has put this power to proper use.

Most if not all of the physical processes are non-linear and to model them, a reasonable amount of approximation is necessary. For simple systems, mathematical expressions give precise descriptions of the system behavior. For more complicated systems with significant amounts of data available, model-free methods provide robust methods to reduce ambiguity and uncertainty in the system. But for complex systems where not much numerical data exists, fuzzy reasoning furnishes a way to understand the system behavior by relying on approximate input-output approaches. The underlying strength of fuzzy logic is that it makes use of linguistic variables rather than numerical variables to represent imprecise data.

4.3 Fuzzy Systems

The starting point in the construction of a fuzzy system is the forming of a knowledge-base consisting of IF-THEN rules. These rules are obtained from human experts based on their respective domain of knowledge and from observations that they made. Combining these rules into a single system is a natural step forward that allows us

to obtain an output that achieves the assigned goals. Theoretically, based on rule combination, three types of fuzzy systems exist, which are

- a) pure fuzzy systems;
- b) Takagi-Sugeno-Kang fuzzy systems;
- c) fuzzy systems with fuzzifier and defuzzifier.

The basic configurations of each of these systems are shown in Figures 4.1-4.3. The knowledge base consists of fuzzy IF-THEN rules. The fuzzifier transforms the real-valued input variables into a fuzzy set and the defuzzifier transforms back these fuzzy sets into real-valued variable outputs. The system shown in Fig 4.3 incorporates all the essential features of fuzzy systems given by the definition.

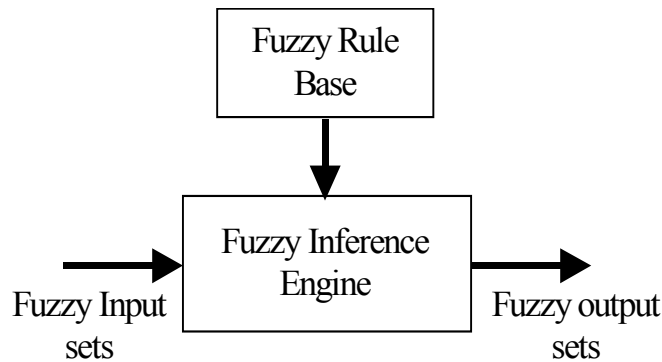


Fig. 4.1. Configuration of a pure Fuzzy system.

4.4 Fuzzy Sets

The key difference between classical sets and fuzzy sets is that in the former, the transition for an element in the universe between membership and non-membership in a given set is abrupt and well defined, that is the element either belongs or does not belong to the set. By contrast, for elements in fuzzy sets, the membership can be a gradual one, allowing for the boundaries for fuzzy sets to be vague and ambiguous.

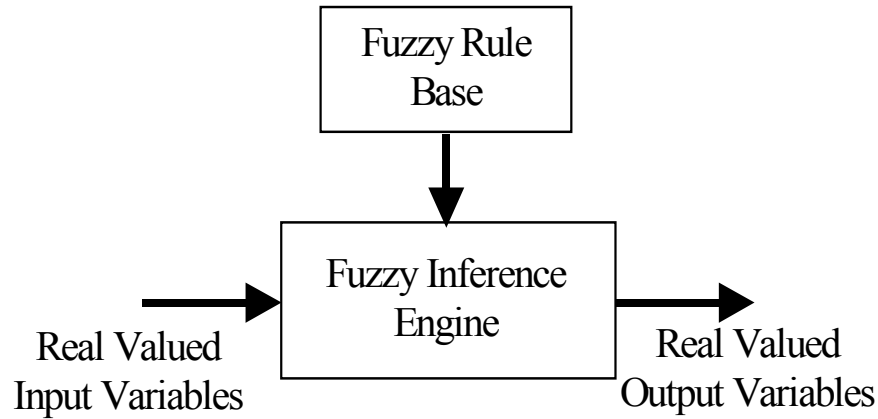


Fig. 4.2. Configuration of a Takagi-Sugeno-Kang fuzzy system

4.4.1 Membership Function

A fuzzy set is characterized by a membership function whose value ranges from 0 to 1. It consists of members with varying degrees of membership based on the values of the membership function. In mathematical terms, the fuzzy set A in the universe U can be represented as a set of ordered pairs of an element x and its membership function $\mu_A(x)$. Formally we have

$$A = \{ (x, \mu_A(x)) \mid x \in U \} \quad (4.1)$$

where U is continuous. The reader is referred to [4] and [5] for a detailed description of the fuzzy sets and the set operations that can be performed on them.

A membership function is a continuous function in the range [0-1]. It is usually decided from human expertise and observations made and it can be either linear or non-linear. Its choice is critical for the performance of the fuzzy logic system since it determines all the information contained in a fuzzy set.

In the INEZ system dealt with in this report, the membership functions will help in automating the fuzzy control. The rules were framed through numerous simulations, which are carried out to determine the best possible set of rules aimed at pushing the

stability limits of the system to its maximum. The membership functions can be estimated by studying the behavior of the bus voltages for different loading conditions and for different contingency cases. They should be able to accommodate all the non-linearities of the system, making their determination a complex task. Examples of membership functions are given next.

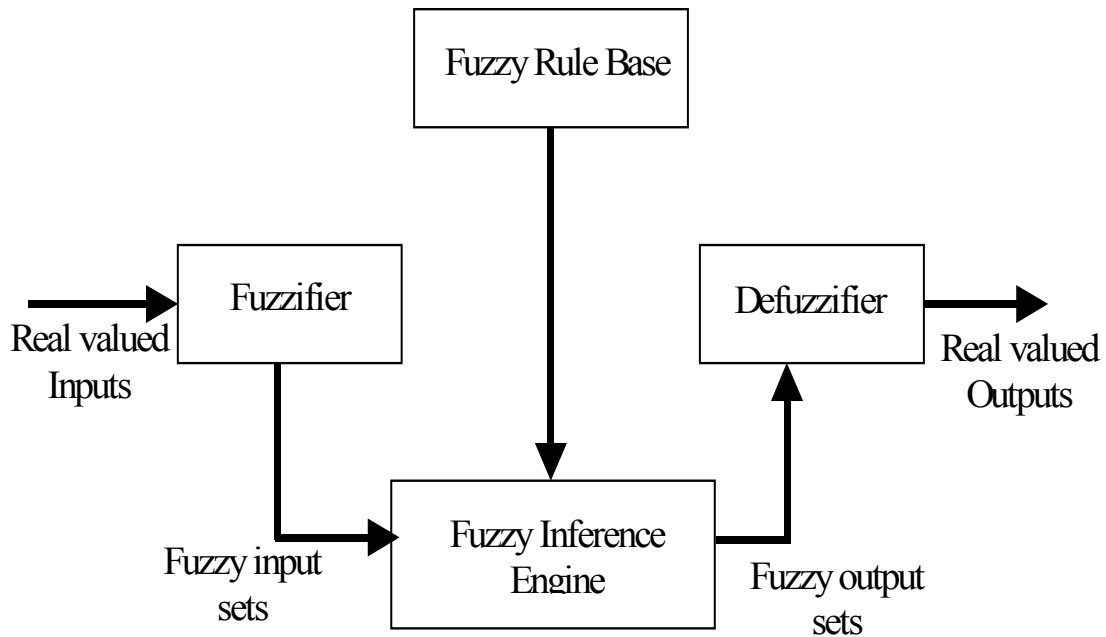


Fig. 4.3. Configuration of a fuzzy system with fuzzifier and defuzzifier.

4.5 Fuzzifier

The fuzzifier is a mapping from the real valued point, $x^* \in U$, to a corresponding fuzzy set $A' \subset U$, which is the input to the fuzzy inference engine. The fuzzifier needs to account for certain criteria while performing this mapping. The first of these criteria states that the input is a crisp point x^* , so that its mapping in U is a fuzzy set A' that has a large membership value. The second criterion states that the fuzzifier must be able to suppress the noise inherent in real valued inputs. The third criterion is that the fuzzifier must be able to simplify the computations in the fuzzy inference engine.

Three types of fuzzifiers have been proposed by [4], which are singleton, Gaussian, and triangular fuzzifiers. They are defined as follows:

- **Singleton fuzzifier:** This maps a real valued point $x^* \in U$, with a membership function $\mu_{A'}(x)$ into a fuzzy singleton $A' \in U$. Specifically we have

$$\mu_{A'}(x) = \begin{cases} 1 & \text{if } x = x^* \\ 0 & \text{otherwise} \end{cases} \quad (4.2)$$

- **Gaussian fuzzifier:** This maps a real valued point $x^* \in U$ into a fuzzy set $A' \subset U$ with a membership function given by

$$\mu_{A'}(x) = e^{-\frac{(x_1 - x_1^*)^2}{a_1}} \dots e^{-\frac{(x_n - x_n^*)^2}{a_n}}, \quad (4.3)$$

where $\{a_i, i = 1, \dots, n\}$ are positive parameters.

- **Triangular fuzzifier:** This maps a real valued point $x^* \in U$ into a fuzzy set $A' \subset U$ with a membership function written as

$$\mu_{A'}(x) = \begin{cases} \left(1 - \frac{|x_1 - x_1^*|}{b_1}\right) \dots \left(1 - \frac{|x_n - x_n^*|}{b_n}\right) & \text{if } |x_i - x_i^*| \leq b_i, i = 1, 2, \dots, n \\ 0 & \text{otherwise} \end{cases} \quad (4.4)$$

where $\{b_i, i = 1, \dots, n\}$ are positive parameters. Note that all these fuzzifiers satisfy the first criterion as mentioned above, that is to say they have a large membership value at the input point.

It can be observed that the singleton fuzzifier simplifies the computations involved in the fuzzy inference engine for any type of membership functions, while the other two fuzzifiers simplify the computations if the membership is either Gaussian or

triangular, respectively. On the other hand, the Gaussian and triangular fuzzifiers can suppress noise while the singleton fuzzifier cannot.

4.6 Defuzzifier

As the name suggests, the defuzzifier's task is the reverse operation to the fuzzifier. It maps the fuzzy output set, $B' \subset V$, from the fuzzy inference engine to a real-valued point (crisp point), $y^* \in V$. In other words, it can be said that the defuzzifier gives the real point that best describes the fuzzy set B' . Naturally, there exist many choices for choosing this point, but the most suitable point can be determined by considering certain criteria. The point y^* should represent B' from an intuitive point of view; for example it should exhibit a high membership in B' . Furthermore, the defuzzifier has to have computational simplicity; this is particularly important because most of the fuzzy controllers are usually used in real time. Lastly, the defuzzifier must have continuity.

4.6.1 Centroid Defuzzifier

The centroid defuzzifier specifies the crisp point y^* as the center of the area covered by the membership function of B' . If the membership function is viewed as a probability density function of a random variable, the centroid defuzzifier gives its mean value. One inherent disadvantage of this method is that it is computational intensive.

4.6.2 Center Average Defuzzifier

The center average defuzzifier takes the weighted averages of all the fuzzy sets that are output from the inference engine, where the weight of each set is based on the height of that particular set to determine the point y^* . This is a good approximation since the fuzzy set B' is either a union or an intersection of the inference engine's output. This is the most commonly used defuzzifier in fuzzy systems because of its computational simplicity and intuitive plausibility.

4.6.3 Maximum Defuzzifier

The maximum defuzzifier chooses y^* as the point at which the associated membership function achieves its maximum value. If more than one point satisfies this condition, then the maximum, or minimum, or mean of all such points is taken. While this type of defuzzifier is computationally simple and intuitively plausible, it lacks continuity wherein a small change in the value of B' results in a large change in y^* .

4.7 Fuzzy Rule Base – IF-THEN rules.

Fuzzy logic has been centered on the point that it makes use of linguistic variables as its rule base. Li-Xin Wang [4] said that *“If a variable can take words in natural language as its values, it is called linguistic variable, where the words are characterized by fuzzy sets defined in the universe of discourse in which the variable is defined”*.

Examples of these linguistic variables are slow, medium, high, young and thin. There could be a combination of these variables too, i.e. “slow-young horse”, “a thin young female”. These characteristics are termed atomic terms while their combinations are called compounded terms. In real world, words are often used to describe characteristics rather than numerical values. For example, one would say “the car was going very fast” rather than say “the car was going at 100 miles per hour”.

Terms such as slightly, very, more or less, etc. are called linguistic hedges since they add extra description to the variables, i.e. very-slow, more or less red, slightly high, etc.

Let α be the basic linguistic atomic term defined as

$$\alpha = \int_y \mu_\alpha(y) / y, \quad (4.5)$$

Some examples of hedges might be expressed as [5]:

- “Very” α can be expressed as say $\alpha^2 = \int_y [\mu_\alpha(y)]^2 / y$;
- “Very, very” α can be expressed as say α^4 ;
- “Plus” α can be expressed as say $\alpha^{1.25}$;
- “Slightly” α can be expressed as say $\sqrt{\alpha} = \int_y [\mu_\alpha(y)]^{0.5} / y$.

Each of the atomic and composite terms has a syntax represented by its linguistic label and a semantics given by its membership function. The latter gives the flexibility of an elastic meaning to a linguistic term and facilitates the incorporation of bias into its meaning. This forms one of the most important benefits of using fuzzy logic, by which it facilitates the encoding and automation of human knowledge expressed as natural language propositions.

At the heart of the fuzzy rule base are the IF-THEN rules. A fuzzy IF-THEN rule is expressed as

IF<*fuzzy proposition*>, THEN <*fuzzy proposition*>.

Propositions are linguistic variables or atomic terms as described previously. This type of rule-based system is different from the classical expert systems in that the rules may not necessarily be derived from human expertise; they may also be derived from other sources. Three types of linguistic variable forms exist. These are

- 1) Assignment statements such as:
 - “A is not high and not very low”;
 - “Speed of car = fast”;
 - “Apple’s color = red”;
 - “Size of cup = large”.
- 2) Conditional statements such as:
 - “IF the size of cup is large, THEN it holds more water”;

- “IF x is large, THEN temp is high”.
- 3) Unconditional statements such as:
- “Go to x”;
 - “Stop”;
 - “Turn the heat on”.

It is interesting to study the relationship among the set of rules upon which the fuzzy system operates and understand how these rules are interpreted.

In the INEZ case, the rules were framed on the basis of the observations made from simulations. Numerous load flow calculations were carried out to emulate the various possible contingency situations and to identify the best possible combination of capacitor bank switchings and parameter values (gains and set-points) of the voltage regulators and controllers. Examples of such rules are

- “IF the line between 05INEZ and 05BSAND is open, THEN switch on one capacitor bank at 05INEZ”;
- “IF the load at 05HATFLD increases by a large amount, THEN increase the setpoint of UPFC slightly”.

These are a few basic rules; the major rules consist of multiple nested loops that take into account multiple contingencies.

4.8 Description of the Fuzzy Inference Engine

The fuzzy inference engine makes use of the fuzzy logic principles that allow us to combine the fuzzy IF – THEN rules in the rule base. The aim here is to form a mapping from the fuzzy input set, A' , to the fuzzy output set, B' . We have seen that a fuzzy IF-THEN rule is interpreted as a fuzzy relation between the input and output spaces, U and V, respectively.

When there is only one IF – THEN rule, then the mapping is quite easy. The main difficulty arises when a set of rules have to be interpreted since any practical fuzzy rule base has more than one rule. There are two ways to draw an inference in such a scenario with multiple rules, which are the composition-based inference and the individual rule-based inference. They are described next.

4.8.1 Composition based Inference

In this method, all the rules are combined to form a single fuzzy relation in $U \times V$, which is then interpreted as a case with a single IF – THEN rule. So, the performance of this method is centered on how this combination is done. A good way to approach this problem is to first understand what the set of rules mean intuitively and then, combine them via appropriate logical operators.

There are two opposite arguments to the operators that could be used to combine the rules. These are the union and the intersection operators. The union operator is used when the rules are considered to be independent conditional statements. On the other hand, the intersection operator is used when the rules are viewed to be strongly coupled.

4.8.2 Individual Rule-Based Inference

In this type of inference, each rule provides a fuzzy set in the output space. These individual sets are combined to give a single output from the fuzzy inference engine. As in the case of the composition-based inference, they can be combined via the union or intersection operators.

4.9 Hierarchical Fuzzy Control

So far, we have seen various concepts associated with fuzzy logic and control. This section deals with the fuzzy control scheme that has been proposed for the INEZ

system. In this research, the proposed control system is limited to pre-framed rules derived from the numerous simulations carried out for various contingency cases.

In order to design a fuzzy system with a good amount of accuracy, an increase in the number of input variables to the fuzzy system results in an exponential increase in the number of rules required. If there are n input variables and m fuzzy sets are defined for each of these, then the number of rules in the fuzzy system is m^n . This can be shown with the help of a small example. Suppose there are 5 input variables and for each variable 3 fuzzy sets are defined, then the total number of rules is $3^5 = 243$. Now, suppose the number of fuzzy sets is increased to 5 (to increase the accuracy of the system), then the new number of the rules would be $5^5 = 3120$. This is a significant increase in the number of rules.

It is impractical to implement a fuzzy system with such an exponential growth of the number of rules. If we take the case of the INEZ system, there would be at least 2 input variables from each bus, which are nodal voltage magnitude and phase angle. For a total of 16 buses, the number of variables would be 32 variables. Even if we take 2 fuzzy sets, the total number of rules to be framed would be $2^{32} = 4294967296$. This huge number would make the control system highly impractical for real-time applications. This problem is common to any type of control system. The complexity of the control scheme increases with the number of variables involved; hence the need for hierarchical control.

The idea behind the construction of a two-level hierarchical scheme is to make a layered structure of control where each layer takes into account a certain number of variables and gives a single variable as the output. Hence the complexity of the system reduces, and along with it, the number of rules to be framed. For the INEZ case, the output is also in the form of layers where in the higher level of the control scheme, the gains and setpoints of the UPFC and SVC are controlled as the operating point of the system evolves.

Once the control parameters have reached their maximum limits, the second level comes into operation by switching on capacitors in a pre-defined sequence; the latter has been determined via extensive simulations carried on the system. This provides fast and effective control of the system voltage since the UPFC and SVC are fast acting devices with a time lag of couple of seconds in the worst case; hence avoiding wear and tear of the mechanically switched capacitors. This hierarchy can be implemented in linguistic terms with the help of nested IF loops. An example of such nested rules is given in Table4.1.

Table 4.1: Example of nested if loops exhibiting the hierarchy of operations

<p>IF the load at bus 05HATFLD increases by 5%, THEN change the setpoint of SVC to 1.06 and setpoint of UPFC to 1.06, AND IF line between 05BORLND and 05 HATFLD is open, THEN change the setpoint of SVC to 1.07 and setpoint of UPFC to 1.03, AND IF line between 05BUSSYV and 05THELMA is open, THEN change the setpoint of SVC to 1.1 and setpoint of UPFC to 1.08 and switch on 2 capacitor banks at 05INEZ and one capacitor bank at 05THELMA</p>
--

The IF-THEN loops given in Table 4.1 illustrate the hierarchical control structure displayed in Fig. 4.4 It can be observed that the first action taken is the change in setpoints of SVC and UPFC, while the capacitors are switched on after the maximum limits of the SVC and UPFC are reached. This provides fast and effective voltage control of the system.

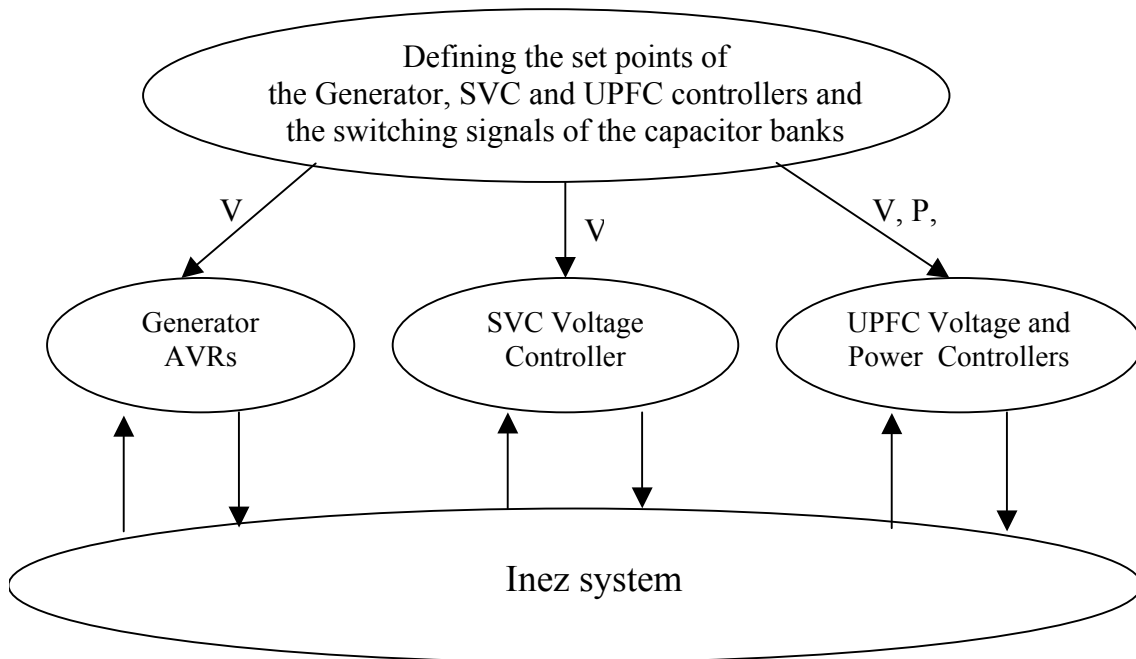


Fig. 4.4. Hierarchical voltage control scheme for the Inez system.

The entire rule-base that has been proposed possesses a structure similar to the type described above. There are few inherent difficulties associated with this type of control. Because there are a large number of possible factors affecting the voltage at each bus, the number of cases to be investigated becomes extremely large. One approach to overcome this difficulty would be to resort to pattern recognition. The latter would allow us to identify similar sets of actions taken to control the voltage. From the numerous contingency cases that were simulated and from the knowledge that was gained about the appropriate actions that need to be taken to cope with voltage instability, clusters can be formed using a supervised learning method. This greatly simplifies the number of cases to be considered in real time because all the steps have been predetermined. The only real-time calculation that has to be performed is to identify the cluster to which the present system state belongs. There are extremely fast algorithms available to deal with this situation. The next section gives a brief review of the basic concepts and methods of pattern recognition.

4.10 Basic concepts of Pattern Recognition (PR)

In one sense, we can define a “*pattern*” as a particular arrangement of structural elements. An example is cloud patterns. In another sense, a pattern can be defined as a prototype or model according to which objects are formed. An example is foundry patterns (molds), etc. Assigning an object to the class of patterns it belongs to can be termed *Identification*.

According to Nadler and Smith [30], pattern recognition problem can be generalized and stated as follows: “*Given a collection of objects belonging to a predefined set of classes and set of measurements on these objects, identify the class of membership of each of these objects by suitable analysis of the measurements*”. The goal is here to design an optimal recognition system with the condition of optimality being to achieve the lowest possible error rate.

As displayed in Fig.4.5, the process of identifying the membership class of an object can be broken down into a number of steps, which include measurement, noise filtering and signal conditioning, segmentation, description, and decision. Pattern Recognition systems are complex and hierarchical. This is to help solve complex problems since it is easier to solve it by dividing its contents into a set of smaller, less complex sub-problems assumed to be independent from each other.

4.10.1 Sensors and Acquisition

The data collected in digital form from the sensors provide input to the PR system. These sensors can be either online or offline. The offline mode of operation is carried out by storing the data in some memory location for future processing.

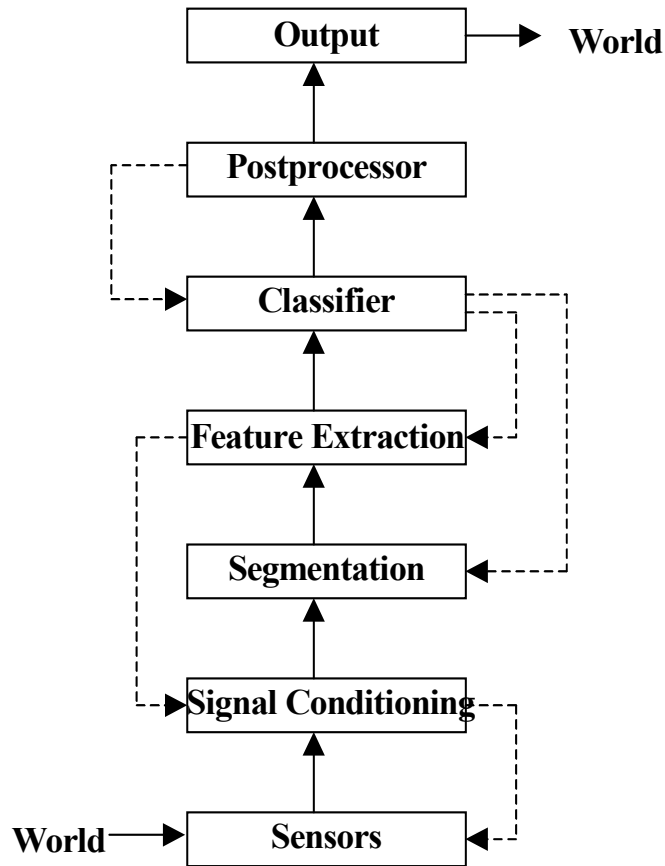


Fig. 4.5. Generic block diagram of a Pattern Recognition System.

4.10.2 Signal Conditioning or Preprocessing

Preprocessing operations are critical for the performance of a PR. They modify the raw measurements obtained from the Analog-to-Digital Converter (ADC) in some useful way. This is to improve the data, compress of data volume, segment and extract preliminary features, and facilitate object identification.

4.10.3 Segmentation (Low level Feature Extraction)

Segmentation algorithms are used to separate or isolate discrete objects from the information provided by a set of measurements. This is to facilitate further analysis and data processing for object classification. In order to carry out a reasonable segmentation,

it is necessary to detect certain features that may or may not be included in the list of features utilized for recognition later in the PR system. These are referred to as low-level features, because they are obtained from direct measurements. They help to achieve object segmentation, a task usually considered as part of preprocessing.

4.10.4 Feature Extraction

As functions of measurements, features are used for segmenting objects and grouping them into distinct classes. Features serve many purposes in a PR system, which include the following tasks:

- Reduce the dimensionality of the pattern space where the classification is actually carried out;
- Render the features more amenable to the decision process;
- Select useful information and summarize them to enhance the reliability of object recognition.

There are two basic approaches to feature design, which are

- A number - crunching approach, based on the statistical theory, which seeks to obtain features by manipulating the measurements as purely numerical variables;
- An approach that makes use of semantic content. This stems from structural PR where the features, in some intuitive way, correspond to human perception.

4.10.5 Selecting Features

For any PR problem, there are a huge number of possible features to be considered, of which only few are useful. While proper selection of features can greatly enhance the performance of the PR procedure, improper selection could lead in misleading interpretations. The accuracy of the results obtained from the PR method greatly relies on feature selection, making it a highly critical step in PR.

There is no general solution for feature selection. Features are generally designed by hand, using the experience, intuition, and/or cleverness of the designer. This is owing to the fact that the random variation in the measurements results in an inevitable randomness in the variables determining the features. In the INEZ voltage stability case, possible features could be the distance to voltage collapse in the form of reactive reserve margins, which are obtained from a continuation power flow method [33, 34]. Other possible features include the load index of the system, the derivative of the voltage with respect to the real and reactive power of the loads, and the reactive power distance to voltage collapse.

4.10.6 Classification

Classification is the final step in the grouping of unknown objects, referred to as the system condition. It gives a particular function that helps to form the clusters. Irrespective of the decision method, the number of decision classes must be at least one greater than the number of defined classes. The decision units can be combined to form hierarchical and compound structures, the aim being to obtain highly reliable final decisions.

Once the clusters have been formed, the sequence of steps to be taken for each of these clusters are found out by simulating each of these conditions, and then deciding what would be the best possible sequence of operations to achieve maximum loadability and stability of the power system. The control actions to be taken would then be implemented using fuzzy logic, hence making the control system more efficient, effective, reliable and most important of all, fast.

4.11 Chapter Summary

The field of fuzzy systems and control has been developing at a fast pace. Researchers around the world have been testing out the application of fuzzy logic to various problems, including power system applications. With the simplicity and speed of control that fuzzy logic offers, it is definitely a very good proposition to be pursued for implementing the hierarchical control proposed in this chapter.

The rules are easily established from the desired operation of the overall system. The method is flexible in that the general structure of Fig. 4.3 is appropriate for many control or coordination problems. The input/output signals of the system of Fig. 4.3 are nonlinear due to the way that the inference is carried out. By performing an interpolation between rules, this structure can approximate to any degree of accuracy any arbitrary smooth (nonlinear) mapping. In addition, with regard to the flexibility of fuzzy logic systems, the type of control that is implemented can vary from nearly linear (i.e. PID control) to a strongly nonlinear control such as sliding-mode control. This is accomplished primarily by changing the parameters of the membership functions.

Chapter 5

Design and Implementation of the INEZ system in Eurostag

This chapter gives the details of the modeling of various components of the INEZ power system as implemented in Eurostag. Screen shots from the software have been included to give an idea about the implementation part of the models. It is to be noted that the data used in the entire modeling of various transmission system parameters are real-time data provided by American Electric Power (AEP).

5.1 Transmission Line Model

The transmission line has been modeled as a pi-equivalent circuit that consists of a series impedance comprised of a series resistance R and series reactance X between the terminal nodes, and a shunt impedance comprised of a capacitive susceptance B and insulation conductance G connected between the conductor and the ground.

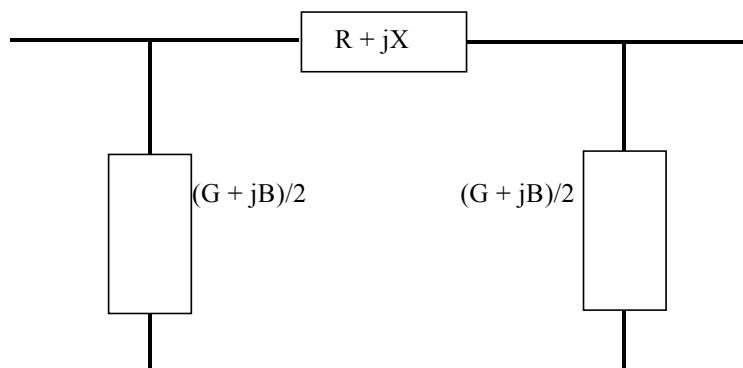


Fig. 5.1. Equivalent pi- circuit of a transmission line.

The screenshot shows a software window titled "Edition" for modeling a line. The window displays the following parameters:

Parameter	Value	Unit
Type	LINE	
Class	BRANCH	
Page	1	
Sending node	05BSAND	
Receiving node	05INEZ	
Opening status	closed at both sides	
Parallel code	1	
Total line resistance	0.01001	p.u.
Total line reactance	0.06203	p.u.
Semi shunt conductance	0	p.u.
Semi shunt susceptance	0.035	p.u.
Line rated power	523	MVA

Fig. 5.2. Modeling of a line in Eurostag. Note: The original image has been adjusted to enhance visibility

In Eurostag, the data required for the modeling of the line is as shown in the screen capture displayed in Fig 5.2. It is to be noted here that all the parameters data used in emulating the INEZ system in Eurostag are real time data provided by AEP.

5.2 Load Modeling

While the load in the INEZ area is primarily induction motors used for mining, it includes spread residential and commercial-type load too. In order to emulate these load, constant impedance load was modeled at all buses as shown in Fig 5.3.

The screenshot shows a dialog box titled 'Edition' with a close button (X) in the top right corner. The dialog is divided into two main sections: 'Type: NODE' and 'Class: NODE'. Below this, there is a 'Page 1' indicator. The main area contains several input fields for node parameters:

Node name	05BUSSYV	Area name	A List ...
Base voltage	138. kV	Generated active power	0. MW
Generated reactive power	0. Mvar	Reactive load	15. Mvar
Active load	50. MW	Active losses	0. kW
Shunt capacitor	0. Mvar	Initial voltage magnitude	0.97746 p.u.
Initial voltage angle	-35.11 degrees		

At the bottom of the dialog, there is a 'Help:' label followed by an empty text box, and two buttons: 'Ok' and 'Cancel'.

Fig. 5.3. Constant impedance load as entered at each node in Eurostag.

5.2.1 Dynamic Load Modeling

The dynamic load has been modeled as 3 large 653.6-MVA induction motors connected to nodes 05DINGES, 05CEDARC, and 05BORLND, respectively. This modeling provides a reasonable approximation of the load over the entire INEZ region by making the total load about 70% dynamic and 30% constant impedance. The data entered for the induction motors are obtained from a standard library model given in Eurostag as displayed in Fig. 5.4 The induction motor can be modeled in two different ways in Eurostag [8]; the model that has been used in this case is the so-called “full” model. In this model, the dynamics of the rotor fluxes are calculated assuming the existence of a double rotor cage. This model provides a good compensation of the electrical torque during start-up and loading, thereby minimizing the slip. The induction motor is represented as a synchronous motor whose excitation winding is short-circuited. For a much more detailed explanation of the model used, the reader is referred to [8].

The screenshot shows a dialog box titled 'Edition' with a close button (X) in the top right corner. The dialog is divided into two pages, 'Page 1' and 'Page 2'. The current page displays the following parameters and their values:

Parameter	Value	Unit
Type	INDUCTION	
Class	MACHINE	
Machine name	LOAD3	
Connection node name	05BORLND	
Rated apparent power	653.6	MVA
Proportion of active load	0.1	
Proportion of reactive load	0.05	
Constant of inertia	1.	MW s./MVA
Model type	Full	
Leakage resistance - winding 2	0.0116	
Negative sequence resistance		p.u.
Zero sequence resistance		p.u.
Stator leakage resistance	0.00438	
Stator leakage reactance	0.15	
Rotor-stator mutual reactance	2.6	
Leakage resistance - winding 1	0.25	
Leakage reactance - winding 1	0.01	
Leakage reactance - winding 2	0.1	
Negative sequence reactance		p.u.
Zero sequence reactance		p.u.

At the bottom of the dialog, there is a 'Help:' field, an 'Ok' button, and a 'Cancel' button.

Fig. 5.4. Parameter's values of the induction motor model used to represent the load of the INEZ subsystem.

5.3 Generator Modeling

The INEZ system has 2 generators, one connected to Node 05BSAND and the other one connected to Node 05BAKER, with ratings of 260 MW (300 MVA) and 800 MW (907MVA), respectively. Real time data provided by AEP was utilized to model these two generators in Eurostag. The generators were modeled as synchronous machines according to PARK's classical theory [8]. Of the two generator's models available in Eurostag was picked. It includes four equivalent models, which are the exciter winding, the damper winding in the direct axis with magnetic coupling with the exciter winding, and two dampers in the quadrature axis.

While in general, the stator transformation electromotive forces are neglected in Eurostag they are not to make the machine internal fluxes sensitive to the network's frequency. The saturation of the magnetic circuits can be modeled according to two methods. In the first method, the generator parameters defined for the magnetic condition prevailing at the time of initial conditions are adjusted and kept constant throughout the whole simulation. In the second method, the coupling inductances in the two axes are mathematically modeled as a function of the position and amplitude of the air-gap flux. Also the step-up transformer is integrated into the generator model. Figures 5.5–5.6 show the parameters required by Eurostag to model the synchronous generators.

5.4 Step-down Transformer Modeling

There is one step-down transformer in the Inez system, which is connected between the 05BAKER and 05BSAND buses. Out of the 4 types of transformer models available in Eurostag, the simplified transformer with a fixed real transformer ratio has been used. The data required to model this type of transformer is shown in Fig 5.7. Suppose it is linking two voltage levels V_1 and V_2 with an apparent nominal power S_t and a short circuit voltage rated to p percent of V_1 . The rated current on side 1 is expressed by

$$I_{nom} = \frac{S_T}{\sqrt{3}V_1} \quad (5.1)$$

The leakage impedance on side 1 is expressed by [8]:

$$Z_1 = \frac{pV_1 / \sqrt{3}}{I_{nom}} = \frac{pV_1^2}{S_T}, \quad (5.2)$$

yielding
$$Z_1 = \frac{pC_1^2 V_{1b}^2}{S_T}. \quad (5.3)$$

Therefore
$$Z_2 = \frac{p.C_2^2.V_{2b}^2}{S_T} \quad (5.4)$$

where $C_1=V_1/V_{1b}$ and $C_2=V_2/V_{2b}$. As displayed in Fig. 5.7., the transformer equivalent circuit is composed of an ideal transformer, a series impedance taking into account losses due to load current and a shunt admittance representing no-load losses.

The screenshot shows a software window titled "Edition" for a "SYNCHRONOUS - EXT. PAR." machine. The parameters are as follows:

Parameter	Value	Unit
Machine name	BAKER	
Connection node name	05BAKER	
Rated apparent power	907.	MVA
Rated turbine power	807.23	MW
Rated generator active power	800.	MW
Base voltage machine side	345.	kV
Proportion of generated active power	1.	
Proportion of generated reactive power	1.	
Model type	Full	
Transformer included in machine model	yes	
Machine transformer resistance	0.0038	p.u.
Machine transformer reactance	0.22	p.u.
Machine transformer rating	235.	MVA
Rated voltage, machine side	345.	kV
Rated voltage, network side	345.	kV
Saturation	without saturation	
Coefficient md of the saturation curve		
Coefficient mq of the saturation curve		
Coefficient nd of the saturation curve		
Coefficient nq of the saturation curve		
coupling behaviour	Running	

Fig. 5.5. First set of data for a synchronous generator as modeled in Eurostag.

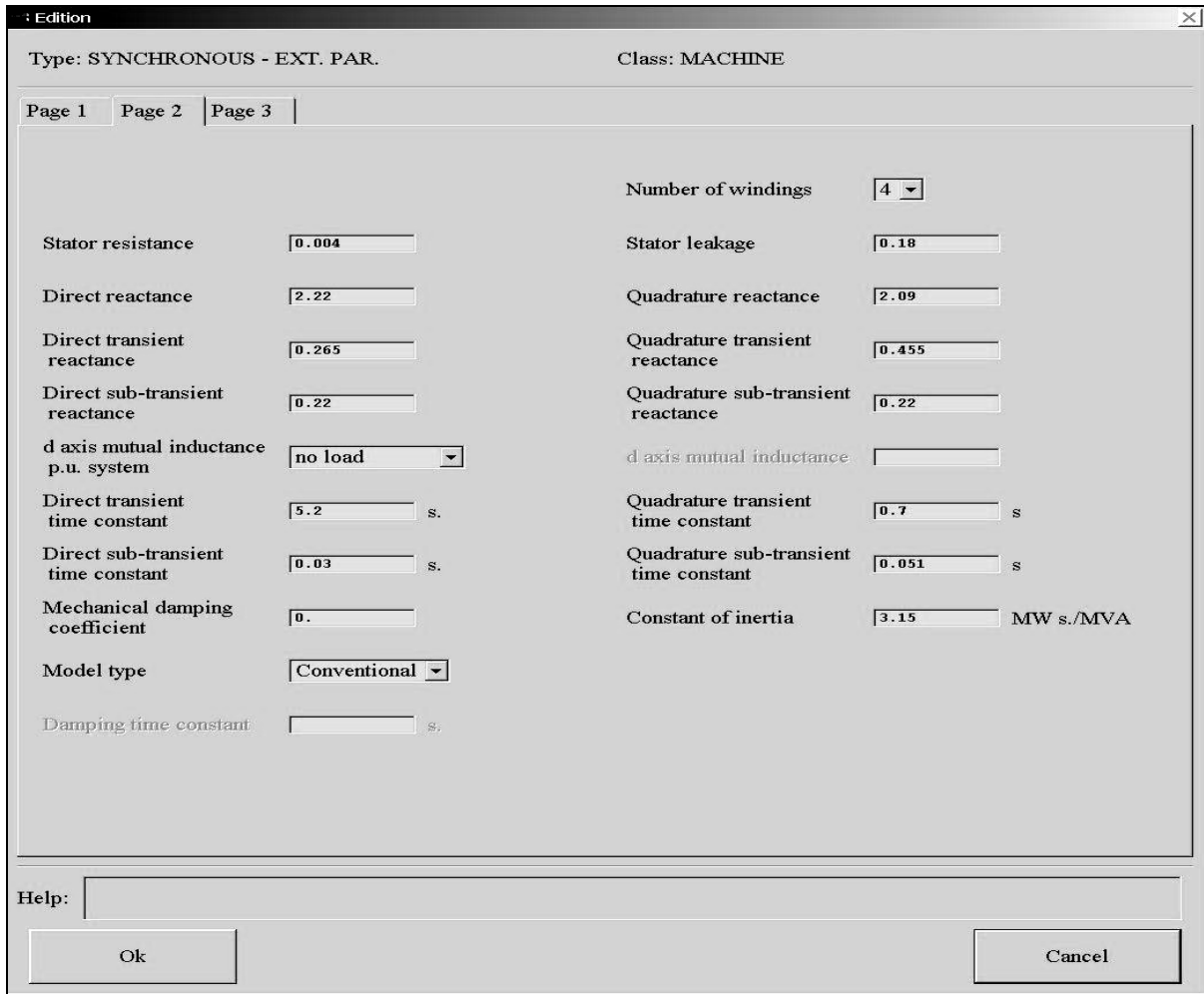


Fig. 5.6. Second set of data of a synchronous generator as modeled in Eurostag.

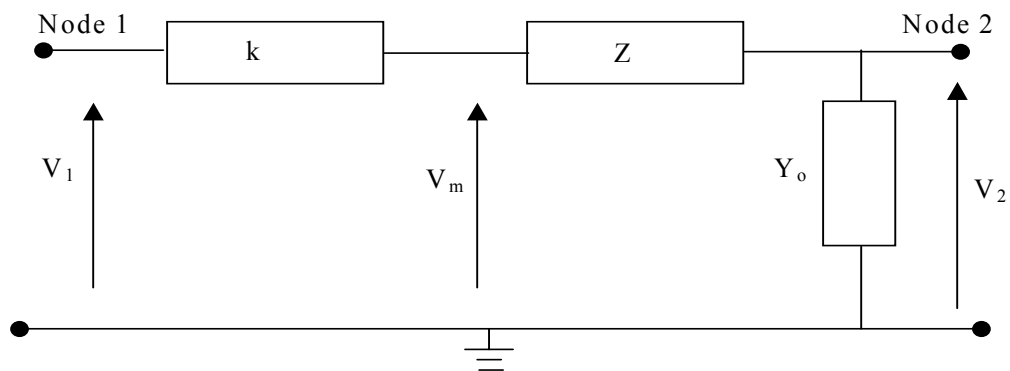


Fig. 5.7. Transformer equivalent circuit.

The screenshot shows a software window titled ': Edition' with a close button (X) in the top right corner. Below the title bar, it displays 'Type: FIXED RATIO TRANSFORMER' and 'Class: BRANCH'. The main area is labeled 'Page 1' and contains several input fields and buttons:

- Sending node:** A text box containing '05BAKER' and a 'List ...' button.
- Receiving node:** A text box containing '05BSAND' and a 'List ...' button.
- Opening status:** A dropdown menu currently showing 'closed at both sides'.
- Parallel code:** A text box containing '1'.
- Resistance:** A text box containing '0.00046' followed by 'p.u., SNREF base'.
- Reactance:** A text box containing '0.01827' followed by 'p.u., SNREF base'.
- Shunt conductance:** A text box containing '0.' followed by 'p.u.'.
- Shunt susceptance:** A text box containing '0.' followed by 'p.u.'.
- Transformer rated power:** A text box containing '876.' followed by 'MVA'.
- Transformer ratio:** A text box containing '1.0124' followed by 'p.u.'.

At the bottom of the window, there is a 'Help:' label followed by an empty text box, and two buttons: 'Ok' and 'Cancel'.

Fig. 5.8. Transformer modeling in Eurostag.

5.5 Capacitor Banks

The INEZ system has 10 capacitor banks spread throughout the network at different buses. These have been modeled as a set of capacitors connected in parallel on a node, yielding step values for the capacitances. It is possible to connect several banks to the same node. The banks can be switched on in steps at any time using the events available in the dynamic simulation tool of Eurostag. The capacitor banks in the INEZ system are as displayed in Fig. 5.9 and their representation in Eurostag is shown in Fig. 5.11.

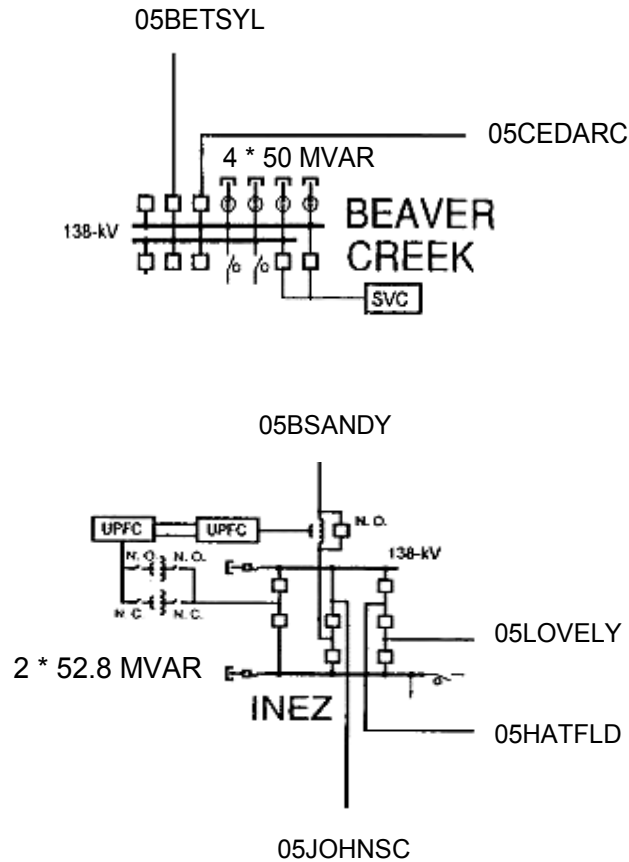


Fig. 5.9. Capacitor banks at the Beaver Creek and Inez buses.

5.6 Static Var Compensator (SVC) Modeling in Eurostag

In Eurostag [8], the SVC is modeled as an impedance injector connected to the network at a particular node. The control of the SVC is achieved with Macroblocks. The standard model of SVC available in the library of Eurostag has been used to model the SVC of the INEZ system with changes made to the setpoint, rating, and gain. The structure of the SVC as used in Eurostag is shown in Fig. 5.11.



Fig. 5.10. Generalized Block diagram of SVC with conductance G and susceptance B [8].

Eurostag provides two sets of parameters for the SVC, of which one set has been used because it gave better performance in terms of voltage support for this system. The SVC control is achieved by the macroblock main scheme as displayed in Fig. 5.15.

The screenshot shows a dialog box titled "Edition" with a close button (X) in the top right corner. Below the title bar, it displays "Type: CAPACITOR or REACTOR BANK" and "Class: BANK". The main area is labeled "Page 1" and contains several parameter fields:

- Bank name:
- Connection node:
- Number of steps:
- Active losses on each step: kW
- Reactive power of each step: Mvar
- Maximum number of steps:

At the bottom, there is a "Help:" label followed by an empty text box, and two buttons: "Ok" and "Cancel".

Fig. 5.11. Capacitor bank as modeled in Eurostag.

5.7 Unified Power Flow Controller (UPFC)

In order to connect the UPFC to the transmission network at Node 05INEZ, a PQ node called UPFCNODE is created. The 05INEZ node and the UPFCNODE are joined by a series branch having a 1000-p.u. reactance in order to prevent the injector from stopping in case of line opening. The dynamic model of the UPFC used in Eurostag is depicted in fig 5.13.

The whole UPFC is represented by two current injectors, one acting as the shunt part and the other one acting as the series part. The shunt part injects reactive power into the network at the point of connection while the series part supplies a series voltage to provide voltage support. The UPFC control is implemented with 4 Macroblocks as shown in Fig. 5.15-5.18. The standard library model of the UPFC has been used to model the UPFC of the INEZ system with some changes made to the setpoint, control points, ratings, and gain.

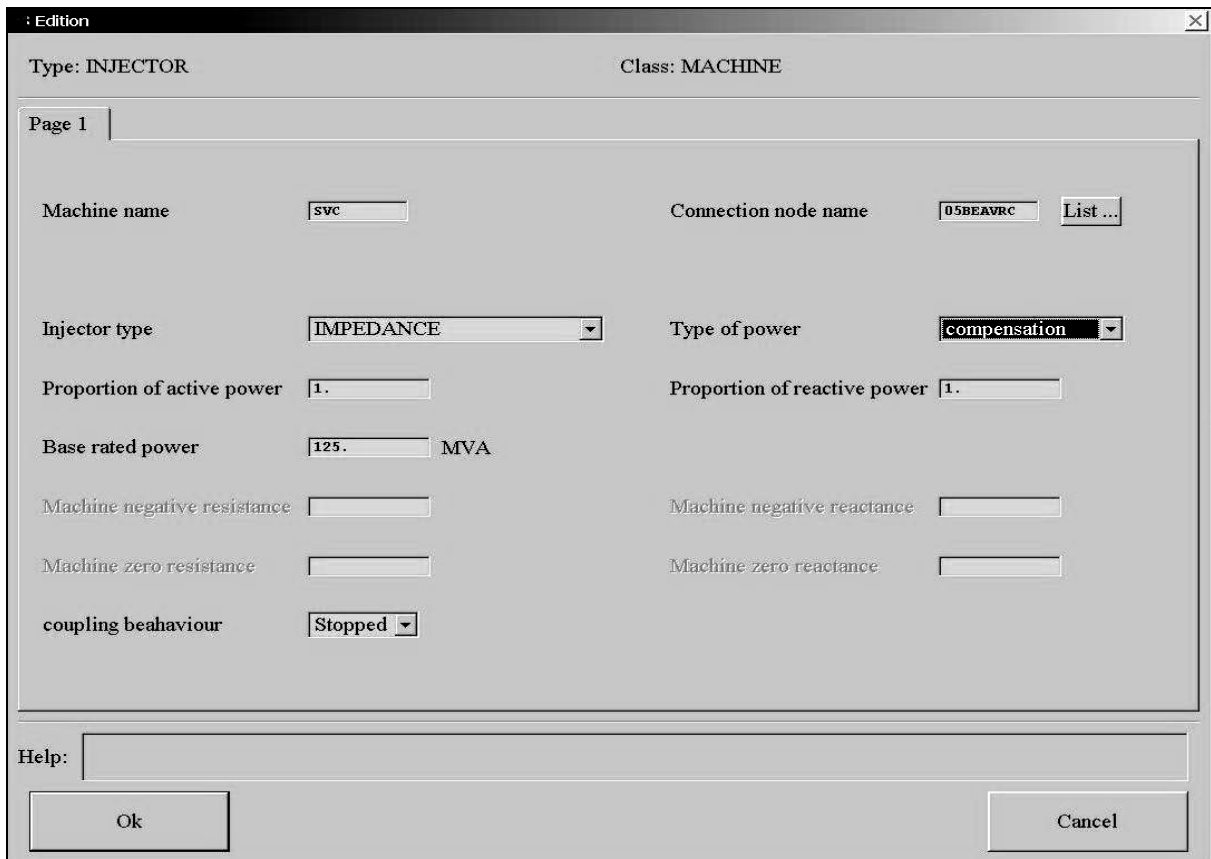


Fig. 5.12. SVC Implementation in Eurostag.

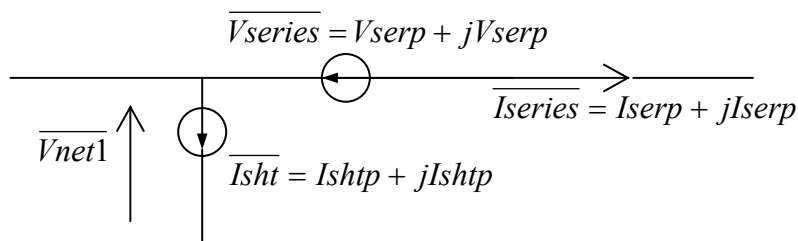


Fig. 5.13. Dynamic model of UPFC in Eurostag [8].

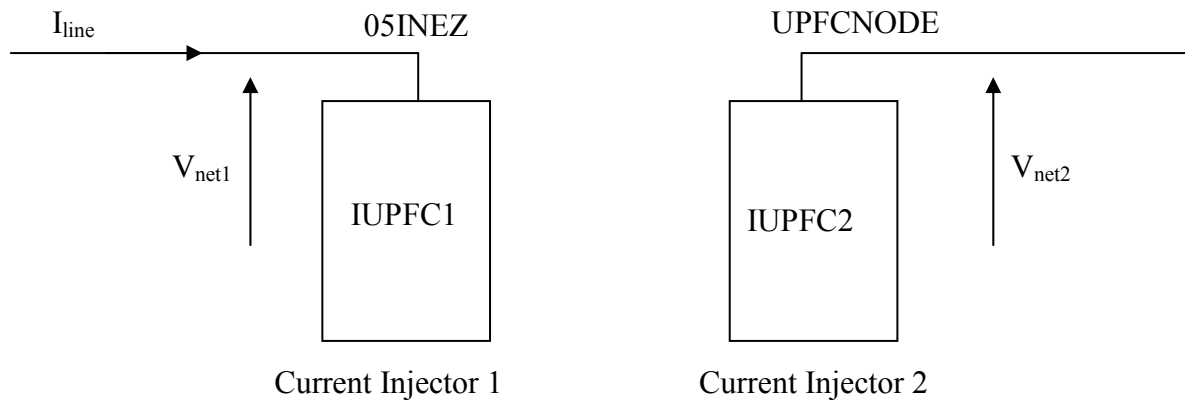


Fig. 5.14. Model of the complete interface between the UPFC and the transmission network [8].

5.8 Chapter Summary

This chapter gives a brief description of the devices used and their modeling in Eurostag. The model diagrams, principles, and their implementation have been discussed with appropriate figures. Few mathematical equations giving a brief idea about the modeling of various devices have also been included. For further reference and detailed description of the models used, the user is referred to [8].

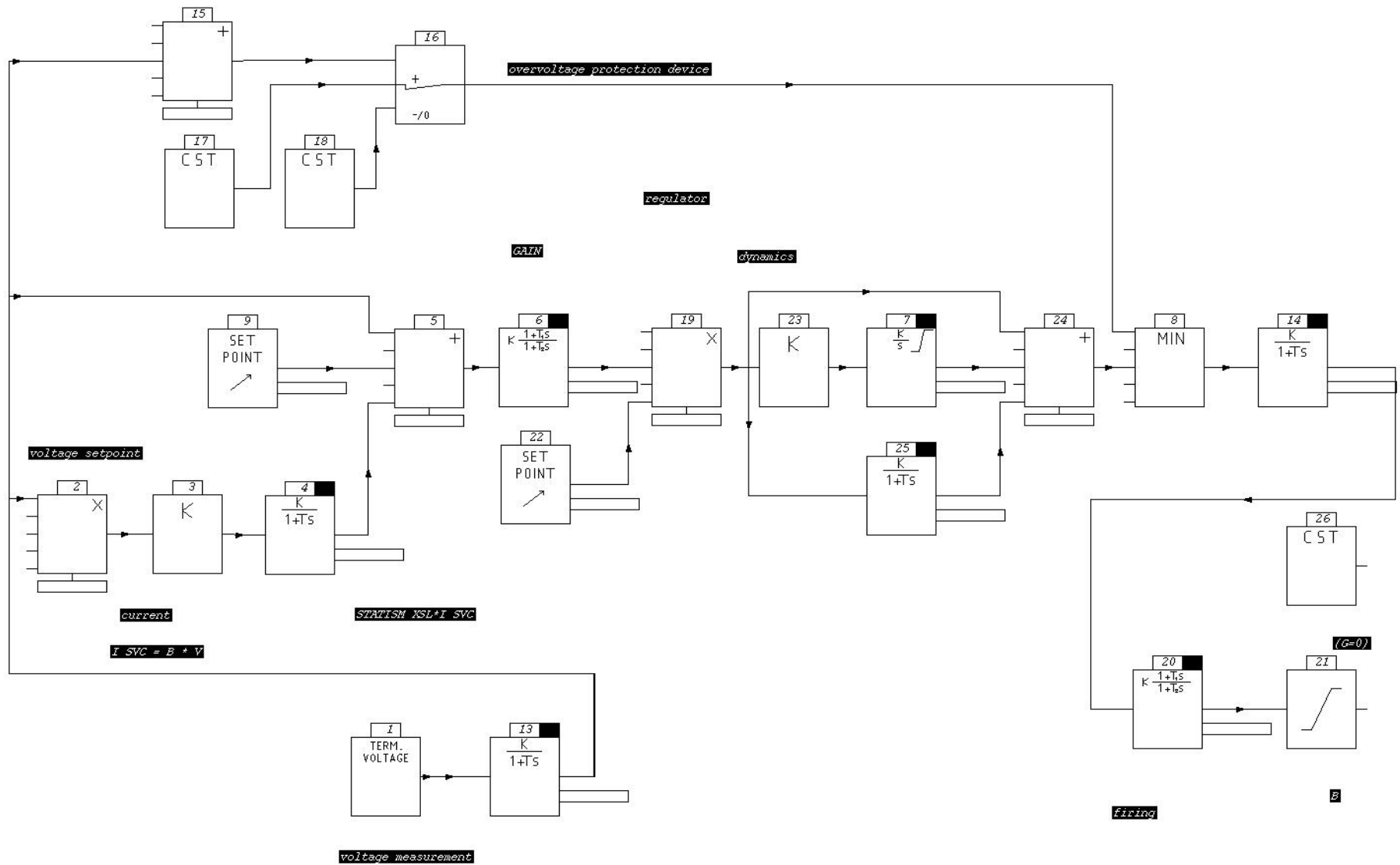


Fig. 5.15. Macroblock main scheme of the SVC [8].

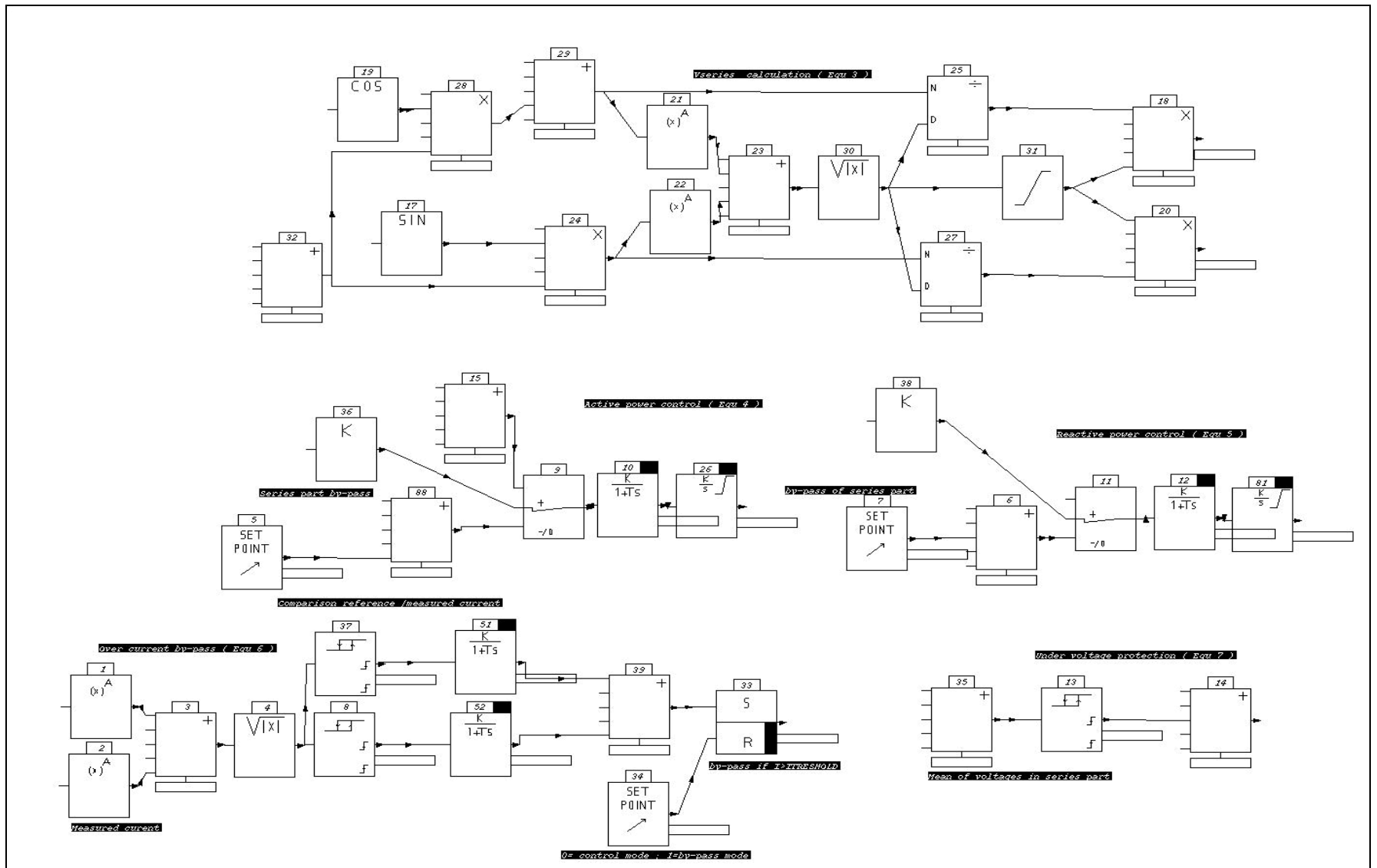


Fig. 5.16. Macroblock upfc_se (series part control) connected to 05INEZ node [8].

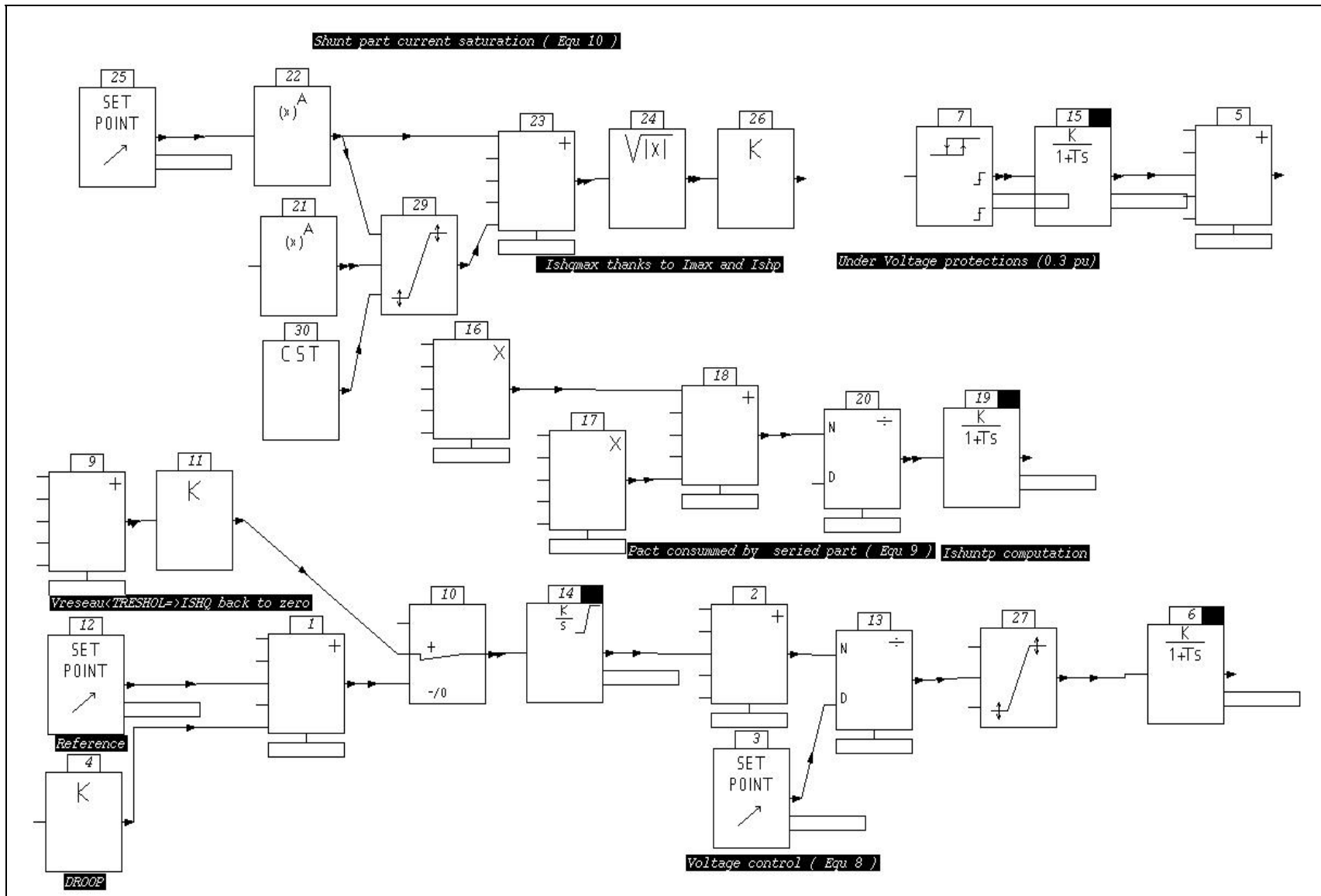


Fig. 5.17. Macroblock upfc_sh (shunt part control) connected to 05INEZ node [8].

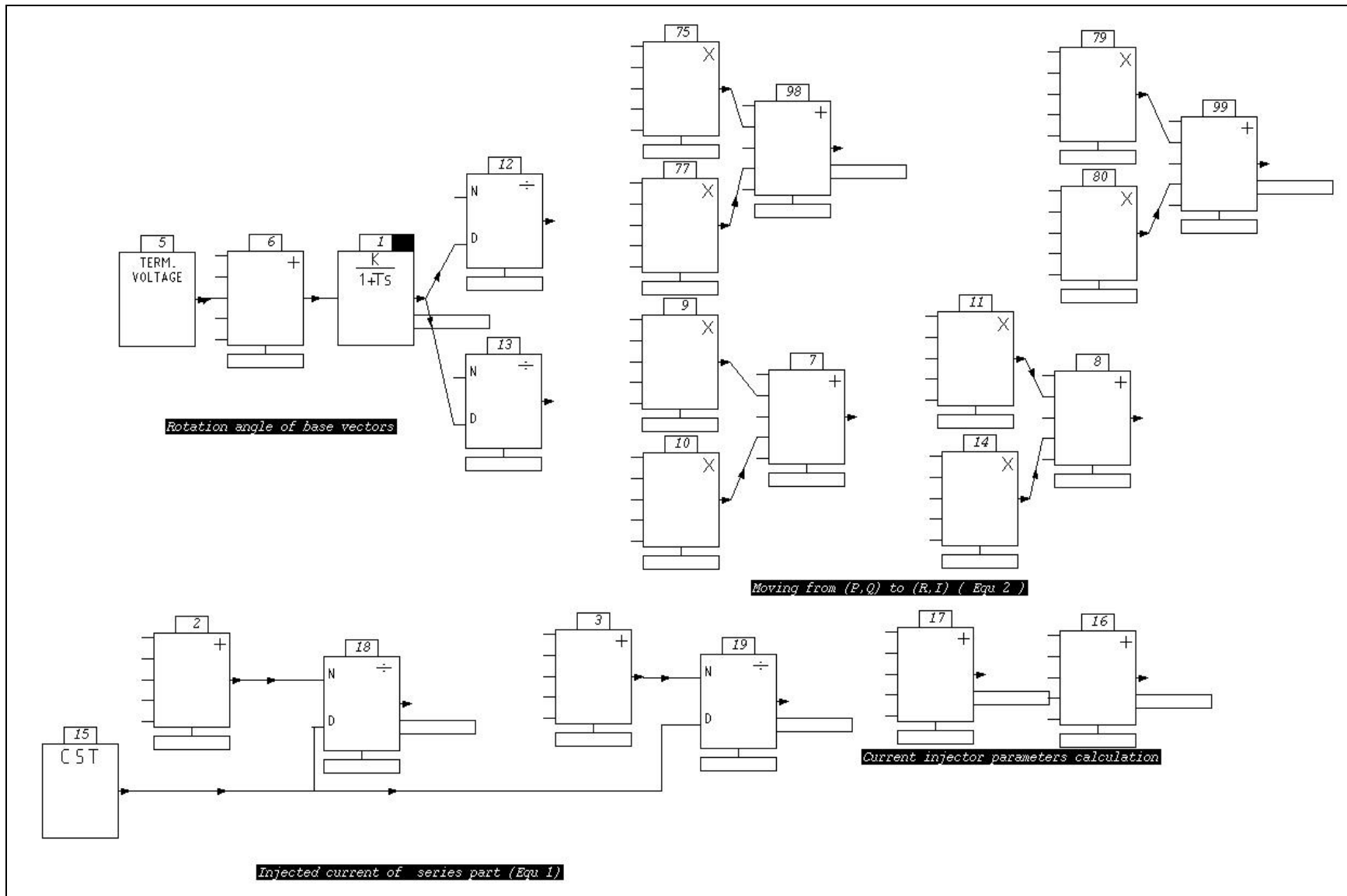


Fig. 5.18. Macroblock interup1 (Injector 1) connected to 05INEZ node [8].

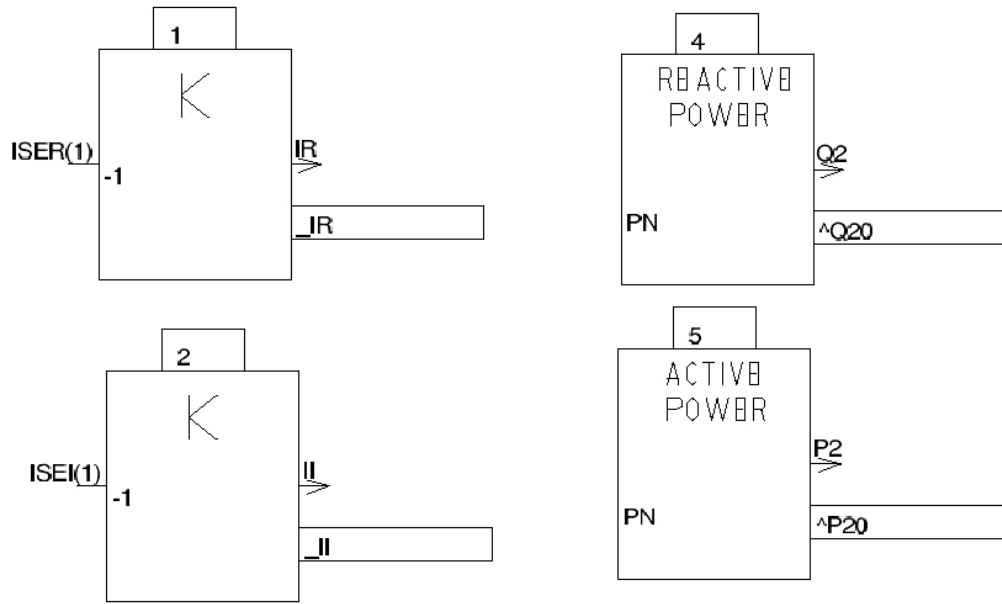


Fig. 5.19. Macroblock interup2 (Injector 2) connected to UPFCNODE [8].

Chapter 6

Simulation Results of the INEZ system

This chapter presents and analyzes simulation results obtained on the INEZ system. Numerous graphs showing the behavior of the system in various conditions have been included to illustrate the analysis. Few interesting results have also been included and explained.

6.1 Steady-State Analysis

For the steady-state analysis, the P-V and the Q-V curves were plotted for the INEZ system. The P-V and Q-V curves were drawn by simultaneous and gradual increase of the P and Q load at each bus in steps of 1%. Figures 6.1 and 6.3 and Figures 6.2 and 6.3 depict the P-V and Q-V curves of the system without and with the UPFC and SVC connected respectively. In all these figures, a dashed vertical line indicates the P and Q values at which one of the bus voltages reaches its minimum admissible limit. This voltage limit is equal to a voltage drop of 10% from the nominal value of 138 kv, yielding a minimum voltage of 124.2 kv. Note that the voltages that undergo the fastest drop are those on buses 05BORLND, and 05DINGES. Interestingly, the minimum voltage limit is always reached first by the 05CEDARC bus voltage for both P and Q load increase.

From Figures 6.1-6.4, it can be observed that there is a considerable increase in the loadability limits of the system. These graphs show that the UPFC and SVC help to

increase the loadability limit of the system by providing appropriate voltage support to the system. The UPFC and SVC gain, setpoints, and time constants are equal to the values provided in the library models of Eurostag.

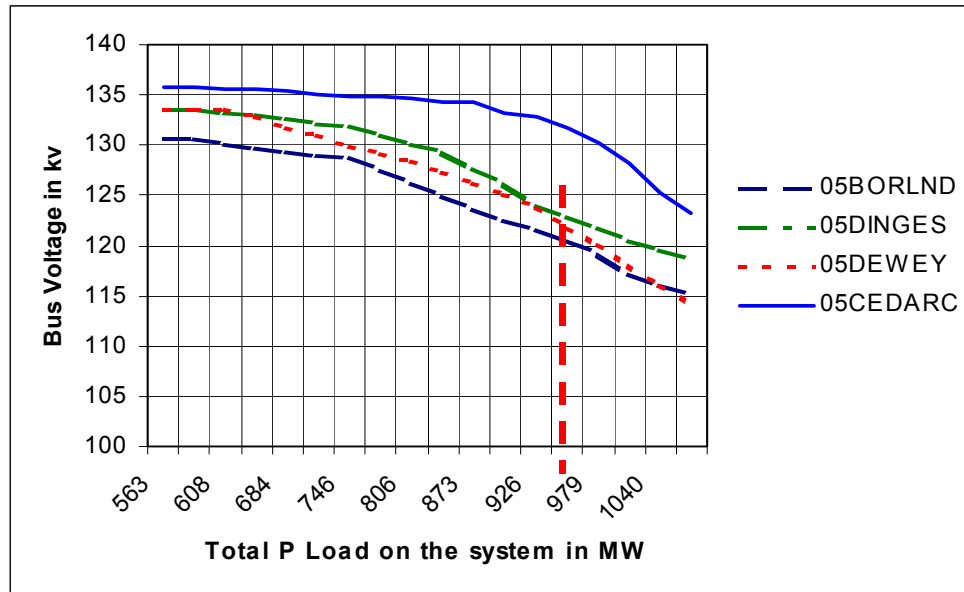


Fig. 6.1. P-V plots of the system without UPFC and SVC. The minimum voltage of 124 kV is reached at around a total load of 950MW on the system.

6.2 Transient Analysis

The transient behavior of the system was studied for three types of scenarios. In the first scenario, the total load on the system was evenly increased by 5% at all the buses without any topological changes in the system. In the second scenario, the total load was increased by 5% and after a short interval of 15 seconds, a single line was opened. This was repeated sequentially for all the lines and the bus voltage profiles were recorded and investigated. The third scenario was an increase of load by 5% followed by successive opening of two lines at a time in short time intervals of 25 seconds. The sections below give details of the observations made for each of these cases.

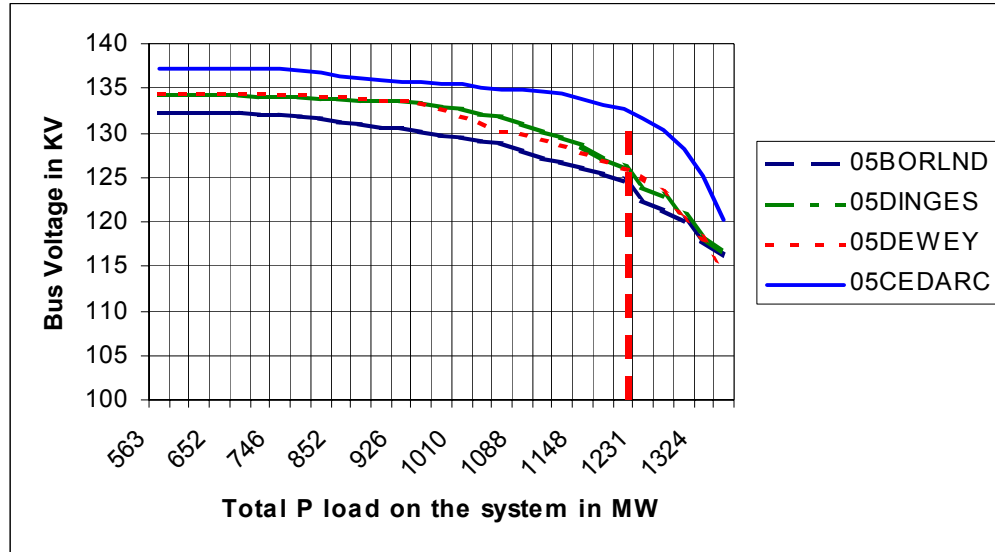


Fig. 6.2. P-V plots of the system with the UPFC and SVC. The minimum voltage of 124 kV is reached at around a total load of 1275MW on the system.

6.2.1 5%-Load increase on the system

Figures 6.5-6.14 depict the system behavior for different contingency cases. Fig. 6.5 and 6.6 display plots of the voltage magnitude and angle at 05INEZ and 05BAKER buses of the INEZ system without the UPFC and SVC connected to it. The system is operating under heavy loading conditions and close to its stability limits. At time $t = 5$ seconds, as the load on the network is increased by 5%, the system undergoes a voltage collapse. This indicates that the system is highly vulnerable to voltage collapse in the event of load increase while operating under heavy loading.

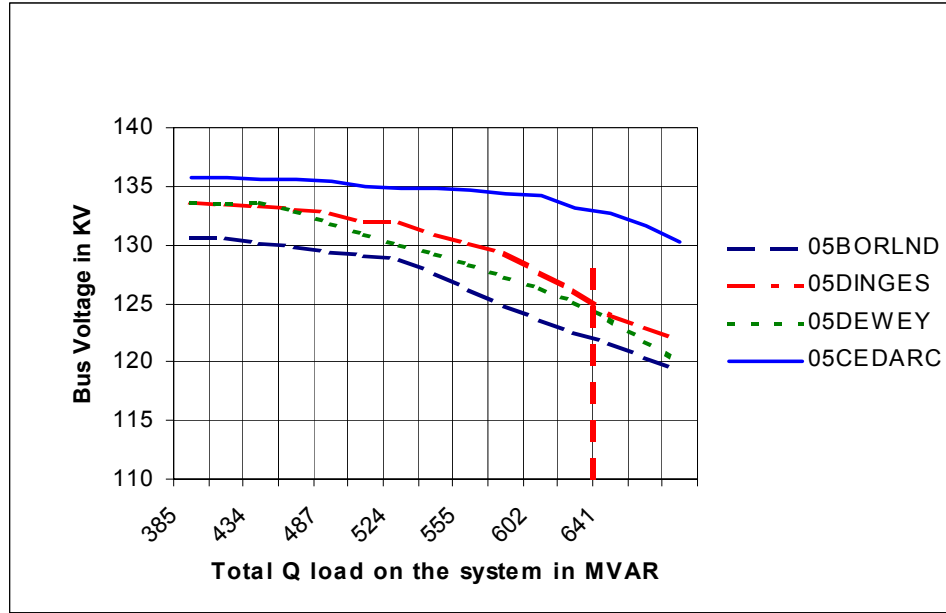


Fig. 6.3. Q-V plots of the system without UPFC and SVC. The minimum voltage of 124 kV is reached at around a total load of 640MVAR.

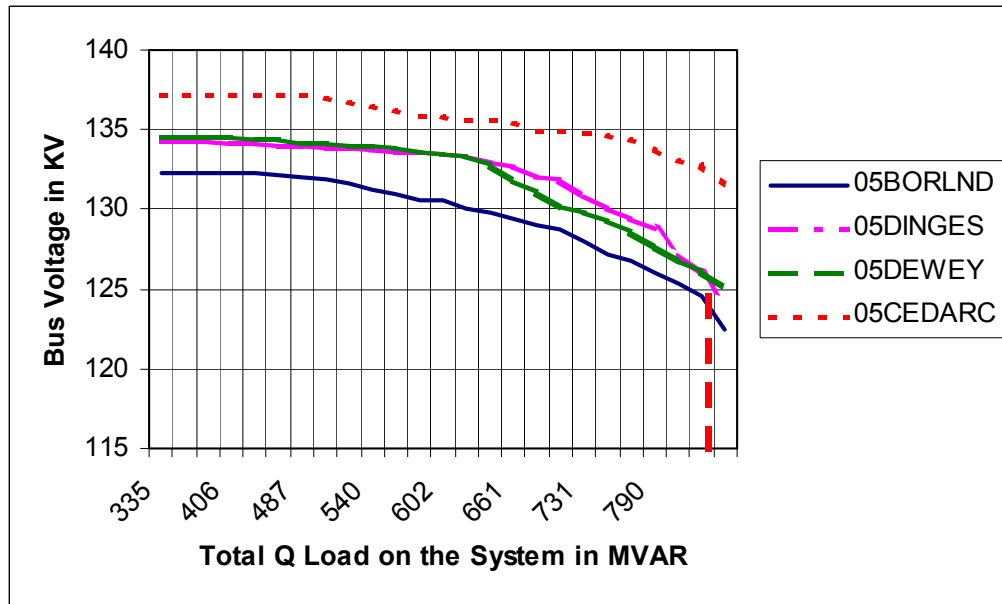


Fig. 6.4. Q-V of the system with the UPFC and SVC. The minimum voltage of 124 kV is reached at around a total load of 870MVAR.

Now the SVC and UPFC were connected to the system and the same case was rerun. The results obtained are shown in Figs. 6.7-6.8. It can be seen that the system voltage is stable for the same case as before, demonstrating the voltage support provided by the SVC and the UPFC. Note that similar results were obtained at all the other buses in the system.

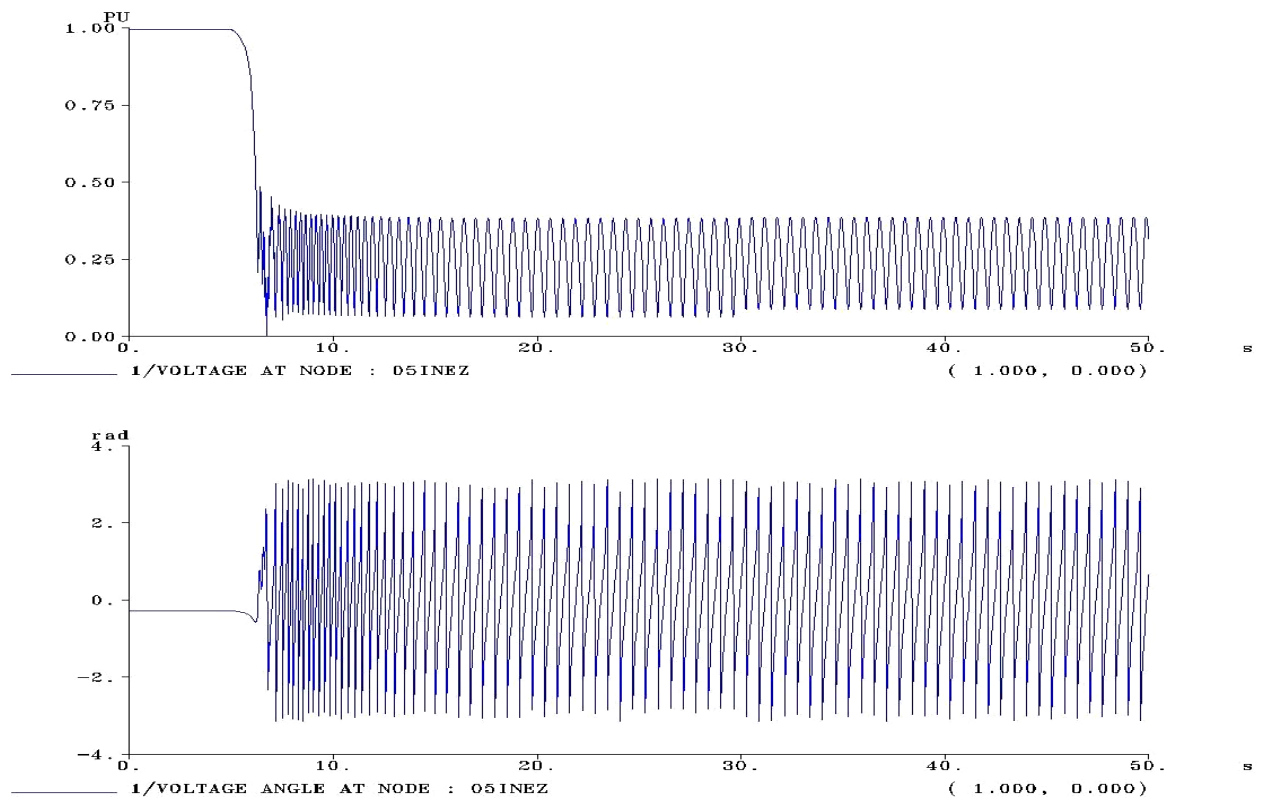


Fig. 6.5. Voltage magnitude and angle plot of the 05INEZ node with the UPFC and SVC not connected to the network.

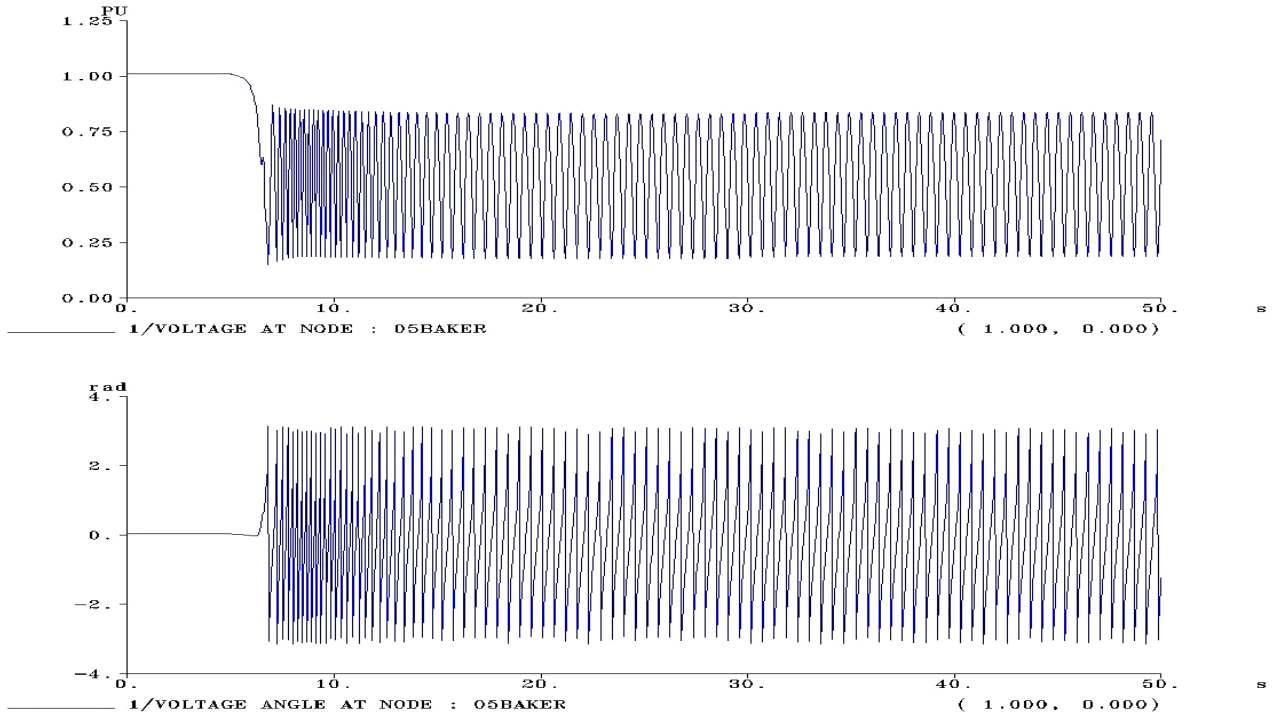


Fig. 6.6. Voltage magnitude and angle plot of the 05Baker node with the UPFC and SVC not connected to the network.

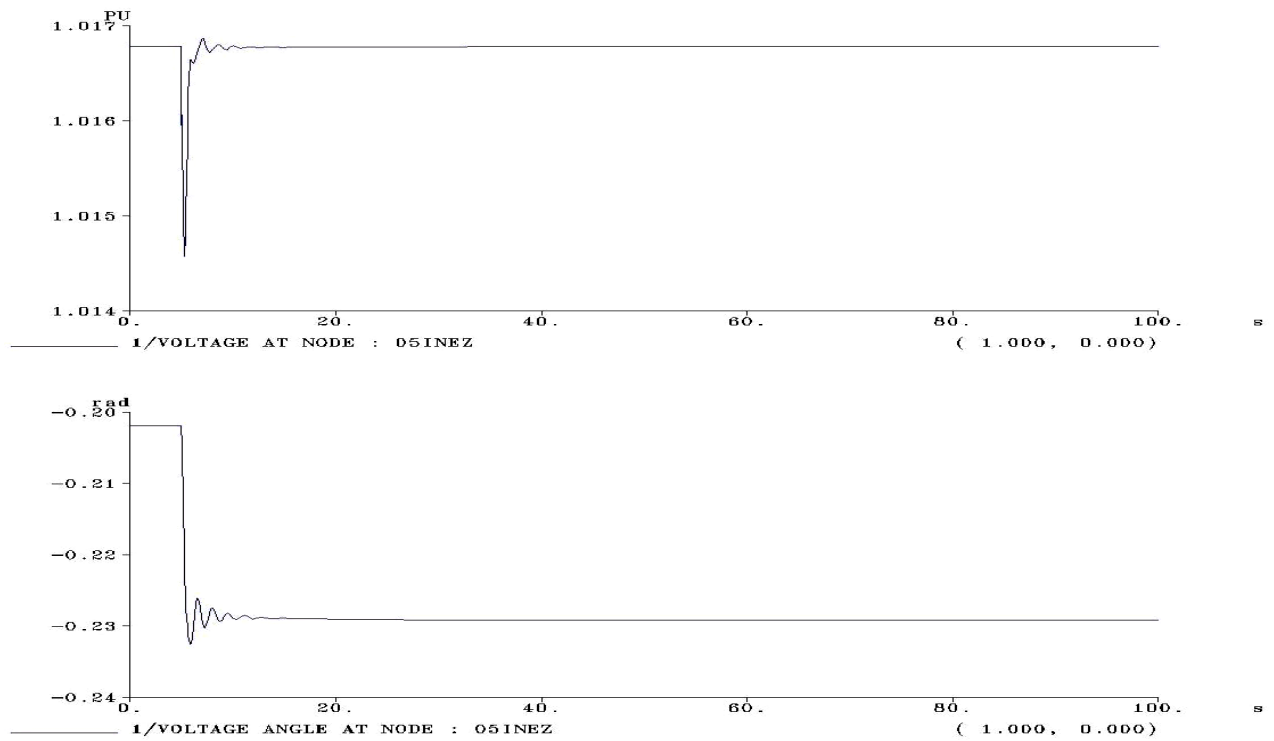


Fig. 6.7. Voltage magnitude and angle plot of the 05Inez node with the UPFC and SVC connected to the network.

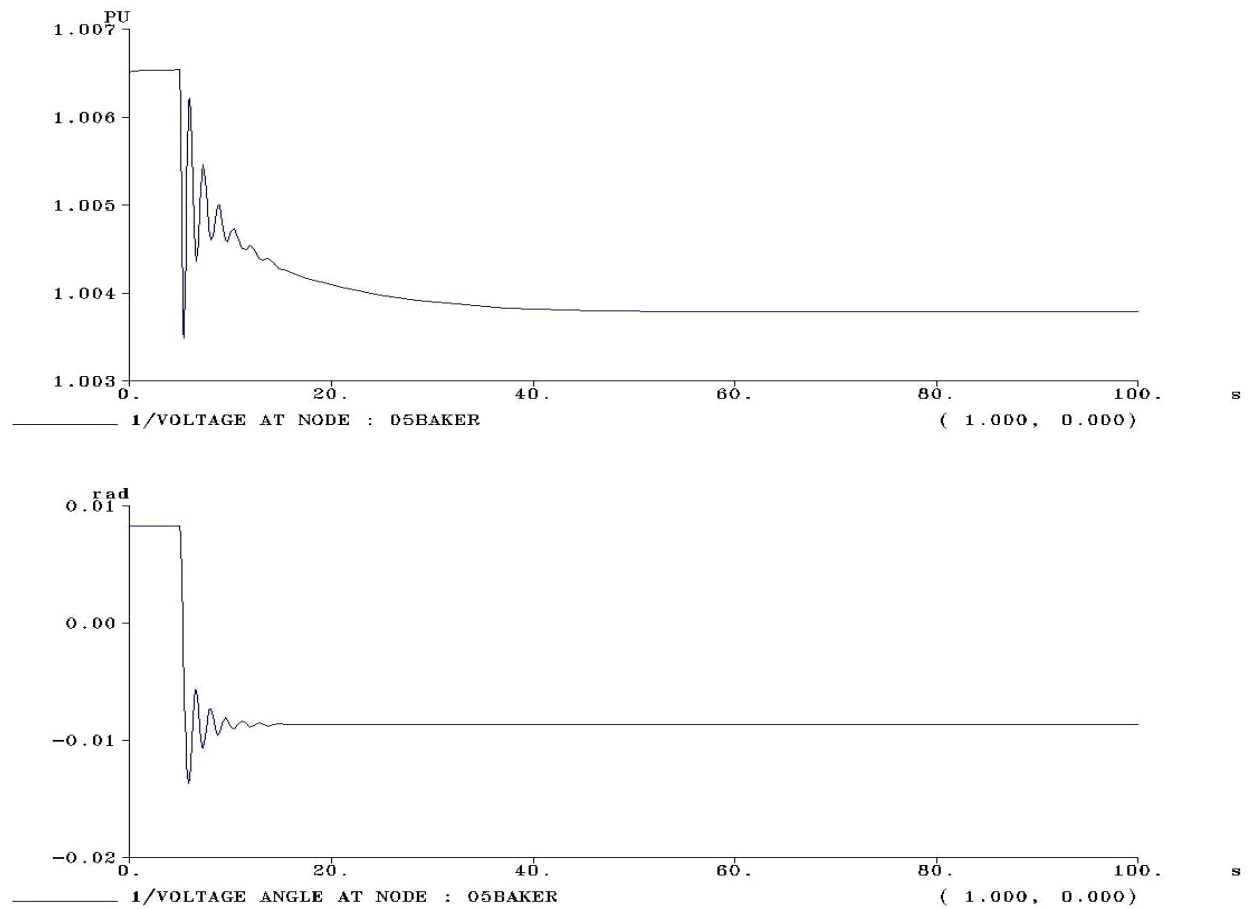


Fig. 6.8. Voltage magnitude and angle plot of the 05Baker node with the UPFC and SVC connected to the network.

6.2.2 Single-contingency Cases

The system along with the UPFC and the SVC was tested for single contingency cases with the sequential opening of one line at a time. The procedure consisted of an increment of the P and Q load at every bus of the network by 5% at time $t = 5$ seconds followed by the opening of line between 05HATFLD and 05BORLND at time $t = 20$ seconds. The results obtained are displayed in Figures 6.9-6.10. We observe that thanks to the damping action of the UPFC and the SVC, the system voltages regain their stability

after few highly damped oscillations. It is to be noted that at this stage, the parameters of the SVC and the UPFC have neither been tuned nor coordinated.

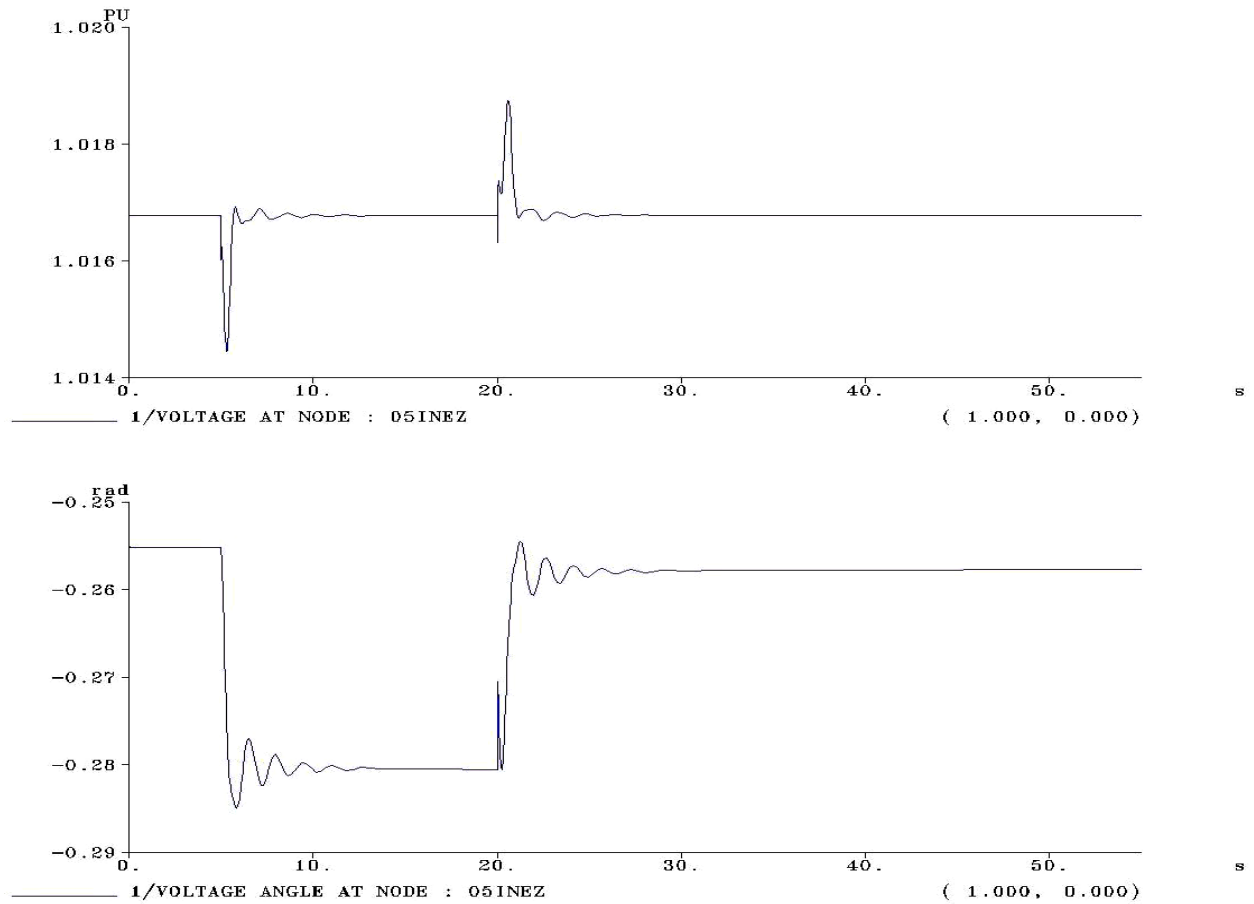


Fig. 6.9. Voltage magnitude and angle plot of the 05Inez node with the UPFC and SVC connected to the network when Line 05HATFLD-05BORLND is disconnected at t=20 seconds following an increment in P and Q load by 5% throughout the network.

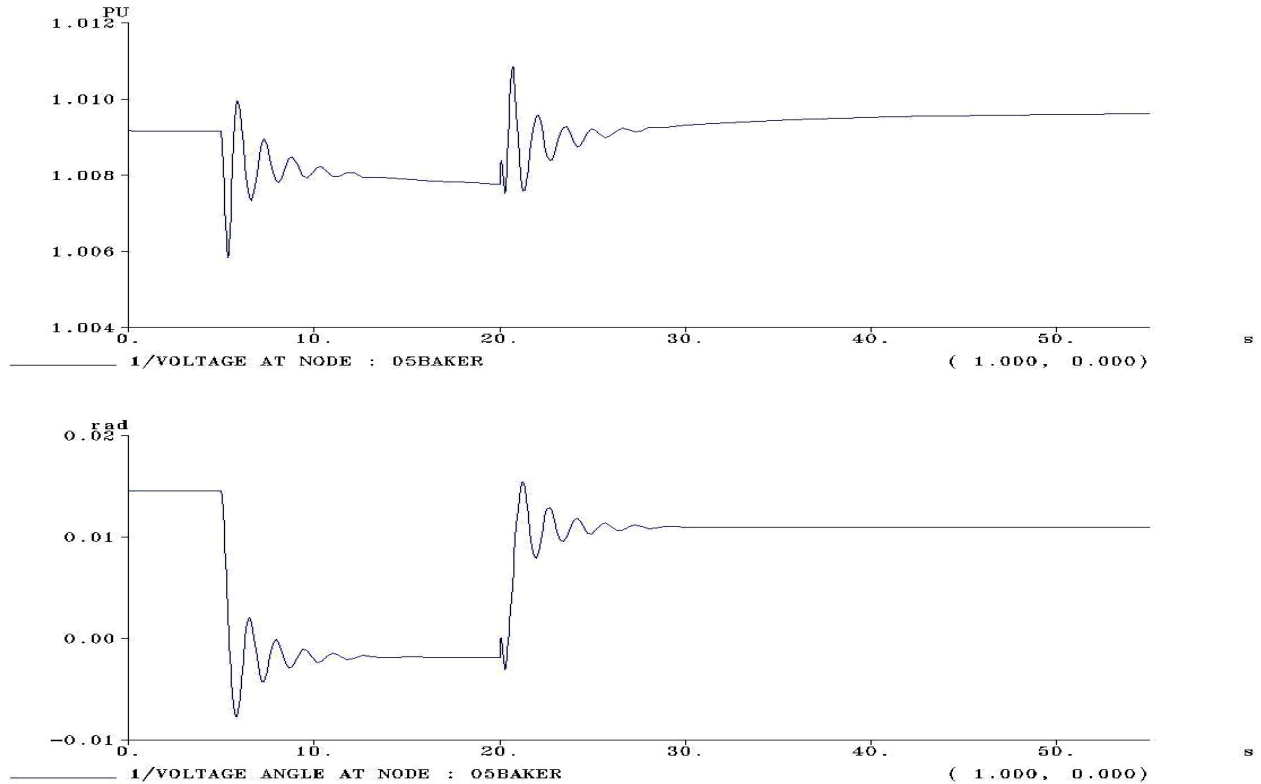


Fig. 6.10. Voltage magnitude and angle plot of the 05Baker node with the UPFC and SVC connected to the network when Line 05HATFLD-05BORLND is disconnected at $t=20$ seconds following an increment in P and Q load by 5% throughout the network.

6.2.3 Double-Contingency Cases

In these series of simulation, double contingencies were simulated. First the P and Q load over the network was evenly increased by 5% followed by the opening of two lines at a time. Figs. 6.11 and 6.12 display the voltage and voltage angle plots for a double contingency case on Line 05HATFLD-05BORLND and Line 05BUSSYV-05THELMA. Here, at time $t = 5$ seconds, the network load was increased; then at time $t = 20$ seconds the line between 05HATFLD and 05BORLND was opened, and finally at time $t = 45$ seconds, the line between 05BUSSYV and 05THELMA was disconnected. As observed, the system exhibits a voltage collapse even with the presence of the SVC and the UPFC. This was because their actions were neither coordinated nor their

parameters have been tuned. To overcome this problem, numerous simulations were carried out for different combinations of parameter values and capacitor bank configurations. The simulations were carried out in two steps. First, the set-points and gains of the SVC and UPFC were incrementally increased step by step and the stability of the system checked. Once their maximum values were reached while the system still suffered from voltage collapse, then switchings of capacitor banks were undertaken. This coordinated action resulted in a voltage profile as shown in Figs. 6.13 and 6.14.

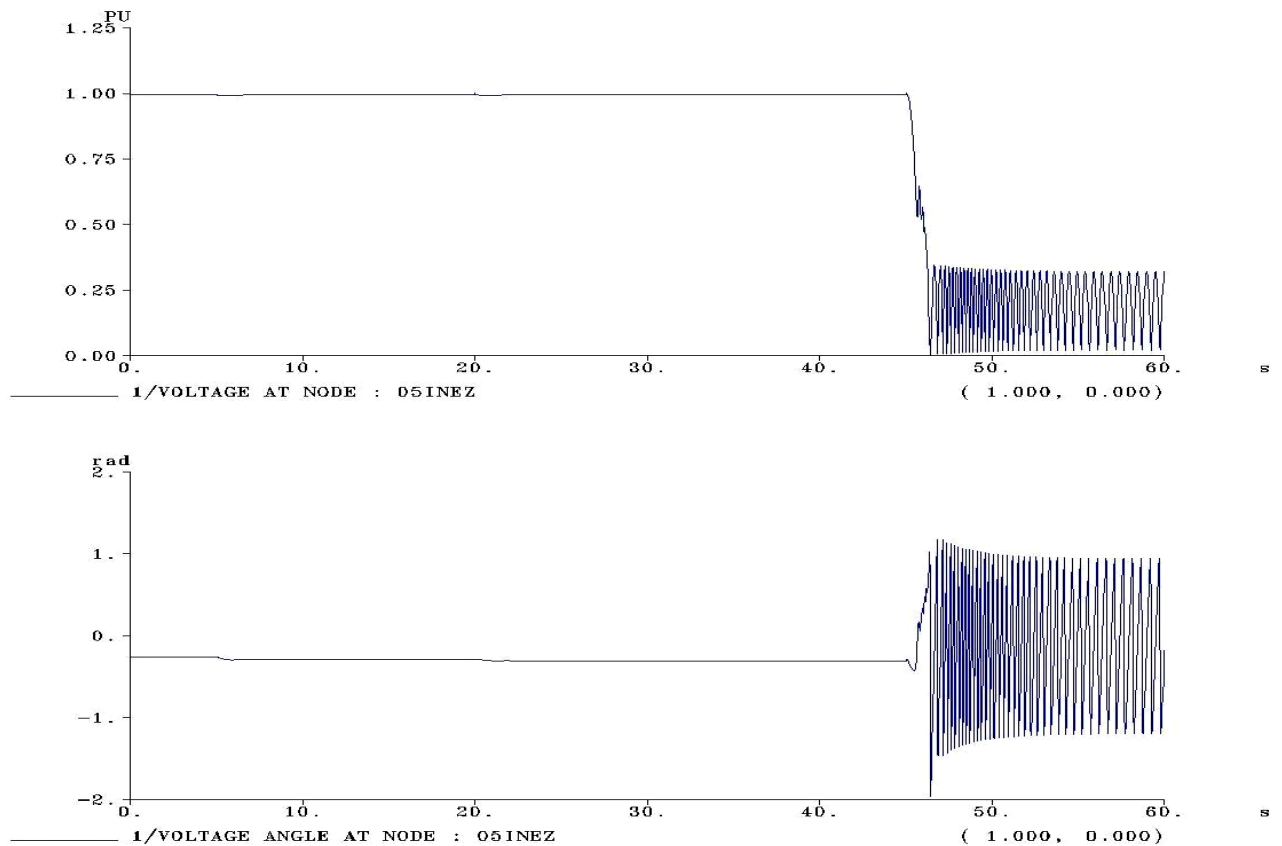


Fig. 6.11. Voltage magnitude and angle plot of the 05INEZ node with the UPFC and SVC connected to the network with Line 05HATFLD-05BORLND and Line 05BUSSYV-05THELMA opened.

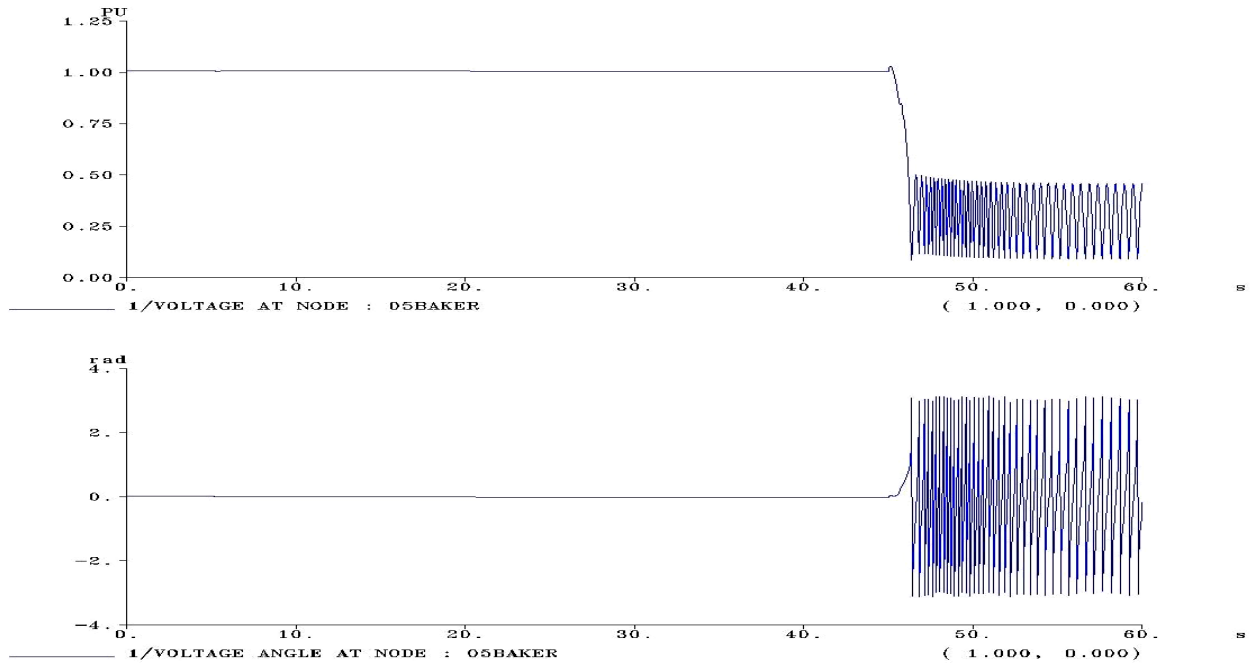


Fig. 6.12. Voltage magnitude and angle plot of the 05BAKER node with the UPFC and SVC connected to the network with Line 05HATFLD-05BORLND and Line 05BUSSYV-05THELMA opened.

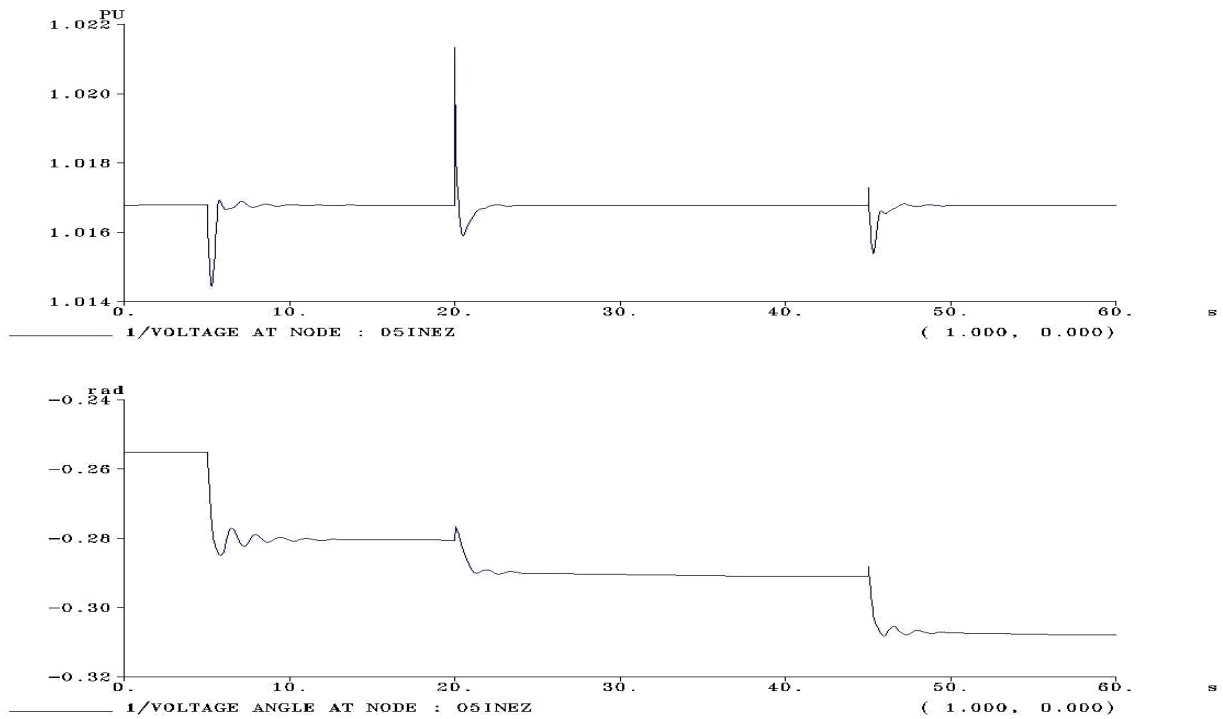


Fig. 6.13. Voltage magnitude and angle plot of the 05INEZ node with the UPFC and SVC connected to the network with Line 05HATFLD-05BORLND and Line 05BUSSYV-05THELMA opened and with actions of the controllers coordinated.

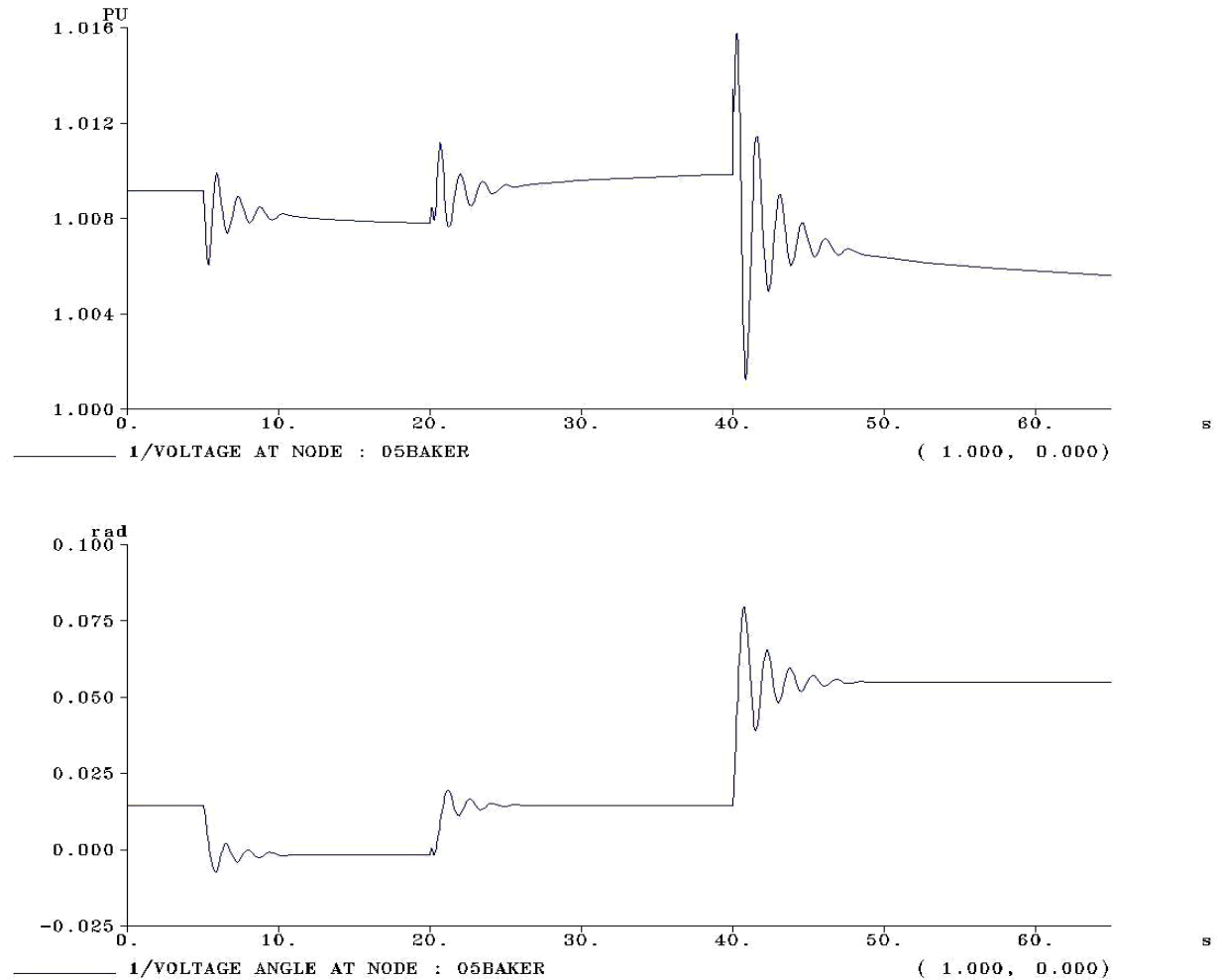


Fig. 6.14. Voltage and voltage angle plot of the 05BAKER node with the UPFC and SVC connected to the network with Line 05HATFLD-05BORLND and Line 05BUSSYV-05THELMA opened and with actions of the controllers coordinated.

It can be seen from Figures 6.13 and 6.14, that no voltage collapse occurs after the actions of the UPFC and SVC have been centrally coordinated by a second-level controller. Similar tests were conducted for numerous contingency cases and suitable set of actions were found out for each of these cases.

6.3 Fuzzy Logic Controller

A fuzzy logic control scheme was implemented and tested. To this end, simple IF-THEN rules were implemented. These rules were then manually implemented in Eurostag and the desired stable voltage profile was obtained. Listed in Table 6.1 are a few IF-THEN rules that have been used to implement the proposed two-level hierarchical scheme.

Table 6.1: Example of nested if loops exhibiting the hierarchy of operations
<p>IF the load at bus 05HATFLD increases by 5%,</p> <p>THEN change the setpoint of SVC to 1.06 and setpoint of UPFC to 1.06,</p> <p> AND IF line between 05BORLND and 05 HATFLD is open,</p> <p> THEN change the setpoint of SVC to 1.07 and setpoint of UPFC to 1.03,</p> <p> AND IF line between 05BUSSYV and 05THELMA is open,</p> <p> THEN change the setpoint of SVC to 1.1 and setpoint of UPFC to 1.08 and switch on 2 capacitor banks at 05INEZ and one capacitor bank at 05THELMA</p>

The rationale of these IF-THEN statements is as follows: When the load at the bus 05HATFLD increases by 5%, the setpoints of the SVC and the UPFC are both changed to 1.06 p.u. The setpoint values have been determined from the simulations that were carried out on the system for optimum values. Now, following the increase of the load and the tripping of the line 05BORLND-05HATFLD, the setpoints of the SVC and the UPFC were both changed to 1.03 p.u. As in the previous case, the values of the setpoints have been determined based on the numerous simulations performed as described in section 6.2.

In the second set of simulations, a second contingency is performed by opening the line between 05BUSSYV and 05THELMA. It turns out here that adjustments of the SVC and UPFC setpoints are not sufficient to prevent voltage collapse; in addition connecting of some capacitor banks are required. The two capacitor banks needed to be switched on are those located at bus 05INEZ and at the bus 05THELMA. Similar types of rules have been framed for other contingency cases. In certain cases the stability limit of the system has been stretched by a value of about 175 MW.

The implementation of fuzzy control can be automated by using the Macroblocks feature available in Eurostag. The automatic control was designed but not implemented owing to the fact that the implementation requires extensive transient analysis simulations and incorporation of protective devices. This would require taking into account the operating characteristics of these protective devices and their behavior in different contingency cases.

6.4 Self-excited Dynamic Non-Linear Oscillations

Instabilities in a power system are of a number of types. They include steady-state instability, transient instability, dynamic instability, frequency collapse, voltage collapse, and subsynchronous resonance, to cite just a few.

So far we investigated steady-state and dynamic instabilities triggered by some perturbations. We will now explore self-excited non-linear dynamic oscillations due to the interactions between the synchronous generators and the induction motors of the dynamic loads.

The stability of an equilibrium point is indicated by the location of the eigen values of the Jacobian matrix evaluated at that point. For example, steady-state voltage collapse occurs at the saddle-node bifurcation point. This is the point of maximum loadability beyond which there is no equilibrium point. At this point, one of the eigenvalues becomes zero implying the singularity of the Jacobian matrix; the load flow program diverges.

Due to non-linear dynamic interactions between the induction motors and the synchronous generators, another type of bifurcation, called the Hopf bifurcation, is anticipated to occur [14].

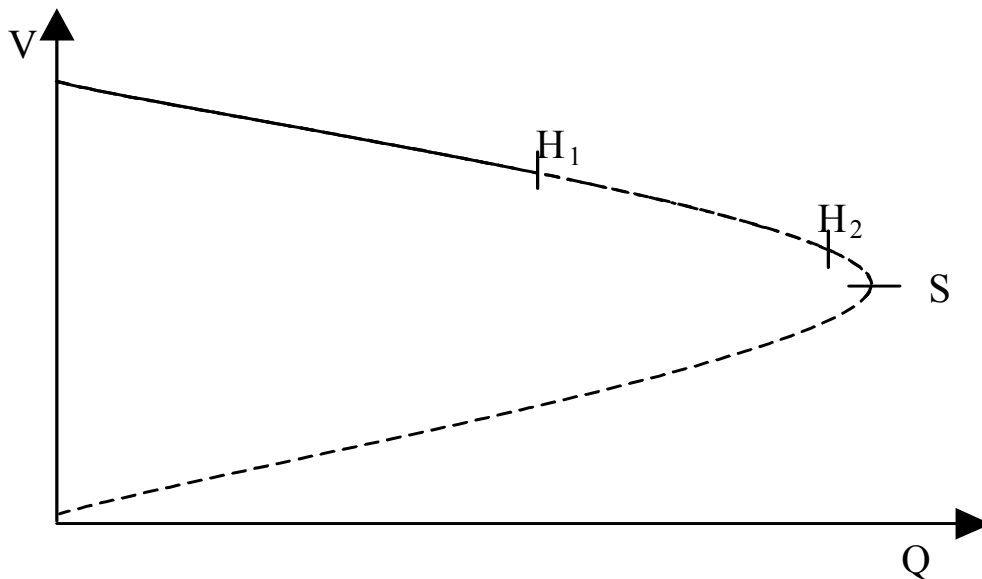


Fig.6.15. Variation of the voltage magnitude V with the reactive power load Q .

The Hopf bifurcation point is the point beyond which a conjugate pair of eigen values of the Jacobian matrix transversally cross over the imaginary axis from the left-hand-side onto the right side of the complex plane. Thus, the operating point goes into self-excited oscillatory mode. It is to be noted that in this case there is no voltage collapse

with the oscillations occurring around 1 p.u. In Fig. 6.15, the points H_1 and H_2 denote the Hopf bifurcation points and S denotes the saddle-node. The solid line denotes stable operating points and the dotted line represents the unstable foci.

Let us investigate the dynamics of the INEZ system in the vicinity of the bifurcation point H_1 . The system possesses a stable equilibrium point at values of Q slightly less than H_1 . As the value of the Q load increases beyond H_1 , the equilibrium point loses stability and a limit cycle is born. As Q is increased further, the limit cycle undergoes a sequence of period-doubling bifurcations, culminating in a chaotic attractor. At this point, if the value of Q is increased by a value large enough, the oscillations grow to a higher value, possibly resulting in voltage collapse.

Simulations were carried out on the INEZ to study these self-excited non-linear oscillations. The network load was gradually increased in small steps of 1 percent per 5 seconds initially, and then much smaller steps in the end over an interval of 100 seconds and the voltage at various buses was plotted against the time in seconds. These plots are displayed in Figures 6.16 - 6.19.

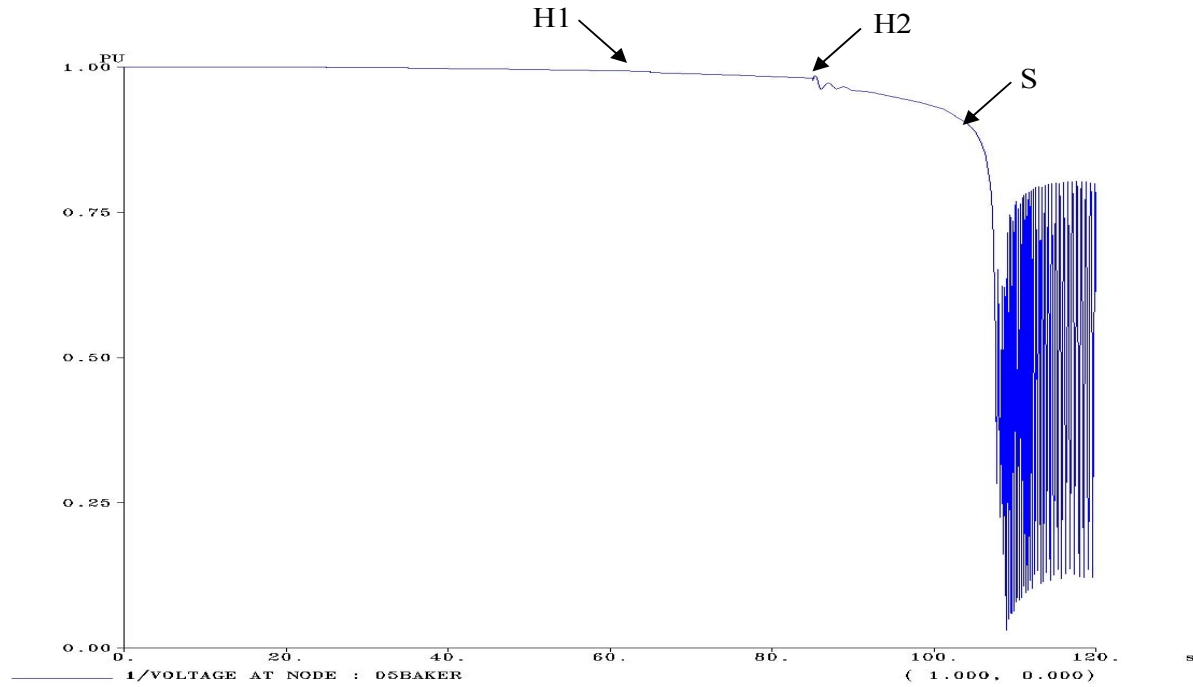


Fig. 6.16. Voltage versus Time plot at the 05BAKER node. There is a voltage collapse at time $t = 105$ seconds.

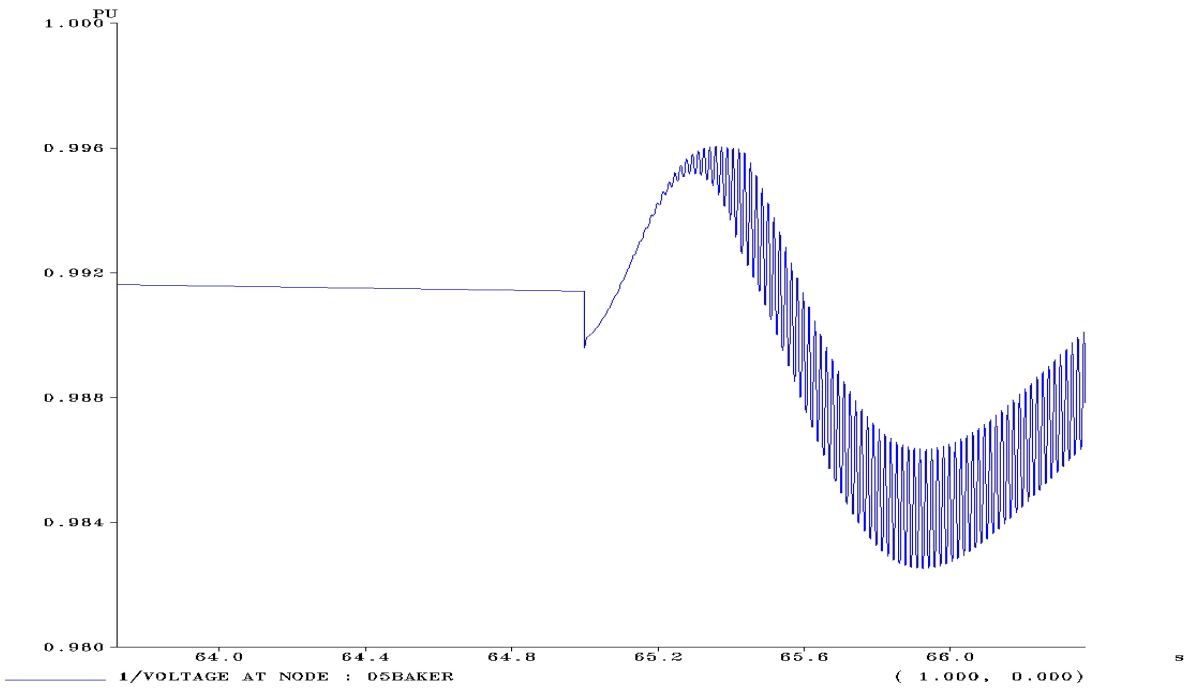


Fig. 6.17. Zooming in at point H₁ in Fig. 6.16, showing persistent oscillations at time $t = 65$ seconds.

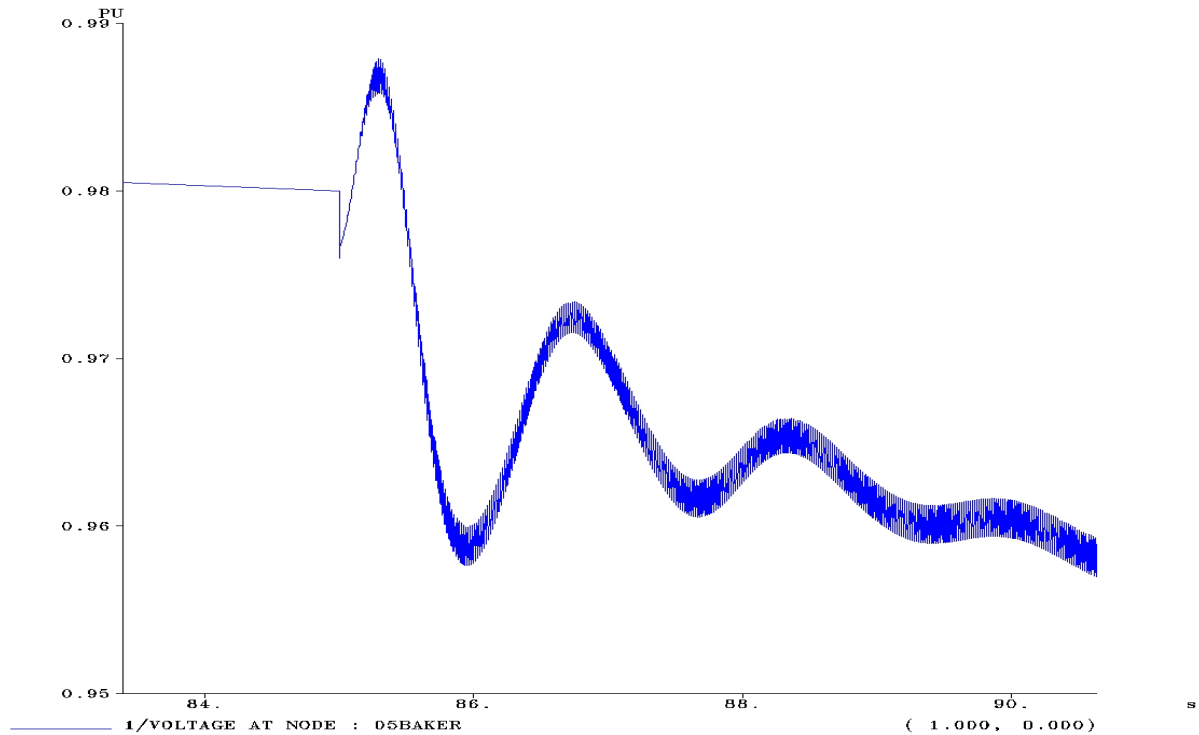


Fig. 6.18. Zooming in on point H2 in Fig. 6.16, showing damped oscillations at time $t = 85$ seconds.

In Figs. 6.17 and 6.18, it is observed that the oscillations are around 1 p.u, indicating that there is no voltage collapse, but rather frequency rich sustained oscillations.

One interesting observation made was that these oscillations occurred only at buses where there was either a generator or a dynamic load attached to. As indicated in Fig 6.19, at all the other buses there was a voltage collapse with no oscillations. This point represents the saddle-node bifurcation point, S, as shown in Fig 6.15. These observations further confirm that the Hopf bifurcations occur only at buses where there are machines present.

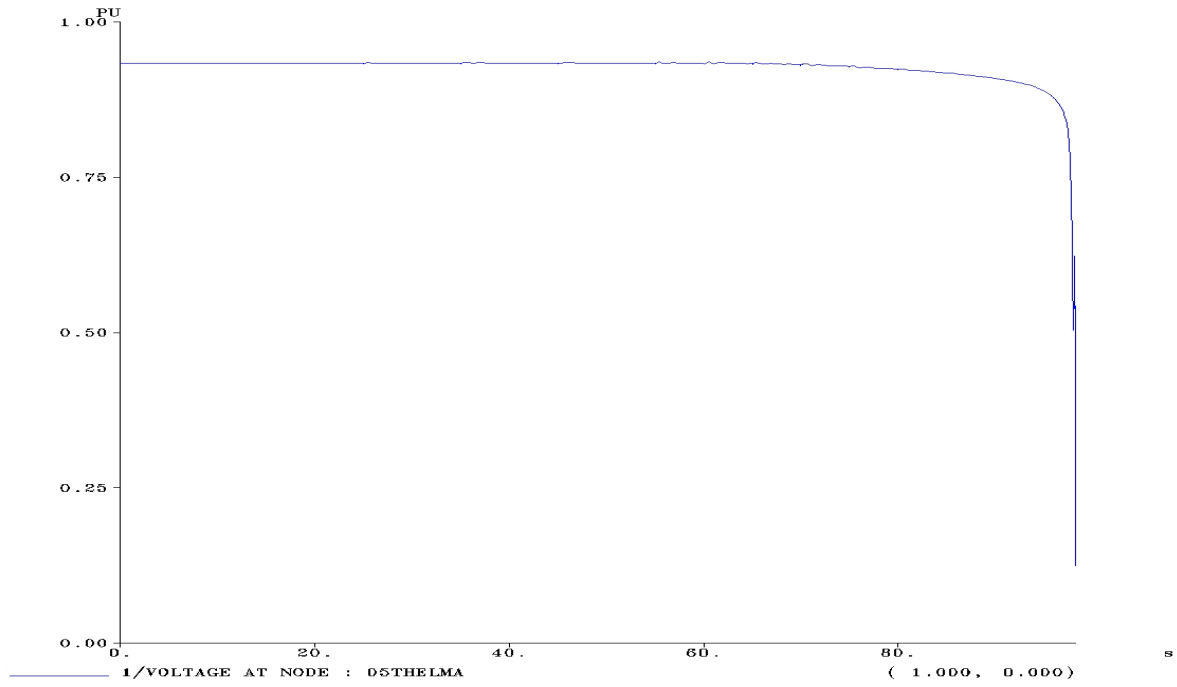


Fig. 6.19. Voltage-Time plot at Node 05THELMA.

Chapter 7

Conclusions

Extensive studies of the behavior of the INEZ power system for different contingency cases revealed that this system performs well under light to medium load conditions, but is subject to instabilities and voltage collapse under heavy load conditions. This instability problem has been addressed by the fine tuning of the UPFC and the SVC, wherein the maximum loadability of the system has been increased by a considerable value, and thus enabling the system to operate closer to its thermal limits. This is owing to the presence of FACTS devices like the UPFC and SVC, which are fast and highly effective means of controlling the voltage and power flow on the network when appropriately tuned and coordinated.

Control coordination of these devices is achieved by means of a two-level hierarchical fuzzy control scheme. It serves as a centralized control that aims at damping the oscillations that may take place in the system should a single or a double contingency occur. The control scheme has increased the overall loadability of the network by a significant value as substantiated through simulations using Eurostag.

Simulation studies performed on the system have also revealed the existence of dynamic interactions between the synchronous generators and the induction motors, resulting in self-excited sustained non-linear oscillations. By an appropriate tuning of the parameters of the FACTS devices and the fuzzy controller, an effective damping of these self-excited oscillations was achieved.

Future work

As a future work, automatic fuzzy control can be implemented. To this end, extensive transient studies need to be carried out to account for the actions of the protective devices in the system. Also more studies need to be performed on the dynamic interactions between the synchronous generators and induction motors. The control scheme needs to be further tuned to take the non-linear interactions into account and control the parameters of the UPFC and SVC accordingly to provide more effective damping of the resultant machine oscillations.

As suggested in Chapter 4, another possible improvement to the implementation of fuzzy control would be the incorporation of pattern recognition to improve the coordination of the controllers' actions.

References

- [1] Carson W. Taylor, *Power System Voltage Stability*, McGraw-Hill, New York.
- [2] Thierry Van Cutsem and Costas Vournas, *Voltage Stability of Electric Power Systems*, Kluwer Academic Publishers, Boston.
- [3] Prabha Kundur, *Power System Stability and Control*, McGraw-Hill, New York.
- [4] Li-Xin Wang, *A Course in fuzzy systems and control*, Prentice Hall, NJ 1997.
- [5] Timothy J. Ross, *Fuzzy logic with engineering applications*, McGraw-Hill, New York.
- [6] Daniel McNeill and Paul Freiberger, *Fuzzy Logic*, Simon and Schuster, Inc., New York.
- [7] Narain G. Hingorani and Laszlo Gyugi, *Understanding FACTS, concepts and Technology of Flexible AC Transmission Systems*, IEEE press, NJ.
- [8] Eurostag, *Eurostag Software Release Notes*, Tractebel-EDF, Release 4.1, Dec 2000.
- [9] R. Mohan Mathur and Rajiv K. Varma, *Thyristor – Based FACTS Controllers for Electrical Transmission systems*, John Wiley & Sons, Inc. and IEEE Press.
- [10] Yong Hua Song and Allan T Johns, *Flexible ac transmission systems (FACTS)*, TJ International Ltd.
- [11] IEEE Task Force on Load Representation for Dynamic Performance, “Standard Load Models for Power Flow and Dynamic Performance Analysis”, *IEEE Transactions on Power Systems*, Vol.10, No. 3, May 1995.
- [12] IEEE Task Force on Load Representation for Dynamic Performance, “Biography on Load Models for Power Flow and Dynamic Performance Simulation”, *IEEE Transactions on Power Systems*, Vol.10, No. 1, Feb. 1995.
- [13] D. J. Hill, “Nonlinear Dynamic Load Models for Voltage Stability Studies,” *IEEE Transactions on Power Systems*, Vol. 8, No. 1, May 1992.
- [14] Ali H. Nayfeh, Ahmad M. Harb and Char-Ming Chin, “Bifurcations in a Power System Model”, *International Journal on Bifurcation and Chaos*, Vol. 6, No. 3 (1996) p 497-512
- [15] L. Zadeh, “Fuzzy sets,” *Information and Control*, vol.8, pp.338-353, 1965.

- [16] T.J. Ross, *Fuzzy Logic*, McGraw-Hill, Inc., New York, 1995.
- [17] R. Mihalič, P. Žunko and D. Povh, “Improvement of Transient Stability using Unified Power Flow Controller”, *IEEE Transactions on Power Delivery*, Vol. 11, No. 1, January 1996, p. 485-492.
- [18] Karl Schoder, Azra Hasanovic and Ali Feliachi, “Enhancing Transient Stability using a Fuzzy Control Scheme for the Unified Power Flow Controller (UPFC)”, *Procedures IEEE Midwest Symposium on Circuits and Systems*, Lansing MI, Aug 8-11, 2000.
- [19] Karl Schoder, Azra Hasanovic and Ali Feliachi, “*Power System Damping using Fuzzy Controlled Unified Power Flow Controller*”, 0-7803-6672-7/01 © 2001 IEEE.
- [20] C. Travares da Costa Jr., J. A. L. Barreiros, R. C. L. de Oliveira, W. Barra Jr., “Power System Stabilizer Scheduled by a Fuzzy Logic Based Supervisor from a Local Compensator Network”, *2001 IEEE Porto Power Tech Conference*, 10th – 13th September, Porto, Portugal.
- [21] J. G. Vlachogiannis, “Fuzzy logic application in load flow studies”, *IEE proceedings, Generation, Transmission, Distribution*, Vol. 148, No. 1, January 2001.
- [22] M. Pamiani and M. R. Iravani, “Voltage Control Stability and Dynamic Interaction Phenomena of Static Var Compensators”, *IEEE Transactions on Power Systems*, Vol. 10, No. 3, August 1995.
- [23] R. Gutman, J. J. Keane, M. Ea. Rahman, O. Veraas, “Application and Operation of a Static Var System on a Power System – American Electric Power Experience, Part I: System Studies, Part II: Equipment Design and Installation,” *IEEE Transactions on Power Apparatus and Systems*, Vol. PAS-104, No. 7, pp. 1868-1881, July 1985.
- [24] M. Rahman, M. Ahmed, R. Gutman, R. J. O’Keefe, R. J. Nelson, and J. Bian, “UPFC Application on the AEP System: Planning Considerations,” *IEEE transactions on Power Systems*, Vol. 12, No. 4, pp. 1695-1701, Nov. 1997.
- [25] C. Schauder, E. Stacey, M. Lund, A. K. Mehraban, A. Edris, “AEP UPFC Project: Installation, Commissioning and Operation of the ± 160 MVA STATCOM (Phase),” *IEEE Transactions on Power Delivery*, Vol. 13, No. 4, pp. 1530-1535, Oct. 1998.

- [26] B. A. Renz, A. Keri, A. S. Mehraban, C. Schauder, E. Stacey, L. Kovalsky, L. Gyugyi, A. Edris, "AEP Unified Power Flow Controller Performance," *IEEE Transactions on Power Delivery*, Vol. 14, No. 4, pp. 1373-1381, Oct. 1999.
- [27] J. Bian, D. G. Ramey, R. J. Nelson, A. Edris, "A Study of Equipment Sizes and Constraints for a Unified Power Flow Controller," *IEEE Transactions on Power Delivery*, Vol. 12, No. 3, pp. 1385-1391, July 1997.
- [28] P. Petitclair, Y. Besanger, S. Bacha, and N. Hadjsaid, "Facts Modeling and Control: Application of STATCAM on Power System," *Proceedings of the 1997 Annual Meeting of the IEEE Industry Applications Society*, New Orleans, Louisiana, Oct. 5-9, 1997.
- [29] S. Ammari, Y. Besanger, J. C. Passelergue, N. HadjSaid, D. George, "On the Interaction Between Facts Controllers and Power System Environment," *Submitted to the IEEE Transactions on Power Systems*.
- [30] Morton Nadler and Eric P. Smith, "*Pattern Recognition Engineering*".
- [31] L.K. Wong, Frank H. F. Leung and Peter K. S. Tam, "A Fuzzy Sliding Controller for Nonlinear Systems", *IEEE Transactions on Industrial Electronics*, Vol. 48, No. 1, February 2001.
- [32] C. M. Valle, A. O. Borges, G. C. Guimarães and H. R. Azevedo, "Fuzzy Logic Controller Simulating an SVC Device in power System Transient Stability Analysis", *2001 IEEE Porto Power Tech Conference*, 10th – 13th September, Porto, Portugal.
- [33] Hsiao-Dong Chiang, Alexander J. Flueck, Kirit S. Shah, Neal Balu, "CPFLOW: A Practical Tool for Tracing Power System Steady-State Stationary Behavior Due to Load and Generation Variations", *IEEE Transactions on Power Systems*, Vol. 10, No. 2, May 1995.
- [34] Venkatraman Ajjarapu, Colin Christy, "The Continuation Power Flow: A Tool for Steady State Voltage Stability Analysis", *IEEE Transactions on Power Systems*, Vol. 7, No. 1, February 1992.

Educational Qualification

- **Master of Sciences** in Virginia Polytechnic Institute and State University (Virginia Tech). Overall GPA 3.5. Aug2001- May 2003
- **Bachelor of Engineering** in Electrical and Electronics Engineering, Osmania University. First Class with Distinction. Oct 1997- June 2001

Technical skills

Simulation Languages: Eurostag 3.1/4.0, Matlab 5.1/6.1

Operating systems: Windows 95/98/2000, Windows NT, MS DOS, and UNIX

Programming Languages: C, C+ +, Java

RDBMS: MS SQL server 7.0, Sybase, MS Access

GUI Tools: Visual basic 6.0, MS Access

Internet Technologies: HTML, Macromedia Dreamweaver, Fireworks, Flash and M.S. Front page.

Professional Experience

- **Graduate Research Assistant**, Alexandria Research Institute, Virginia Tech. (August 2001-January 2003)
Responsibilities: Design and develop a control system using fuzzy logic. Project funded by American Electric Power and Electric Power Research Institute. Eurostag, a simulation package developed by EDF of France was used as the primary tool to implement this control system.
- **Graduate Support Technician**, Alexandria Research Institute, Virginia Tech. (January 2003- Present)
Responsibilities: Network and IT support, Website Development.
Design and maintenance of several websites using HTML, JavaScripts, Microsoft FrontPage 2000, Macromedia Dreamweaver and Fireworks. IIS 5.0 Web Server Management and Installation, Wireless LAN maintenance; Installation of Windows terminals and Peripherals; Network security; Helpdesk Support for all computer related issues for Virginia Tech Faculty.
- **Faculty**, Innovation InfoTech, Secunderabad, India. (Feb 2000-May 2001)
Responsibilities: Conducted hardware (Computer Assembling and Installation) and software (C & C++) training classes at this cutting edge career training school for 20 batches of 15 students each.

Course Projects

- **Control Coordination of the UPC and the SVC located in the AEP's INEZ area using Fuzzy logic. (Master's Thesis Project)**
Tools: Eurostag 4.0/3.1
This was a research project funded by American Electric Power and Electric Power Research Institute. The objective was to develop a hierarchical scheme using fuzzy logic that coordinate the actions of the SVC and the UPFC controllers in order to increase the voltage stability margins of the system under normal and contingency operating conditions. This required the extensive use of EUROSTAG, a simulation package with a graphical interface where the control system was designed and built.
- **Real Time Data Acquisition of Analog Input for Nuclear Power Plant. (Undergraduate Final Project)**
Tools: C
The objective of this 2-month project was to write a device driver for the Analog Input Board, a part of the I/O system of a control panel of a Nuclear Power Plant, using C language. As an application of real time data acquisition, a part of the nuclear power plant was simulated and the output of the board was given as input to this simulation and the various control parameters were calculated. This simulation was carried out using the ADIOS 3000 system developed by Electronic Corporation of India Ltd.
- **Analysis of the performance of Robust estimators**
Tools: Matlab 6.1
This project was to study the performances of various Estimators discussed in the class. Programs were written in Matlab to estimate the parameters and the results were documented. The performances of the Huber, Huber type Skipped Mean and the Tukey's bi-weight M-estimator were analyzed and the results were presented

- **Speech signal analysis and synthesis using correlation methods**
Tools: Matlab 6.1
The project dealt with writing programs to analyze a given speech segment to determine the voiced and unvoiced components using the Fast Fourier Transform function of MATLAB.
- **Design of a filter using least-squares method**
Tools: Matlab 6.1
The objective was to design an IIR filter to eliminate the noise from a complex noisy speech signal. The filter was designed using the **least-squares method** and the accuracy of the design was judged by the quality of the filtered signal.
- **Designed and maintaining the site** www.ari.vt.edu/workshop
- **Designed and maintaining the site** www.netvisionresources.com

Other Projects

- **Module generation for automating the bank transactions for online banking.**
Tools: Visual Basic 6.0 as front end and backend MS SQL Server 7.0 as an RDBMS.
A case study was done for automating the banking system. The details of the customers were stored in the SQL Server database. The aspects of automating the banking transactions including the transactions using the ATMs of the bank were incorporated into the module. Security features included the validation of credit cards and verification of user identification numbers while using the ATMs. The users were authenticated before cash was transacted from their accounts. Inter bank transactions were also incorporated in the module.
- **A case study for Toy Universe Incorporation**
Tools: Java as front end and backend MS SQL Server 7.0 as an RDBMS.
The website was designed using HTML and Java. The site was to serve the purpose of allowing the visitors to make purchases. The mode of payment was using credit cards only. The cards were verified for validity and the requests were processed. The site dealt with maintaining a database of all the visitor's requests using MS SQL server 7.0. A good amount of security was incorporated using various tools available in Java.
- **Client Server Application Development and Object Oriented Programming Using SQL Server, DB-Library and C ++.**
Tools: C ++ as front end and backend Sybase as an RDBMS.
The company wanted to computerize its shares issues and maintenance. The share transactions were to be maintained with a certain amount of security with limited access only to the directors of the company. The printing of share certificates was also handled.

Relevant Course Work

Linear Control Systems, Advanced Control Systems, Power Electronic Devices, Power Systems Engineering, Electrical Machines, Electro Magnetic Theory and Electrical Measurements and Instrumentation.

Achievements and Extra Curricular Activities

- Won the first prize in a State Level Technical paper presentation contest conducted by IEEE held at SriNidhi Institute of Science and Technology, by presenting a paper on **Magneto Hydrodynamics**.
- Won the first prize in a National level Technical Symposium in 1999, held at Vasavi College of Engineering and Technology, Hyderabad by presenting a paper on **Mobile Communications**.
- Won the first prize in a National Level One Day Technical Symposium in 2000, held at GITAMS, Vishakapatnam by presenting a paper on **Virtual Reality**.
- Won the first prize in a Technical paper meet in 2001, held at GNITS, Hyderabad by presenting a paper on **Image Processing**.
- Presented a paper on TCP/IP in a National level Technical Symposium in 1999, held at Hyderabad.
- President of the Indian Students Association of Virginia Tech for the Northern Virginia Campus.
- Won first prizes for AD-CAMPAIGNS conducted in the various youth festivals conducted in Hyderabad.
- Won second prize in arts and handicrafts contest conducted by FEVICOL for three consecutive years, during high school.